



HAL
open science

Molecular studies of ATP-sensitive potassium channels : gating, pathology, and optogenetics

Gina Catalina Reyes-Mejia

► **To cite this version:**

Gina Catalina Reyes-Mejia. Molecular studies of ATP-sensitive potassium channels : gating, pathology, and optogenetics. Structural Biology [q-bio.BM]. Université Grenoble Alpes, 2016. English. NNT : 2016GREAV012 . tel-01497530

HAL Id: tel-01497530

<https://theses.hal.science/tel-01497530>

Submitted on 28 Mar 2017

HAL is a multi-disciplinary open access archive for the deposit and dissemination of scientific research documents, whether they are published or not. The documents may come from teaching and research institutions in France or abroad, or from public or private research centers.

L'archive ouverte pluridisciplinaire **HAL**, est destinée au dépôt et à la diffusion de documents scientifiques de niveau recherche, publiés ou non, émanant des établissements d'enseignement et de recherche français ou étrangers, des laboratoires publics ou privés.

THÈSE

Pour obtenir le grade de

**DOCTEUR DE LA COMMUNAUTE UNIVERSITE
GRENOBLE ALPES**

Spécialité : **Biologie Structurale et Nanobiologie**

Arrêté ministériel : 7 août 2006

Présentée par

Gina Catalina REYES MEJIA

Thèse dirigée par **Dr. Michel VIVAUDOU**

préparée au sein du **l'institut de Biologie Structurale**
dans **l'École Doctorale Chimie et Science du Vivant**

Etudes moléculaires du canal potassique sensible à l'ATP: "gating", pathologie et optogénétique

Thèse soutenue publiquement le **23 Septembre 2016**
devant le jury composé de :

Pr. Franck FIESCHI

Président

Dr. Thomas GRUTTER

Rapporteur

Dr. Gildas LOUSSOUARN

Rapporteur

Dr. Guillaume SANDOZ

Examineur

Dr. Michel VIVAUDOU

Directeur de thèse



Université de Grenoble
École Doctorale Chimie et Science du Vivant

Thèse pour obtenir le grade de
DOCTEUR EN SCIENCES DE L'UNIVERSITÉ DE
GRENOBLE

Specialité: Biologie Structurale et Nanobiologie

Presented and defended in public by

Gina Catalina REYES MEJIA

On September 23th 2016

Molecular studies of ATP-sensitive potassium channels: Gating, pathology, and optogenetics

Thesis director:

Dr. Michel VIVAUDOU

Jury:

President: Pr. Franck FIESCHI

Reviewer: Dr. Thomas GRUTTER

Reviewer: Dr. Gildas LOUSSOUARN

Examiner: Dr. Guillaume SANDOZ

List of Abbreviations

ABC	ATP-Binding Cassette
ADP	Adenosine diphosphate
ATP	Adenosine triphosphate
BR	Bacteriorhodopsin
CFTR	Cystic Fibrosis Transmembrane Conductance Regulator
ChR	Channelrhodopsin
CL	Caged ligand
COPI	Coat Protein Complex I
CS	Cantù Syndrome
CTD	Cytoplasmic domain
ED	Aspartate and Glutamate
ER	Endoplasmic Reticulum
GPCR	G Protein-Coupled Receptor
HR	Halorhodopsin
ICCR	Ion Channel-Coupled Receptor
iGluR	Ionotropic glutamate receptor
Kir	Inward rectifier K ⁺ channel
KCO	Potassium Channel Opener
Kv	Voltage dependent K ⁺ channel
LC-CoA	Long chain Co-Enzyme A ester
MAQ	Maleimide Azobenzene Quaternary Ammonium
MEA-TMA	Maleimide Ethylene Azobenzene Trimethyl Ammonium
NBD	Nucleotide-binding domain
PCLs	Photochromic ligand
PHHI	Persistent Hyperinsulinemic Hypoglycemia of Infancy
Pi	Phosphate
PIP ₂	Phosphatidylinositol-4,5-bisphosphate
Po	Open probability
PTL	Photoswitched tethered ligand
SPARK	Photoisomerizable Azobenzene Regulated K ⁺ channel
SUR	Sulfonylurea receptor
TM	Transmembrane segment
TMD	Transmembrane domain
VFTM	Venus Flytrap Mechanism
YCF1	Yeast Cadmium Factor 1

Table de Contents

Objectives	8
Introduction	9
1. Potassium channels	10
1.a. The inward rectifying potassium channels (Kir).....	11
1.a.1. Inward rectification	12
1.a.2. Kir channel structures	13
2. ABC transporters	18
2.a. Transport mechanism	21
3. ATP-sensitive potassium channels	22
3.a. K_{ATP} channel summary.....	22
3.b. The sulfonylurea receptor	25
3.b.1. Isoforms and localization.....	25
3.b.2. Structural organization.....	25
3.c. Kir6 channels.....	26
3.d. SUR/Kir6 assembly and functional coupling	27
3.d.1. SUR/Kir6 association	27
3.d.2. SUR/Kir6 functional coupling	30
4. K_{ATP} channel mechanism and regulation.....	31
4.a. Physiological regulation of the K_{ATP} channel by SUR	31
4.a.1. Regulation by Mg-nucleotides, specifically Mg-ADP.....	31
4.a.2. Regulation by Zinc.....	32
4.a.3. Regulation by G-proteins.....	32
4.b. Physiological regulation of the K_{ATP} channel by Kir6.....	33
4.b.1. Regulation by nucleotides	33
4.b.2. Regulation by lipids.....	34
4.c. K_{ATP} channel physiology and physiopathology	35
4.c.1. K_{ATP} channels in the pancreas	35
4.c.2. K_{ATP} channels in the central nervous system.....	37
4.c.3. Muscle K_{ATP} channels	37
4.d. K_{ATP} channel pharmacology.....	38
4.d.1. K_{ATP} channel inhibitors.....	38
4.d.2. K_{ATP} channel openers.....	39
5. Ion Channel-Coupled Receptors	42
5.a. Principle of the ICCR concept.....	42
5.b. ICCR engineering.....	43
5.c. Applications of the ICCR technology	43
5.d. G Protein-Coupled Receptors.....	44
5.d.1. The GPCR Family.....	45
5.d.2. GPCR ligands	47
5.d.3. GPCR-mediated signaling through G Proteins	48
5.d.4. The M2 muscarinic acetylcholine receptor	49
6. Light as a tool in Biology.....	51
6.a. Optogenetics, optopharmacology and optogenetic pharmacology.....	52
6.a.1. Optogenetics: Rhodopsins at a glance	52
6.a.2. Optopharmacology and optogenetic pharmacology.....	54
6.b. PTL approach in membrane proteins	56

6.b.1. Ionotropic glutamate receptor (iGluR).....	56
6.b.2. Nicotinic acetylcholine, GABA and metabotropic glutamate receptors	57
6.b.3. Potassium channels	58

Materials and Methods..... 61

1. Molecular biology	62
1.a. Genes and expression vectors	62
1.b. Site-directed mutagenesis	63
1.c. Subcloning.....	64
1.d. Amplification of the genetic material.....	65
1.d.1. Transformation of competent bacteria.....	65
1.d.2. Amplification and purification of DNA	65
1.d.3. Miniprep and midiprep methods	66
1.e. Sequencing	67
1.f. In vitro transcription.....	67
2. Heterologous expression in <i>Xenopus laevis</i> oocytes	68
2.a. <i>Xenopus laevis</i> oocytes	68
2.b. Extraction and preparation of oocytes	69
2.c. mRNA Microinjection.....	69
3. Expression in mammalian cells	70
3.a. Transfection DNA mammalian cells	70
3.b. Calcium Phosphate Transfection.....	70
3.c. Lipofectamine transfection	71
4. Electrophysiological characterization of ion channels	71
4.a. Patch Clamp Technique.....	71
4.b. Patch clamp Instrumentation	73
4.c. Patch Clamp configuration	75
4.d. Experimental procedure	75
4.e. Optogenetics experiments	77
4.e.1. Photoswitchable molecule attachment	77
4.f. Data processing and analysis	78
5. Two-Electrode Voltage Clamp (TEVC)	80
5.a. Experimental procedure	80
5.b. Data processing and analysis	81

Results..... 83

1. Identification of the gates of Kir6.2 controlled by regulatory membrane proteins.....	84
1.a. Relevance of the study	84
1.b. Project background and experimental approaches	85
1.c. Gate scanning approach by site directed mutagenesis.	86
1.d. Effect of I296L mutation of the G loop gate	89
1.e. Do mutations at position M314 in Kir3.4 and I296 in Kir6.2 have the same effect?.....	90
1.f. Do GPCR and SUR act on the same gate residues?	92
1.g. Discussions and perspectives	94
2. Design of a light-gated ATP-sensitive K ⁺ channel.....	103
2.a. Objectives.....	103
2.b. Light-inhibited K _{ATP} channel	104
2.b.1. Design of a light-inhibited K _{ATP} channel.....	104
2.b.2. Functional impact of the cysteine mutations	106
2.b.3. Light-dependent block in HEK-293 mammalian cells	109

2.b.4. Light-dependent block in inside-out patches from oocytes.....	111
2.b.5. Thermal stability of the photosensitive ligand MAQ.....	113
2.b.6. Light-dependent block in INS-1E glucose-sensitive cells.....	114
2.c. Light-activated K_{ATP} channel	115
2.c.1. Design of a light-activated K_{ATP} channel	115
2.c.2. Testing light-dependent activation in excised patches	117
2.d. Discussions and Perspectives	117
3. Mechanism of action of Cantù syndrome mutations	120
3.a. Relevance of the study	120
3.b. Project background and experimental approaches	121
3.c. Functionality of the SUR2A variants H60Y and D207E	122
3.c.1. Response to the physiological inhibitor ATP	123
3.c.2. Responses to the physiological opener ADP	124
3.c.3. Response to PIP_2	125
3.c.4. Response to the pharmacological opener P1075	129
3.c.5. Response to the pharmacological blocker glibenclamide.	129
3.d. Discussion and perspectives	130
Bibliography	133

OBJECTIVES

The ATP-sensitive potassium channels (K_{ATP} channels) are formed by the unique interaction of two proteins: The sulfonylurea receptor (SUR) which belongs to the ABC transporter family, and an inwardly-rectifying potassium channel (Kir6). After the discovery of K_{ATP} channels in 1983 by Akinori Noma, they obtained remarkable notoriety due to their implication in the insulin secretion process. Over the past decades huge progress has been made regarding the understanding of their function although many questions remain to be answered. During this thesis we pursued three main lines of investigation: (1) The dysfunction of K_{ATP} channel gating induces pathologies and it has been shown that many gain-of-function mutations in the human Kir6.2 gene directly impaired ATP sensitivity or increased the opening frequency of the gates causing severe neurological disorders. The number of gates in Kir channels is still under discussion. In order to address this we used site-directed mutagenesis together with Ion Channel-Coupled Receptors (ICCRs). ICCRs are artificial proteins created in our group that physically and functionally couple a GPCR to the N-terminus of Kir6.2. Using this method we functionally mapped the gates regulated by the N-terminus membrane protein. (2) K_{ATP} channels are found in many excitable tissues and have been implicated in diverse physiological processes. Due to their wide distribution and physiological functions, the remote control by light of K_{ATP} channels could be used to examine their role in diverse aspects of cellular electrophysiology, and potentially, to develop photopharmacological treatments. The primary objective of this work was the design of a light-gated K_{ATP} channel that will allow us to understand the consequences of forcing its closure or its opening *in vivo*. To accomplish this, we aim to modulate channel activity in both directions, downregulation and upregulation. (3) The only pathology associated primarily with SUR2 mutations is Cantù syndrome (CS). The CS mutations in the SUR2 subunit are believed to cause hyperactivity of K_{ATP} channels although not all mutations have been functionally characterized. The objective was to focus on SUR2 TMD0 mutations and correlate molecular observations and pathological consequences, while gaining insight in the function of the TMD0 in the control of Kir6.2 gating.

This thesis work involved three major families of proteins: ABC transporters, Kir channels and GPCRs. ABC transporters and Kir channels are described in detail in the introduction of this work. GPCRs are not reviewed extensively as they are used only as a tool to map the gates regulated by the Kir6.2 N-terminus.

INTRODUCTION

1. Potassium channels

The cellular membrane is a lipid bilayer that acts as an insulator that separates two environments that have different ionic compositions, the extracellular and the intracellular compartments (MacKinnon, 2004). Ions cannot permeate the lipidic membrane and they require a specific mechanism to be transported. In some cases, the ions go through hydrophilic pores termed ion channels. Ion channels are macromolecules that form pores in the cellular membrane and allows the passive flow of ions. The movement of ions which go through each channel can be measured as an electrical current which can cause fast changes in the membrane potential. Ion channels have three essential properties: they permeate ions, are selective, and their function is regulated by a process of opening and closing which, depending on the stimulus, allows or not ion conduction (MacKinnon, 2004). The cell membrane harbors several kinds of ion channels, each one with a selectivity for a specific ion, such as Na^+ , Ca^{2+} , Cl^- , or K^+ . Some channels however, allow the passage of more than one type of ion, for example ions that share a common negative charge (anions) or a common positive charge (cations). The activity of the whole set of ion channels contributes to the correct cellular behavior.

Potassium ion channels consist of a group of several proteins present in both excitable and non-excitable cells. Members of this family play critical roles in vital cellular signaling processes such as the release of neurotransmitters, heart function, insulin secretion, neuronal excitation, smooth muscle contraction and cellular volume regulation. In the last few years, our knowledge about their structure, function and regulation have advanced based on studies of their biophysical properties, subunit stoichiometry, interactions, regulation by second messengers and ligands (Shieh et al., 2000), and their structure by crystallography or other methods (MacKinnon, 2004; Whorton and MacKinnon, 2011).

Analysis of K^+ channel sequences, confirmed by structure determination, has shown that the selectivity of K^+ channels for potassium ions is associated with a conserved sequence motif TVGYG located in a re-entrant loop present between two transmembrane (TM) α -helices. This sequence motif, conserved across all K^+ channels, was proposed to correspond to the selectivity filter of the pore-forming region of the channel protein. Most K^+ channels are tetrameric and consequently four copies of the filter sequence motif come together to form the pore (Sansom et al., 2002).

There are several families of K^+ channels in animals, such as the voltage dependent K^+ channels (Kv) which are activated by a change in transmembrane voltage; the inward rectifier channels (Kir), which have a higher conductance for K^+ ions moving into the cell

than outwards and are often regulated by intracellular factors; and 2P channels that contain two copies of the selectivity filter motif in one polypeptide chain, two chains coming together to form the intact channel (Tamargo et al., 2004; Shieh et al., 2000).

1.a. The inward rectifying potassium channels (Kir)

Inwardly rectifying potassium channels (Kir, inward rectifiers) constitute a large family of voltage-independent K^+ channels. They have two main physiological functions: stabilizing the resting membrane potential near the K^+ equilibrium potential, and facilitating the transport of potassium through the membrane (Doupnik et al., 1995; Nichols and Lopatin, 1997).

Up to the present time, fifteen Kir channels have been recognized and categorized into seven subfamilies depending on their sequence homology and their properties such as the degree of rectification, unitary conductance and their sensitivity to different mediators. As shown in Figure 1, these subfamilies can be separated into four subgroups (Hibino et al. 2010):

- Classical Kir channels (Kir2.x).
- G protein-gated Kir channels (Kir3.x).
- ATP-sensitive K^+ channels (Kir6.x)
- K^+ transport channels (Kir1.x, Kir4.x, and Kir7.x).

Kir1 channels play an essential role in the kidney, where they are involved in transepithelial transport (Nichols and Lopatin, 1997). Kir2 channels are involved in the control of excitability of cardiac and cerebral tissues (Reimann and Ashcroft, 1999), and Kir3 channels are G protein-activated channels expressed in cardiac, neuronal and neurosecretory cells (Yamada et al., 1998). The Kir4 channels can exist as homomers or heteromers with Kir5 channels. They are expressed in glia, cochlea and kidney (Hibino et al., 2010).

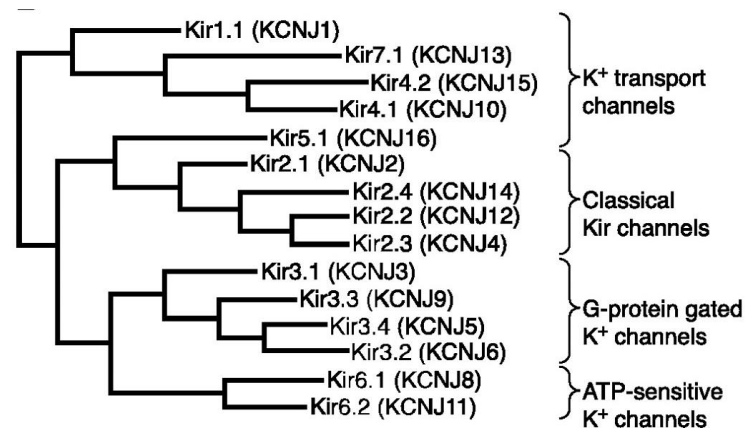


Figure 1. Kir channels phylogenetic tree. Phylogenetic analysis of the fifteen known subunits of human Kir channels. These subunits can be classified into four functional groups (Hibino et al., 2010).

1.a.1. Inward rectification

Inward rectification means that the passage of the ions is easier in the inward direction (into the cell) than in the outward direction (out of the cell). With identical, but opposite, driving forces, the Kir channels have a feeble outward current while the inward flow of potassium is stronger (Figure 2). This property arises from the voltage-dependent block by intracellular cations, such as polyamines and Mg^{2+} , that block at the cytoplasmic side of the pore the outward passage of K^+ ions without affecting inward movement (Bichet et al., 2003). Two residues on the internal face of the pore appear to be essential for the Mg^{2+} and polyamine block, one being located in transmembrane segment 2 (TM2), and the other in the C-terminus of the Kir channel (Yang et al., 1995; Lu and MacKinnon, 1994).

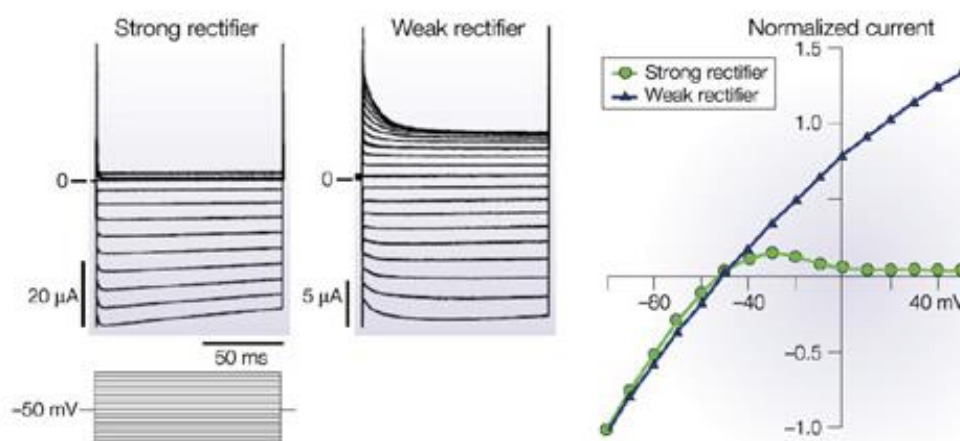


Figure 2. Inward rectification. **A.** TEVC recordings from *Xenopus oocytes* expressing strong and weak Kir channels. **B.** Associated current-voltage relations. The protocol of stimulation shown below the current traces consists of voltage steps of 10 mV increments from -140 mV to +50 mV from a holding potential of -50 mV. Oocytes were bathed in a physiological extracellular solution (Bichet et al., 2003).

Kir channels rectify to different degrees. For example, Kir2.1 and Kir3.1 are strong rectifiers, while Kir1.1 and Kir6.2 are weak rectifiers. This is due to the amino acid residues present in TM2. A neutral residue such as asparagine at position 171 in Kir1.1 channel causes a weak rectification, while a negative charge, such as aspartate at position 172 in Kir2.2, causes a strong rectification (Yang et al., 1995; Lu and MacKinnon, 1994). It has thus been shown that substitution of an asparagine to an aspartate in Kir1.1 converts this weak rectifier into a strong inward rectifier (Lu and MacKinnon, 1994). On the other hand, it has been suggested that polyamines bind to the C-terminal site, which in turn becomes more positively charged and acts as an inactivation domain that plugs the pore from its cytoplasmic side (Reimann and Ashcroft, 1999).

1.a.2. Kir channel structures

All the Kir channels are tetramers made of four identical or similar subunits to form a homomeric or heteromeric channel, respectively. The natural Kir1.x, Kir2.x and Kir6.x probably exists *in vivo* as homotetramers while Kir3.x channels have been shown to predominantly create heterotetramers, formed by the Kir3.2 and Kir3.4 subunits in brain, and the Kir3.1 and Kir3.4 subunits in heart (Krapivinsky et al., 1995; Kofuji et al., 1995).

The major breakthrough in ion channel studies was the atomic-resolution structure of the bacterial K⁺ channel (KcsA) from *Streptomyces lividans* (Doyle et al., 1998). Thanks to this crystal structure, it became possible for the first time to have access to the structural

INTRODUCTION

basis of K^+ selectivity and conductance, which at that time was only theorized from electrophysiological studies. The KcsA channel is a homotetramer formed by four identical subunits making an inverted tepee. Each subunit contains two transmembrane helices (TM1 and TM2), which are linked by a short stretch of approximately thirty amino acids, termed the extracellular loop. The selectivity filter contains the conserved signature of potassium channels (TVGYG). Additionally, as shown in Figure 3, the selectivity filter is structured to form a pile of oxygen rings, which are organized with such a precision that they match the dimensions for coordinating a dehydrated K^+ ion (Zhou et al., 2001; Doyle et al., 1998).

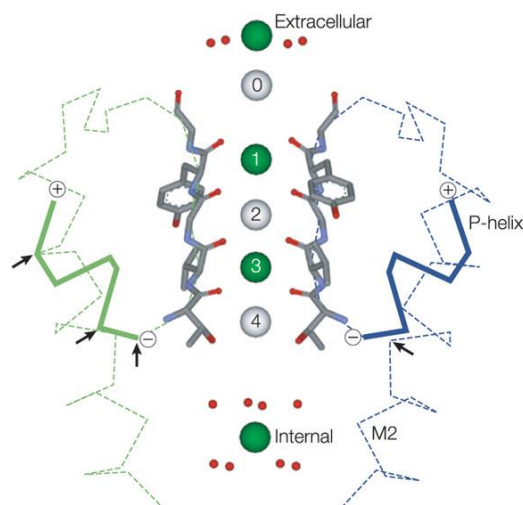


Figure 3. KcsA selectivity filter showing the linear array of K^+ binding sites. The TVGYG signature is shown in ball-and-stick representation. At the extracellular and internal ends of the filter, water molecules surround K^+ ions. As ions enter the filter, their hydration shell is progressively replaced by interactions with the backbone carbonyls of the selectivity filter (positions 0 to 4). The filter contains two ions simultaneously, either at positions 1 and 3 (green spheres), or at 2 and 4 (white spheres) (Bichet et al., 2003)

The first structure at a resolution of 3.2 Å was improved to 2 Å. This high-resolution view of the channel provided a deeper understanding of the potassium conduction. The new structure lets the viewer see K^+ ions actually traversing the pore, as the pictures catch the ions at the different phases of movement (Figure 4). This high-resolution structure provided the complete inner hydration shell of the ion inside the channel aqueous cavity that occurs at the intracellular side of the selectivity filter, midway through the membrane. Eight molecules of water are visible, with their oxygens packed against the K^+ ion. This geometry matches the arrangement of the K^+ -coordination oxygens in the selectivity filter (Zhou et al., 2001).

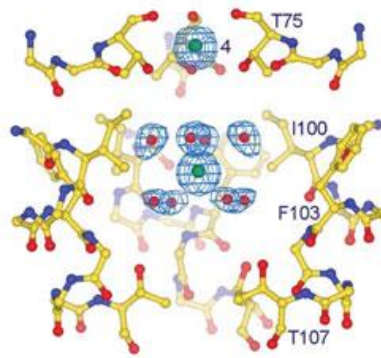


Figure 4. Eight water molecules (red spheres) surround a single K^+ ion (green sphere) in the cavity. Residues forming the cavity are shown in ball-and-stick representation. For clarity, only backbone atoms and the side chains facing the cavity (Thr 75, Ile 100, Phe 103, Gly 104 and Thr 107) are shown. The subunit closest to the viewer has been removed for clarity (Zhou et al., 2001).

An important advance in the field of Kir channels was the structure of the bacterial homolog, KirBac1.1 that showed a structural division into five regions. Interestingly, it has been found that the ion conduction pathway at the intracellular face of the membrane, termed the bundle crossing, contains a physical constriction created by the hydrophobic side chains of four phenylalanines, that has been proposed to form an 'activation' gate (bundle-crossing gate). Furthermore, sequence alignment of other Kir channels indicates that residues with large hydrophobic, aromatic or aliphatic, side chains are favored in this position (Kuo et al., 2003).

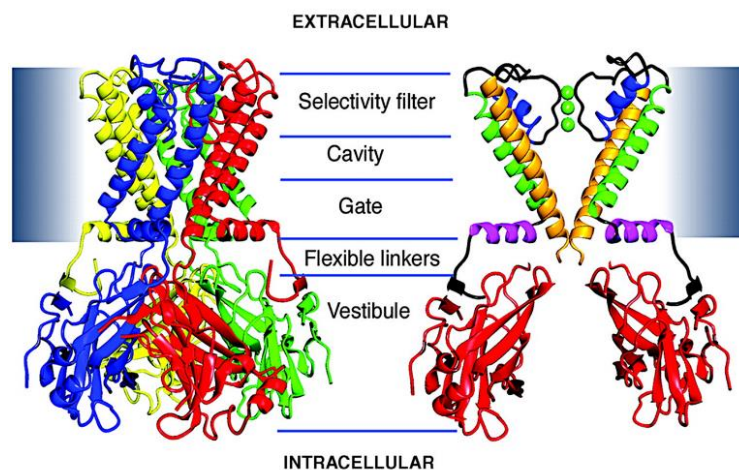


Figure 5. Overview of the KirBac1.1 structure. Five structural elements can be distinguished: the pore helix (blue), the inner helix (yellow), the outer helix (green), the slide helix (pink) and the C-terminal intracellular domain [(Kuo et al., 2003).

INTRODUCTION

Years later, a strong inward rectifier K⁺ channel was structurally characterized, the eukaryotic Kir2.2 channel, providing the basis of the rectification mechanism. However, in the Kir2.2 channel and other eukaryotic Kir channels, the selectivity filter sequence is TXG(Y/F)G(F/Y/G)R, which differs from the canonical signature TXGYGD_X, where X represent an aliphatic residue. Furthermore, there is a common feature in eukaryotic Kir channels, as shown in Figure 6, which is a pair of cysteine residues flanking the pore region. This serves to create a covalent link between the segment just before the pore region and the segment after the selectivity filter by the formation of a disulfide bridge which is essential for both folding and function of the channel (Tao et al. 2009).

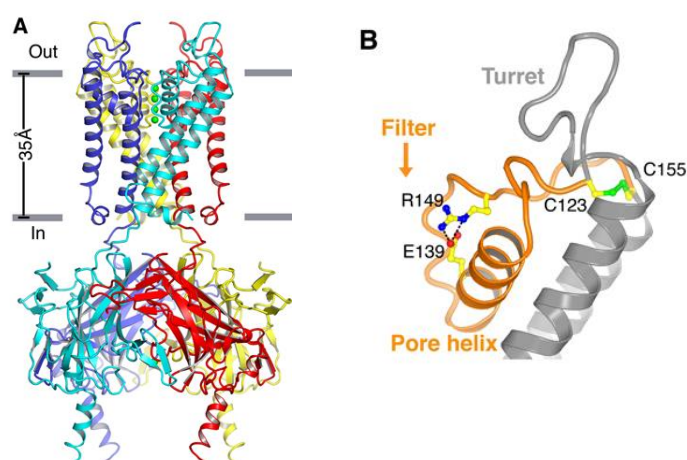


Figure 6. Structure of Kir2.2. **A.** Ribbon representation of the Kir2.2 tetramer side view. **B.** Close-up view of the pore region of a single subunit (in ribbon representation). Side chains of residues E139, R149 and a pair of disulfide-bonded cysteines (C123 and C155) are shown as sticks and colored according to atom type: carbon, yellow; nitrogen, blue; oxygen, red; and sulfur, green. The region flanked by the two disulfide-bonded cysteines is colored in orange (Tao et al., 2009).

Another structural characterization from a representative Kir channel was from the G protein-activated Kir3.2 channel (GIRK2). Despite that Kir2.2 and Kir3.2 are structurally similar, they have two different characteristics. In the Kir3.2 channel, the turrets surrounding the extracellular entry are arranged to create a more open vestibule for ion entry (Figure 7). This difference may explain the pharmacological differences between Kir3 and Kir2 channels, Kir3 channels being inhibited by some toxins such as tertiapin, while the classical inward rectifiers are not. This perhaps is due to the open turrets of Kir3 channels which allow the toxin to fit into the vestibule. The second difference concerns the edge between the transmembrane domain (TMD) and the cytoplasmic domain (CTD). In the Kir2.2 structure (obtained in absence of PIP₂), the TMD and CTD

INTRODUCTION

are distant compared to the corresponding domains of Kir3.2 channels which are tightly juxtaposed (Whorton and MacKinnon, 2011).

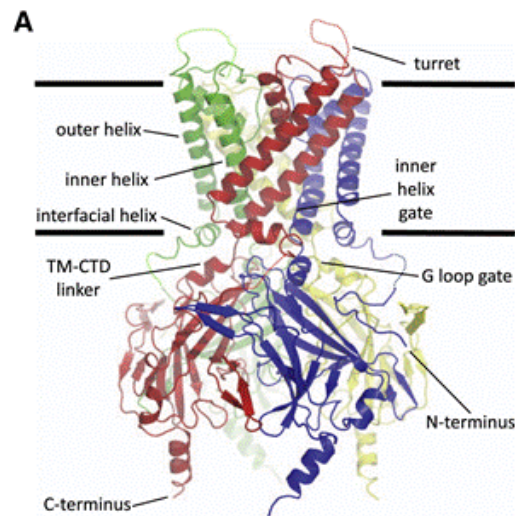


Figure 7. Cartoon diagram of Kir3.2 (GIRK2) structure. Each subunit of the tetramer is a different color. Unresolved segments of the turret and N-terminal linker are drawn in lighter colors. The TM and CT domains are closely juxtaposed thus bringing closer two potential gating regions of the channel (inner helix gate and G loop gate)(Whorton and MacKinnon, 2011).

The structures of the eukaryotic Kir2.2 and Kir3.2 channels expose the presence of two constrictions which perturb the ion conduction pathway and have been proposed to act as functional gates. As is shown in Figure 8, the first narrowing of the channel is located at the end of the inner transmembrane helix, and the second at the top of the cytoplasmic region of the G loop (Whorton and MacKinnon, 2011).

For the Kir2.2 channel, two residues present in the TM2 (I177 and M181 residues) form two hydrophobic seals which shrink the pore, closing it off at the cytoplasmic edge (Tao et al., 2009). The G loop gate is located at the apex of the CTD, just outside the membrane, below the level of the interfacial helix (Whorton and MacKinnon, 2011). Interestingly, in the PIP₂-free structure of Kir2.2 channel, the CTD is extended away from the TMD, so that both gates (from the inner helix and G loop) are positioned far away from each other. Nonetheless, in the structure of Kir2.2 obtained in the presence of a derivative of PIP₂ (with a short-chain), as well as in the structure of the Kir3.2 channel (GIRK2), both gates are closely associated, suggesting their possible cooperation (Niescierowicz, 2013).

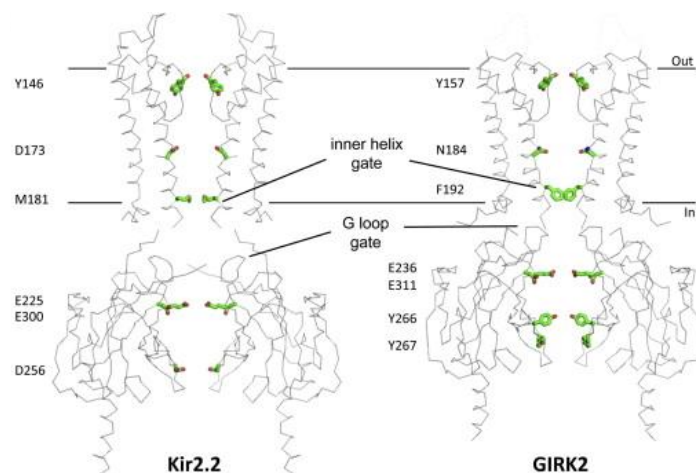


Figure 8. Comparison of the Kir2.2 and GIRK2 Structures. Key gating and rectification residues are highlighted in stick format (Whorton and MacKinnon, 2011).

2. ABC transporters

The passage of both inorganic and organic molecules through the cell membrane is crucial for the living organism. These molecules can be driven through the cell membrane by membrane transport proteins, which can be either passive or active. Passive transporters, also termed uniporters or facilitative transporters, transport substrates down a concentration gradient, while active transporters allow the movement of molecules against their concentration gradient. The active transport can be driven by both the free energy change associated with hydrolysis of adenosine triphosphate (ATP) and the potential energy of the chemical gradient of another molecule, termed as primary and secondary transport, respectively. The primary transporters include a large family of integral membrane proteins termed ATP-Binding Cassette (ABC) transporters (Wilkins, 2015; Vasiliou et al., 2009).

The human genome carries 48 ABC genes. ABC transporters play essential roles in many cellular processes, and many have been associated with severe diseases, such as cystic fibrosis, neonatal diabetes, and macular dystrophy. In addition, some ABC transporters are responsible for the multidrug resistance of bacteria and cancer cells (Wilkins, 2015; Vasiliou et al., 2009).

Biochemical and biophysical studies have provided a wealth of information on ABC protein function. Furthermore, structural data has advanced our knowledge on the transport mechanism and the relevant structure divergences. Today fourteen ABC transporters have been structurally characterized (Table 1) (Beek et al., 2014).

ABC transporters	Reference
BtuCD, Vitamin B ₁₂ transporter (<i>E. coli</i>)	(Locher et al., 2002)
Sav1886, multidrug transporter (<i>S. aureus</i>)	(Dawson and Locher, 2006)
ModB2C2, Molybdate transporter (<i>A. fulgidus</i>)	(Hollenstein et al., 2007)
HI1470/1, Metal-Chelate-type transporter, (<i>H. influenzae</i>)	(Pinkett et al., 2007)
MsbA, lipid 'flippase', (<i>S. typhimurium</i>)	(Ward et al., 2007)
MalFGK2, Maltose uptake transporter complex (<i>E. coli</i>)	(Oldham et al., 2007)
P-Glycoprotein, (<i>M. musculus</i>)	(Aller et al., 2009)
MetNI, Methionine uptake transporter complex (<i>E. coli</i>)	(Kadaba et al., 2008)
TM287-TM288, (<i>T. maritime</i>)	(Hohl et al., 2012)
HmuUV, heme transporter (<i>Y. pestis</i>)	(Woo et al., 2012)
ABCB10, Mitochondrial ABC transporter, (<i>H. sapiens</i>)	(Shintre et al., 2013)
Atm1-type, ABC exporter, (<i>N. aromaticivorans</i>)	(Lee et al., 2014)
Atm1, mitochondrial ABC transporter (<i>S. cerevisiae</i>)	(Srinivasan et al., 2014)
McjD, antimicrobial peptide transporter (<i>E. coli</i>)	(Choudhury et al., 2014)

Table 1. ABC transporters structurally characterized.

ABC transporters can be classified into importers and exporters. The importers are divided into three classes: Type I, Type II, and a third group termed the Energy-coupling factor (EFC) Type III which is functionally and structurally different from both Types I and II, as shown in Figure 9. Bacteria employ both importers and exporters while eukaryotes (with a few exceptions) only employ exporters (Beek et al., 2014).

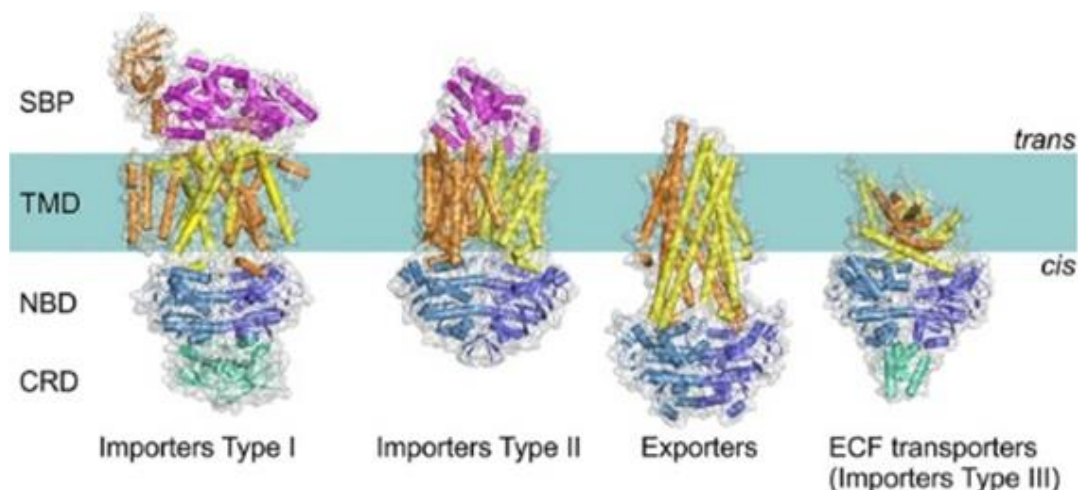


Figure 9. ABC transporters folds. All share a similar general architecture: two NBDs (blue and skyblue) are attached to two TMDs (orange and yellow). In some transporters, additional domains are present (green), which often have a regulatory function. In Type I and II importers, the transported compounds are delivered to TMDs by substrate-binding proteins (SBPs, magenta) located in the periplasm (Gram-negative bacteria) or external space (Gram-positive bacteria and Archaea) (Beek et al., 2014).

All ABC transporters have a fundamental architecture composed of two transmembrane domains (TMDs) and two nucleotide-binding domains (NBDs). The NBDs, which are highly conserved in the structure of all ABC transporters, are the hallmark of the ABC family, while the TMDs show a variable folding (Beek et al., 2014).

Nucleotide-binding domains

All ABC transporters possess two NBDs, which bind and hydrolyze ATP. The NBDs consist of two sub-domains: the larger RecA-like domain and the α -helical domain. The NBDs can be recognized at the sequence level by seven highly conserved motifs, as is shown in Figure 10:

- (1) The A-loop contains a conserved aromatic residue (usually a tyrosine) that helps position the ATP via stacking with the adenine ring.
- (2) The *Walker A* phosphate binding loop with a conserved lysine.
- (3) The *Walker B* motif, which helps the coordination of Mg^{2+} , possesses a conserved glutamate residue that works as base to polarize water.
- (4) The D-loop, important to maintain the geometry of the ATP hydrolysis site.
- (5) The H-loop, which assists the positioning of the water molecule, Mg^{2+} , and the general base.
- (6) The Q-loop, which has a conserved glutamine which allows the formation of an active site during ATP hydrolysis and is also in contact with the TMDs.

(7) The ABC signature motif (LSGGQ), an ABC protein hallmark.

Transmembrane domains

The TMDs have between six and ten α -helices, depending on the transporter class, which are arranged in such a way to form a pathway to allow substrate passage. The TMDs do not share much sequence similarity but have a similar folding which reflects the need to transport a wide range of molecules (Wilkins, 2015).

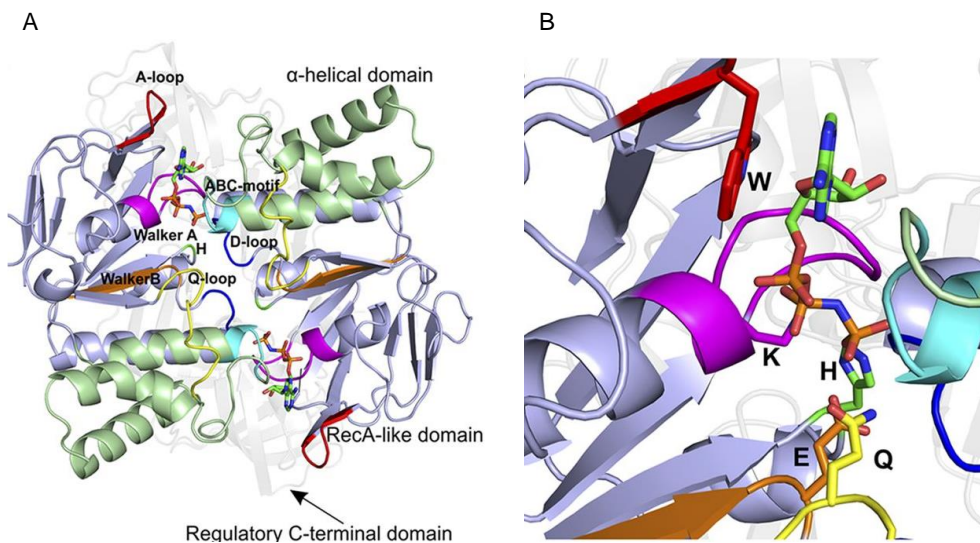


Figure 10. NBD structure (*MalK* dimer of the maltose transporter *MalEFGK2*). **A.** View along an axis perpendicular to the membrane plane from the trans-side onto the NBDs (The TMDs and SBP have been removed for clarity). Domains and highly conserved sequence motifs are color-coded: green, α -helical domain; light blue, RecA-like domain; faded gray, regulatory C-terminal domain; red, A-loop; magenta, Walker A; orange, Walker B; blue, D-loop; green, H-loop; cyan, ABC motif; yellow, Q-loop. The ATP analogue AMP-PNP is shown in sticks. **B.** A closer look onto the nucleotide-binding site. The key amino acids are indicated (see text for details) (Beek et al., 2014).

2.a. Transport mechanism

ABC transporters have an essential catalytic cycle which involves all the significant conformational changes needed to transport a substrate (Wilkins, 2015). This cycle is described in a series of four steps, as shown in Figure 11 for exporters (Linton, 2007):

(1) Substrate binding: The ligand binds to the TMDs in the high-affinity open NBD dimer conformation, which has a high affinity for ATP.

- (2) NBDs dimerization: ATP binding induces formation of the closed NBD dimer, which, in turn, induces a large conformational change in the TMDs sufficient to translocate ligand.
- (3) ATP hydrolysis: ATP hydrolysis initiates dissociation of the closed NBD dimer.
- (4) Nucleotide release: Phosphate (Pi) and adenosine diphosphate (ADP) are released to complete the transport cycle and restore the basal state.

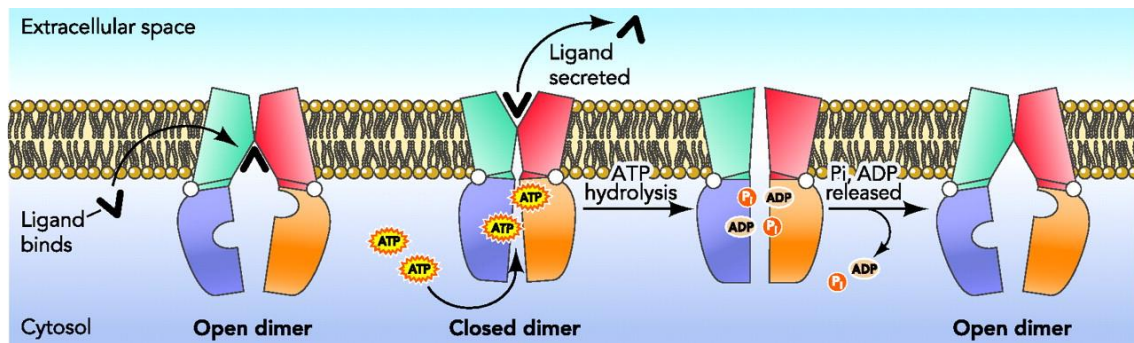


Figure 11. The catalytic cycle of ABC exporters (Linton, 2007)

3. ATP-sensitive potassium channels

3.a. K_{ATP} channel summary

The ATP-sensitive potassium channels (K_{ATP} channels) are formed by the unique interaction of two proteins: The sulfonylurea receptor (SUR, ~140-170 kDa) which belong to the ABC transporter family, and the inwardly-rectifying potassium channel Kir6 (~40 kDa). SUR and Kir6 are mandatory partners, and until now, there is no evidence that they are naturally able to function alone outside of the K_{ATP} channel complex. K_{ATP} channels are able to couple cellular metabolism to the variation of membrane potential because they are regulated by the intracellular ATP/ADP ratio. K_{ATP} channels are present in various tissues, such as heart, skeletal muscle, nervous system, and pancreatic β -cells. Their activity generates a certain cellular response depending on the K_{ATP} localization, such as insulin secretion in the pancreas and regulation of the duration of the action potential in cardiac ventricles.

In the vertebrate genome, the two genes KCNJ8 and KCNJ11 encode the Kir6.1 and Kir6.2 proteins, respectively. The two genes ABCC8 and ABCC9 encode the SUR1 and SUR2 proteins, respectively. The isoforms SUR2A and SUR2B are splice variants of the ABCC9 gene. Remarkably, the genes for Kir6.2 and SUR1 are located next to each other on human chromosome 11p15.1, while the Kir6.1 and SUR2 genes are on chromosome

INTRODUCTION

12p12.1. This suggests that gene expression regulation occurs already at the transcription level (Nichols et al., 2013).

As shown in Figure 12, the K_{ATP} channel is a hetero-octameric complex with a predicted mass of about 950 kDa. Four Kir6 subunits assemble to form the K^+ -selective pore, surrounded by four SUR subunits, which play a regulatory role. The hetero-octameric stoichiometry has been confirmed by both biochemical and electrophysiological studies (Inagaki et al., 1997; Clement et al., 1997), and is consistent with a low resolution (18 Å) three-dimensional structure of the full K_{ATP} channel complex (Mikhailov et al., 2005).

A retention signal (RXR) present on both subunits ensures that only the correctly-assembled channels can reach the plasma membrane. After assembly of the K_{ATP} channel complex, these motifs are masked so that the resultant complex is released from the reticulum endoplasmic (ER) (Zerangue et al., 1999). Tight subunit physical association has been confirmed by co-immunoprecipitation experiments (Lorenz and Terzic, 1999). Nevertheless, the removal of the Kir6.2 retention signal by deletion of its last 36 amino acids permits the formation of a functional Kir6.2 channel in absence of the SUR subunit (Tucker et al., 1997).

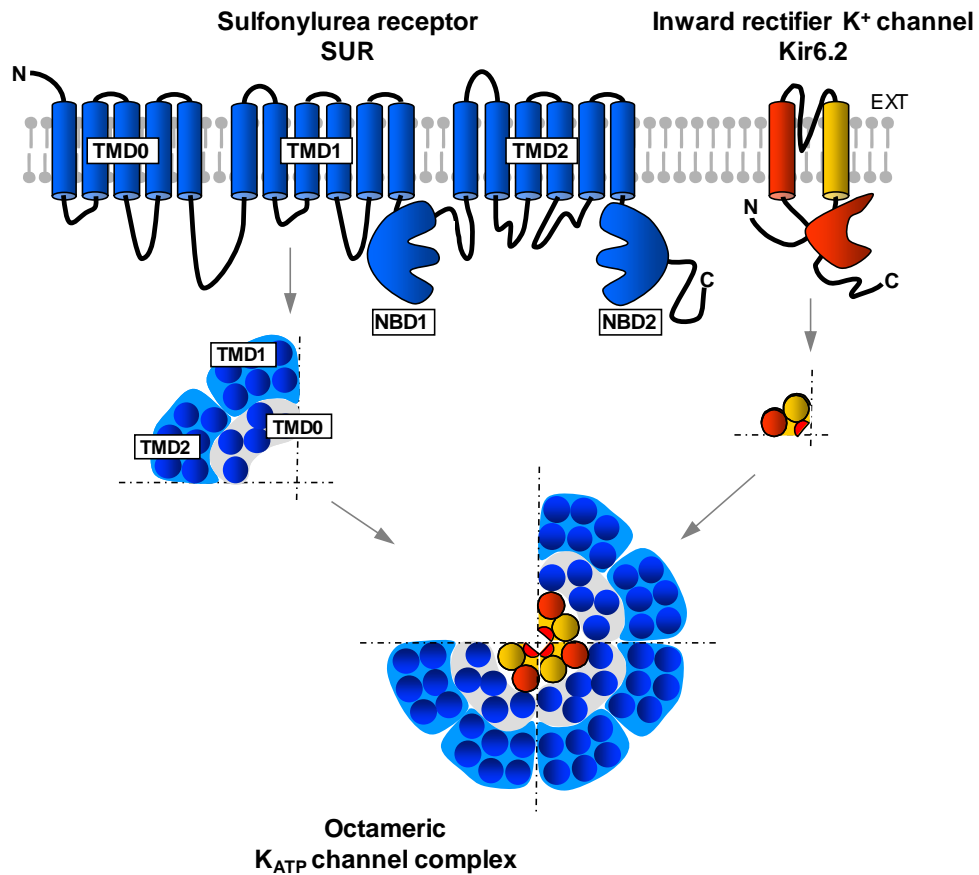


Figure 12. Topology and stoichiometry of the K_{ATP} channel. Four subunits of the inwardly rectifying Kir6.2 channel associate with four subunits of the sulfonylurea receptor forming a functional K_{ATP} channel. Kir6.2 has two transmembrane helices (TM1 and TM2) and a large cytoplasmic domain containing an ATP-binding site. The SUR subunit is composed of three transmembrane domains (TMD0, TMD1 and TMD2) and two nucleotide-binding domains (NBD1 and NBD2) enclosing the Walker A, Walker B and Linker L consensus sequences (Moreau et al. 2005).

3.b. The sulfonylurea receptor

The sulfonylurea receptors (SUR) belong to the ABCC subfamily of ABC transporters, subfamily which also includes MRP1 (multi-drug resistance protein 1), CFTR (cystic fibrosis transmembrane conductance regulator) and YCF1 (yeast cadmium factor 1). Even though these proteins are in the same phylogenetic branch, they differ in terms of function. MRP1 is a multidrug exporter of glutathione conjugates which uses ATP hydrolysis to transport substrates (Cole, 2014). CFTR which is implicated in cystic fibrosis is an ion channel gated by ATP hydrolysis (Vergani et al., 2005), and SUR is a channel regulator which has no identified transport function.

3.b.1. Isoforms and localization

Three isoforms are present in humans: SUR1, SUR2A and SUR2B. SUR1 (1581 amino acids) is mainly expressed in the pancreas associated with Kir6.2, but it has also been found in the brain associated with both Kir6.1 and Kir6.2 isoforms. The SUR2A isoform contains 1549 amino acids and is mostly expressed in heart and skeletal muscle, and in low levels in the brain, ovaries and pancreatic Langerhans islets. The SUR2B isoform contains 1591 amino acids and is mainly expressed in smooth muscle and certain neurons (Aguilar-Bryan et al., 1995; Inagaki et al., 1995; Karschin et al., 1997; Isomoto et al., 1996).

3.b.2. Structural organization

The atomic structure of SUR is unknown, however sequence alignment with other members of the ABC transporters family, whose structures have already been solved, confirms the presence of some common features. As shown in Figure 12, SUR has an N-terminus and a C-terminus that are exposed to the extracellular and intracellular sides, respectively. The hydrophobic profile of the SUR sequence suggests the presence of three transmembrane domains (TMDs) designated TMD0, TMD1 and TMD2, containing five, six and six hydrophobic transmembrane α -helices, respectively (Tusnády et al., 2006). These TMDs are connected by a long loop (L0) and two hydrophilic domains, the nucleotide binding domains NBD1 and NBD2.

TMD1 and TMD2 are common to most eukaryotic ABC proteins, while TMD0 is found only in a few members of the ABC family such as MRP1-3 and YFCF1 (yeast cadmium factor) and is connected to TMD1 through the long cytoplasmic loop (L0). TMD0 is considered as an “additional domain” among ABC transporters and its function is not completely understood. The TMD0s from different ABC proteins show different amino acid sequences, suggesting a variability in its function. In the SUR protein, TMD0 is crucial for the proper addressing of the K_{ATP} channel to the plasma membrane and it has

a critical role in Kir6.2 gating modulation (Chan et al., 2003; Fang et al., 2006). TMD0 cannot abolish the retention of the full-length Kir6 channels (containing the RKR retention signal) but it boosts the expression of Kir6 channels deleted of the retention signal. When Kir6.2 tetramers are forced to the cell surface by deleting the retention signal (RKR motif), they show a low maximum open probability ($P_{O(max)}$) in ligand-free solution. TMD0 alone is able to increase the duration of the opening bursts of the Kir6.2 tetramer, raising its $P_{O(max)}$ by 4-fold, thus suggesting that transmembrane interactions are able to force channel opening (Babenko and Bryan, 2003).

Domains NBD1 and NBD2, which contain standard ATP-binding cassettes, are cytoplasmic. The role of the NBDs appears to be primarily to sense the intracellular levels of ADP, enabling the SUR subunit to confer ADP activation to Kir6.

3.c. Kir6 channels

The Kir6 channels share the same topology as other inward-rectifying potassium channels. They are formed by two transmembrane helices, TM1 and TM2, which are linked by the pore-forming hairpin loop (H5 or P Loop) that carries the canonical signature of potassium channels (although the usual GYG is GFG in Kir6). In addition, they feature a short N-terminal and a large C-terminal cytoplasmic domains (Antcliff et al., 2005). The Kir6.1 channels are mainly expressed in smooth muscle cells (Suzuki et al., 2001; Inagaki et al., 1995). The Kir6.2 channels are highly expressed in the α (glucagon-secreting), β (insulin-secreting), and γ (somatostatin-secreting) cells of pancreatic islets (Karschin et al., 1997). They are also expressed at a lower level in heart, skeletal muscle and brain (Suzuki et al., 1997).

The K_{ATP} core conduction pathway is made by assembly of four Kir6 subunits that arrange to form a central pore that permits the flow of K^+ . The tetrameric Kir6 channel can result from the association of Kir6.1 and Kir6.2 proteins only (homotetramers), or from the association of Kir6.1 and Kir6.2 channels (heterotetramers) (Akrouh et al., 2009). A unique feature of Kir6 channels among Kir channels is that these channels harbor an inhibitory binding site for nucleotides which has a high affinity for ATP and a lesser for ADP and AMP.

3.d. SUR/Kir6 assembly and functional coupling

3.d.1. SUR/Kir6 association

The assembly process at the molecular level of the K_{ATP} channel is poorly understood, as there is no high-resolution structure of any K_{ATP} channel. Nevertheless, there is evidence which suggests that the interaction between monomeric forms of the two subunits (Kir6 and SUR) takes place initially in the endoplasmic reticulum (ER) until their association allows their release. The retention signal RKR sequence present in both proteins (located in SUR1 between helix 11 and NBD1, and in Kir6.2 at the C-terminal tail) are recognized by the coat protein complex I (COPI). COPI prevents trafficking to the cell surface when the two partners are separate. However, when SUR and Kir6 start to associate, the retention signal motif on Kir6.2 is masked by the presence of SUR, preventing COPI binding. At this point, only the retention signal from the SUR subunit is exposed, which is deactivated by the binding of the 14-3-3 protein to this region. Another alternative could be that 14-3-3 recruitment to a binding site near the distal tail of Kir6.2 causes a conformational change in SUR that causes deactivation the SUR retention signal (Heusser et al., 2006).

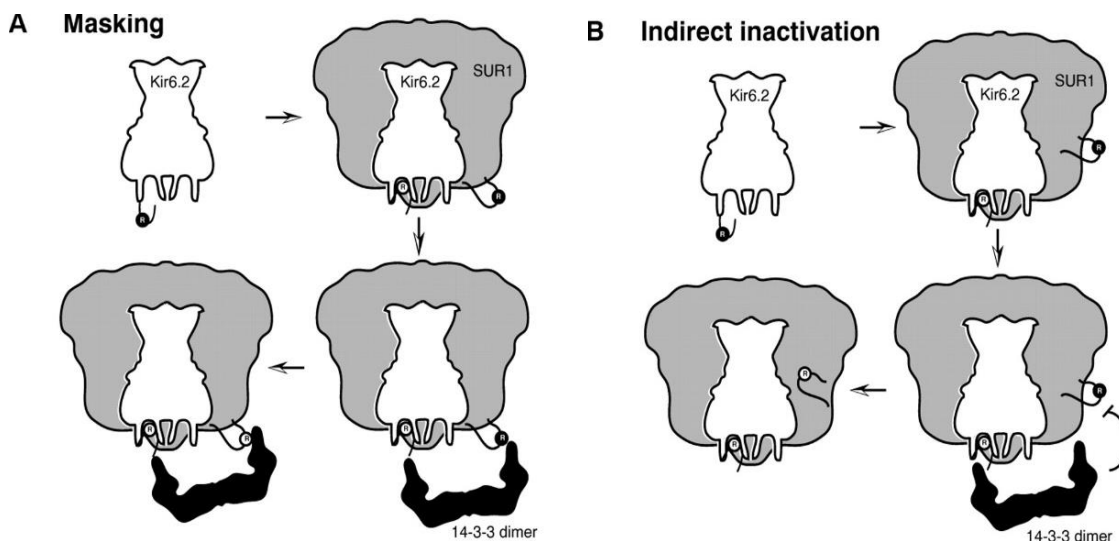


Figure 13. Retention signal (deactivation model). The 14-3-3-binding sites other than the one provided by the distal tail of Kir6.2 remain unknown, the position of the 14-3-3 dimer is hypothetical. Filled circles with white Rs represent active RKR signals, open circles symbolize inactivation of the signal. **A.** The signal of SUR1 could be inactivated by direct binding of 14-3-3 to this region of the protein (masking) or **B.** be indirectly inactivated by 14-3-3 recruitment to a binding site in the vicinity of the distal tail of Kir6.2 (Heusser et al., 2006).

Remarkably, the deletion of the last 26 or 36 amino acids from the Kir6.2 C-terminus (where is the retention signal), yielding Kir6.2 Δ C26 or Kir6.2 Δ C36, respectively, allows

INTRODUCTION

the channel to traffick to the plasma membrane even in absence of the SUR subunit (Tucker et al., 1997).

In the K_{ATP} channel, the Kir6 and SUR subunits have a physical interaction which takes place at different levels with several regions having been proposed as essential for the association of those subunits. The TMD0 has been shown to have a strong interaction with the Kir6 subunit and control K_{ATP} channel gating. Additionally, it has been shown that K_{ATP} channels which lack this domain are not able to traffic to the plasma membrane (Fang et al., 2006). Mutations in TMD0 have been associated to diseases such as Persistent Hyperinsulinemic Hypoglycemia of Infancy (PHHI) (Aguilar-Bryan and Bryan, 1999), and Cantù Syndrome (CS) (van Bon et al., 2012). Today, the molecular pathway involved in CS is still unknown, while the PHHI onset appears to be directly due to the abolition of SUR1/Kir6.2 association, as observed with the A116P and V187D mutations in TMD0 (Aguilar-Bryan and Bryan, 1999).

It has been demonstrated that TMD0 enhances the expression of Kir6.2 Δ C26. Nevertheless, TMD0 is not able to mask the retention signal of non-deleted Kir6. This suggests that interaction with SUR is necessary in another region in order to mask the retention signal in the C-terminal of Kir6, thus indicating that there are other regions than TMD0 involved in the physical interaction between Kir6 and SUR (Chan et al., 2003). Indeed, there is evidence that different regions of SUR interact with Kir6, causing a change in Kir6 sensitivity to inhibition by ATP. Previous studies demonstrated that SUR increases the ATP sensitivity of the K_{ATP} channel while TMD0 does not, as shown in Figure 14. The half maximal inhibitory concentration (IC_{50}) for ATP inhibition of Kir6.2 Δ C26 is approximately 100 μ M while the Kir6.2 Δ C26 expressed with the TMD0 shows an increase in the IC_{50} resulting in a value of approximately 300 μ M. Moreover, the IC_{50} value for the Kir6.2 Δ C26 co-expressed with SUR1 is approximately 15 μ M. These results can be explained by differences in the open probability of the channel (P_o), as single-channel recordings of Kir6.2 Δ C26 expressed with TMD0 and Kir6.2 Δ C26 expressed with SUR1 demonstrated a similar P_o of ~ 0.6 , much higher than the P_o of ~ 0.15 observed for Kir6.2 Δ C26 expressed alone (Figure 15). This increased P_o is mainly due to dramatic changes in the duration of opening bursts (~ 2 ms for Kir6.2 Δ C26 alone vs. ~ 60 ms for Kir6.2 Δ C26+SUR1 and Kir6.2 Δ C26+TMD0). The differences in ATP sensitivity may be intrinsically due to the difference in P_o values, meaning that the lower ATP sensitivity of the Kir6.2 Δ C26+TMD0 compared to Kir6.2 Δ C26 correlates with the higher P_o conferred by TMD0. However, this hypothesis does not fit with the behavior of Kir6.2 Δ C26+SUR1 channels which have a higher P_o but a lower IC_{50} compared to

INTRODUCTION

Kir6.2 Δ C26 alone. ATP IC_{50} might be related to P_o but it is also affected by regions of SUR outside TMD0 (Chan et al., 2003).

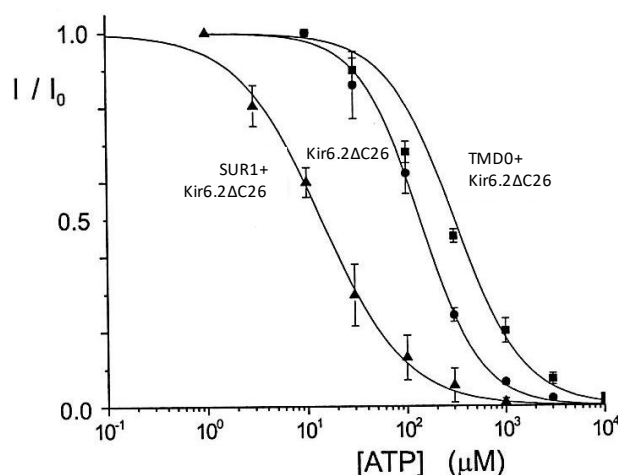


Figure 14. Dose–response curves for ATP inhibition. The IC_{50} values (μM) for Kir6.2 Δ C26, TMD0+Kir6.2 Δ C26 and SUR1+Kir6.2 Δ C26 channels are 138 ± 57 ($n = 3$), 309 ± 14 ($n = 9$) and 14 ± 1 ($n = 2$), respectively. Their Hill coefficients are 1.5 ± 0.1 , 1.3 ± 0.03 and 1.05 ± 0.08 , respectively (Chan et al., 2003).



Figure 15. Kir6.2 Δ C26/TMD0 and Kir6.2 Δ C26/SUR1 channels have similar single-channel properties under nucleotide-free conditions. Single-channel recordings of Kir6.2 Δ C26, TMD0/6.2 Δ C26 and Kir6.2 Δ C26/SUR1 channels.. Single channels were recorded at -80 mV from inside-out patches with 96 mM K^+ on both sides (Chan et al., 2003).

It has been shown that the cytoplasmic segment linking the TMD2 with NBD2 of SUR2A (between residues 1295 and 1358) also have an essential interaction with Kir6.2. Co-precipitation with Kir6.2 demonstrated that this fragment competes with the full-length SUR for binding to Kir6.2 (Rainbow et al., 2004). The specificity of this interaction

between the fragment and the Kir channel was confirmed by trials performed with Kir2.1 channel, which does not associate with SUR to make functional channels.

Another suggested region of interaction includes residues 196-288 of SUR1 and residues 28-32 of Kir6.2. Experiments by co-immunoprecipitation in *Xenopus* oocytes co-expressing Kir6.2 full-length or Kir6.2 with a deletion in the N-terminal (Δ 28-32) and segment 196-288 residues of SUR1, demonstrated that interaction between SUR1(196-288) and Kir6.2 Δ 28-32 is considerably reduced. These results uphold the idea that residues 196-288 of SUR1 are crucial for the binding interaction between SUR1 and the N-terminal of Kir6.2, and this interaction is disturbed by removal of residues 28-32 of Kir6.2 (Craig et al., 2009).

In addition, several studies suggest that both the N-terminus and the C-terminus, plus the transmembrane helix 1 (TM1) are the main regions of Kir6.2 implicated in the physical interaction with the SUR subunit (Schwappach et al., 2000; Tammaro and Ashcroft, 2007; Lodwick et al., 2014).

3.d.2. SUR/Kir6 functional coupling

In addition to the physical interactions between the Kir6 and SUR subunits of the K_{ATP} channel, there is the question of how these subunits communicate to modulate the ion flow in the Kir6 subunit. Only a few regions have been proposed to be involved in the ligand-induced functional coupling between SUR and Kir6. One of these regions is a domain rich in aspartate and glutamate (ED), which has been proposed to act as an allosteric transducer securing functional communication between the Kir6.2 and SUR2A subunits of the cardiac K_{ATP} channel (Karger et al., 2008). The ED contains a stretch of fifteen negatively charged, aspartate and glutamate residues, located in the cytoplasmic loop 6 (LC6) downstream of NBD1, between TMD1 and TMD2. The ED region is positioned far from the known SUR binding sites for openers and blockers of the K_{ATP} channel and essentially contributes in the cooperative interaction between the NBDs that is critical for the conformational arrangement of Mg-ADP induced K_{ATP} channel activation. While ATP inhibition of the wild-type K_{ATP} channel is readily reversed by equivalent concentrations of Mg-ADP, the ED mutants SUR2A/Kir6.2 are incapable to reverse that inhibition. Moreover, it is not known if there are any physical interactions between ED with the Kir6.2, but ED is a crucial part of the allosteric machinery that controls NBDs action and signal transduction to Kir6.2 channel.

Another region in the SUR2A receptor implicated in the communication between the K_{ATP} subunits is the region near the C-terminus, particularly three residues located at this level (E1350, I1310 and L1313) which are crucial in transmitting activation messages from

SUR2A to the Kir6.2 pore-forming subunit. Mutation of these residues results in a drastic reduction of channel activation by Mg-ADP and pharmacological openers mediated by SUR2A (Dupuis et al., 2008). Similar results have shown that mutations in the corresponding SUR1 residues (Q1342, I1347 and L1350) to alanines unexpectedly, in the context of SUR1 and SUR2A, had the opposite impact in the SUR-mediated regulation of Kir6.2 channel. This suggests subtle differences in the molecular mechanism occurring in the two isoforms (Principalli et al., 2015).

Remarkably, the mutations in the three residues of SUR only affect the activation network, but do not affect the inhibitory pathway of the K_{ATP} channel. All these results strongly suggest different transduction pathways between the SUR and Kir6 subunits of the K_{ATP} channel.

4. K_{ATP} channel mechanism and regulation

The K_{ATP} channel is physiologically regulated by molecules that can target one or both subunits: Kir6 and SUR. This regulation is very complex and even with the large amount of functional data a lot remains to be clarified.

4.a. Physiological regulation of the K_{ATP} channel by SUR

Almost all the ABC proteins show transporter activity, but SUR does not. Its only identified function is the gating regulation of the Kir6 pore subunit of the K_{ATP} channel. Mg-ATP binding to the NBDs of SUR cause NBD dimerization and hydrolysis of Mg-ATP that lead to channel opening. Unlike real transporters, the rate of nucleotide hydrolysis by SUR remains very low (Bienengraeber et al., 2000).

The SUR subunit gives the K_{ATP} channel the ability to be activated by nucleotides when these are in complex with magnesium (Mg). SUR is also a target of drugs that can regulate both opening and blocking of the K_{ATP} channel.

4.a.1. Regulation by Mg-nucleotides, specifically Mg-ADP.

Activation by nucleotides require the presence of Mg^{2+} ions and intact NBDs (Gribble et al., 1997b). Previous studies on SUR1 demonstrated that the NBD1 strongly binds ATP rather than ADP, even in the absence of Mg^{2+} ions. Mg-ADP preferentially binds at the NBD2, and this binding can antagonize the Mg^{2+} -independent activity of ATP binding at the NBD1 (Ueda et al., 1997). Mg-ADP stimulates K_{ATP} channels with different affinities depending on the SUR isoform present. In particular, SUR1 and SUR2B are more stimulated than SUR2A. Experiments using chimera and mutant SURs suggested that the 42 amino acids at the C-terminal end of SURs (C42) play a critical role in the ADP-

mediated activation of K_{ATP} channels and that the C42 of SUR2A may reduce ADP-mediated channel activation at the NBD2 (Matsuoka et al., 2000).

Today it is still unclear how Mg-ADP activates the K_{ATP} channel. Nevertheless, it is well accepted that cooperative interaction between the NBDs is crucial for the modulation for Kir6 gating; although the path(s) of allosteric inter-subunit communication remain vague. The deletion of the fifteen negatively charged aspartate and glutamate residues (948-962) from the SUR2A isoform can block the NBDs cooperative interaction, and disturb the regulation of K_{ATP} channel by Mg-ADP. Moreover, three amino acids have been implicated in SUR2A and SUR1 in the transmission of the activation message: E1055, I1310, L1313, and Q1342, I1347, L1350 residues, respectively. When these residues are mutated SUR can no longer transmit the activation message to the channel (Dupuis et al., 2008; Principalli et al., 2015). It has been shown that other nucleotides that form a complex with Mg^{2+} ions can also stimulate the K_{ATP} channel via SUR, including Mg-GDP, Mg-GTP, Mg-UDP and Mg-UTP (Trapp et al., 1997).

4.a.2. Regulation by Zinc

Zinc ions (Zn^{2+}) are strong reversible activators of K_{ATP} channels. Zn^{2+} ions act extracellularly by binding to histidines on the extracellular side of SUR (H326 and H332 in SUR1) (Bancila et al., 2005). Furthermore, in both SUR1+Kir6.2 and SUR2A+kir6.2 channels, Zn^{2+} also caused activation when applied intracellularly (Prost et al., 2004).

4.a.3. Regulation by G-proteins

The activation of G-protein coupled receptors (GPCRs) triggers the release of the G_{α} and $G_{\beta\gamma}$ subunits of heterotrimeric G-proteins, which have been proposed to regulate the activity of K_{ATP} channels by direct binding to SUR. Reports on such regulation are scarce and the effects appear limited (Vivaudou et al., 2009)

4.b. Physiological regulation of the K_{ATP} channel by Kir6

4.b.1. Regulation by nucleotides

ATP strongly inhibits the K_{ATP} channel. Initially, SUR, which contains two NBDs, was proposed as the main inhibitory site of ATP binding (Aguilar-Bryan et al., 1995). However, the discovery that Kir6.2 truncated of 26 C-terminal residues (retention signal) can form a functional tetrameric channel present in the plasma membrane which can be strongly inhibited by ATP (Tucker et al., 1997) demonstrated that ATP inhibition results from binding to Kir6.2. The ATP binding site in Kir6.2 does not resemble any of the classical nucleotide binding sites, such as the NBDs of SUR, and ATP cannot be hydrolyzed by Kir6.2. Since the structure of Kir6.2 is still unknown, we can only rely on functional data to localize the ATP-binding site. To date, most of the data suggest that the ATP-binding site involves both N- and C-terminal domains (Tucker et al., 1998; Proks et al., 1999). As shown in Figure 16, a homology model and ligand docking application allowed to identify a putative ATP-binding site in Kir6.2. Based on this data and functional studies, there are four ATP-binding pockets which are located near the top of the intracellular domain (IC). Each binding pocket lies at the interface between N- and C-terminal domains of the same subunit with a little contribution by the C-terminal of the neighboring subunit (Antcliff et al., 2005).

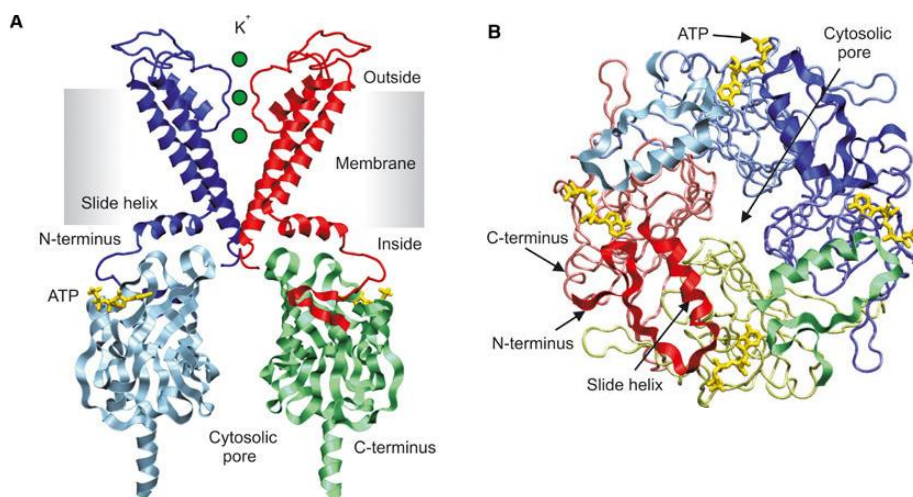


Figure 16. The postulated ATP-binding site of Kir6.2. **A.** Side view of a homology model of the Kir6.2 channel. For simplicity, the TMs of only two subunits and the IC domains of two separate subunits are illustrated. ATP is shown in yellow. **B.** Top view of the cytoplasmic part of the Kir6.2 tetrameric channel. The TMs were removed (residues 64–177). The N-terminal domain is shown in ribbon format and the C-terminal domain in backbone format. Different colors represent individual subunits (Antcliff et al. 2005).

When ATP binds to the Kir6.2 channel, its phosphate tail interacts with R201 and K185 residues at the C-terminal level of one chain, and with R50 at the N-terminal level of the neighboring chain. It has been suggested that the binding of one ATP molecule is enough to produce the conformational changes needed for the channel closure (Markworth et al., 2000). The ligand binding site in Kir6.2 is very selective for nucleotides with an adenine ring and the presence of at least three phosphates. The removal of those phosphates decreases the nucleotide binding affinity (Tucker et al., 1998; Markworth et al., 2000).

When Kir6.2 is expressed alone in its truncated form, the activity of the channel is half inhibited by approximately 100 μM ATP. Co-expression with the SUR subunit decreases this value to approximately 10 μM ATP by reshaping the ATP binding pocket (Dabrowski et al., 2004).

4.b.2. Regulation by lipids

As other Kir channels, Kir6 is well known to be dependent on phosphatidylinositol-4,5-bisphosphate (PIP_2). PIP_2 has a dual role in Kir6 modulation, it increases the channel open probability in absence of ATP, and it antagonizes the inhibitory effect of ATP by decreasing the channel apparent affinity of the channel for this molecule (Hilgemann and Ball, 1996; Fan and Makielski, 1997; Shyng and Nichols, 1998). The precise PIP_2 binding site of the Kir6.2 channel is unknown; however, mutagenic trials have shown that the PIP_2 effect is achieved by electrostatic interactions between the polar head and positively charged residues present in the N-terminal (K39, R54), transmembrane (K67) and C-terminal (R176, R177, R301) regions of Kir6.2 which interact with the polar head of PIP_2 , while the aliphatic chain would be anchored in the plasma membrane (Schulze et al., 2003; Cukras et al., 2002; Shyng et al., 2000; Fan and Makielski, 1997). Interestingly, the structure of the Kir2.2 channel in complex with a PIP_2 analogue suggests an explanation of the effect mediated by this lipid. As is shown in Figure 17, PIP_2 binds at the interface between TMD and CTD provoking a conformational change in the Kir2.2 channel that would stabilize the open conformation of the channel (Hansen et al., 2011).

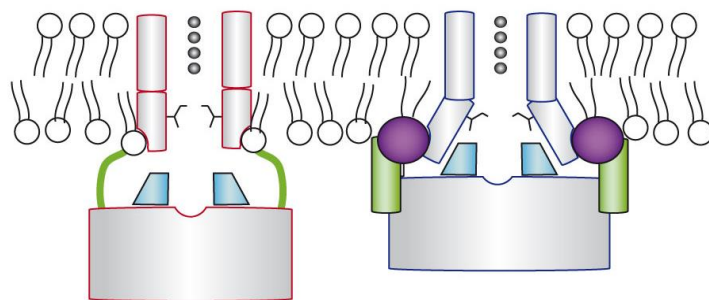


Figure 17. Suggested mechanism of Kir2.2 activation by PIP₂. PIP₂ (purple sphere) binds at an interface between the TMD (grey cylinder) and the CTD (grey rectangle) and induces a large conformational change. The flexible linker (green line) contracts (green cylinder), the CTD moves towards and becomes tethered to the TMD, the G loop (cyan wedge) inserts into the TMD and the inner helix activation gate opens (Hansen et al., 2011).

Other families of anionic lipids shown to regulate Kir6.2 channel activity, such as the long chain Co-Enzyme A esters (LC-CoA), act in a similar way as PIP₂. They decrease the Kir6.2 channel ATP affinity causing its activation (Gribble et al., 1998a). Cholesterol has also been suggested as a possible regulator of Kir6.2 channels but its action remains controversial, some studies proposing an activatory effect and others an inhibitory action (Matthews et al., 2001).

4.c. K_{ATP} channel physiology and physiopathology

The K_{ATP} channels can link the cellular metabolism to the electrical activity of the plasma membrane due to their ability to sense the ADP/ATP ratio inside the cells. At rest K_{ATP} activation causes membrane hyperpolarization while its inhibition generates membrane depolarization. Depending of the localization, variations in the membrane potential will provoke a different cellular response. The K_{ATP} channels are found in many excitable tissues (heart, brain, pancreatic islets and smooth muscle) (Noma, 1983; Ashford et al., 1988; Cook and Hales, 1984; Standen et al., 1989; Winquist et al., 1989) where they have been implicated in diverse physiological processes such as memory and the regulation of male reproductive behavior (Betourne et al., 2009; McDevitt et al., 2009). Mostly, the K_{ATP} channels have been extensively studied in glucose homeostasis and ischemic protection (Rorsman et al., 2008; Flagg et al., 2005; Koster et al., 2005).

4.c.1. K_{ATP} channels in the pancreas

The function of the K_{ATP} channels are best understood in pancreatic β cells, where their activity is connected to insulin secretion (Ashcroft et al., 1984). As shown in Figure 18, plasma glucose is transported into the pancreatic β -cell where it is metabolized to produce ATP. When the glucose level raises, internal ATP concentration increases,

4.c.2. K_{ATP} channels in the central nervous system

K_{ATP} channels are expressed in different regions of the brain, such as the GABAergic neurons which predominantly express the SUR1 and Kir6.2 isoforms, while dopaminergic neurons express SUR1/Kir6.2 and SUR2B/Kir6.2 complexes. Additionally, SUR1 and Kir6.1 isoforms have been found in the hypothalamus (Liss et al., 1999).

The role of the K_{ATP} channel in the brain has been studied by comparing the effects of hypoxia in wild-type and knock-out mice. In the event of hypoxia (caused by a lack of oxygen), neuronal activity decrease in wild-type mice, while in knock-out mice for the Kir6.2 genes, the activity increases (Yamada et al., 2001). Furthermore, these mice are susceptible to widespread attacks after a brief hypoxia. Results with wild-type mice suggest that the K_{ATP} channels can have a protective role against ischemia when, under metabolic stress, the channels start to become more active because of the reduced concentration of ATP. Additional trials demonstrated that transgenic mice overexpressing SUR1 in both hippocampus and cortex are more resistant to ischemic attacks after exposure to kainic acid. This molecule is a potent neuroexcitatory amino acid that acts by activating receptors for glutamate. It is used to study the effects of neurons ablation in animal models because it produces neuronal death if injected in large amounts. The results suggest a protective effect via SUR1 subunit (Hernández-Sánchez et al., 2001).

4.c.3. Muscle K_{ATP} channels

K_{ATP} channels are expressed in the heart, skeletal muscle and smooth muscle. In these tissues, as opposed to the pancreas, under normal metabolic conditions, K_{ATP} channels are predominantly closed, and they do not significantly contribute to cell excitability. Nevertheless, these channels can open when exposed to a severe metabolic stress such as anoxia, metabolic inhibition or ischemia. Recently, it has been found that mutations in the SUR2 gene are associated with a rare condition termed Cantù Syndrome (CS). Most of the cases of CS reported cardiomegaly due to increased myocardial mass (hypertrophy) with larger cardiac chambers but with normal systolic function (Nichols et al., 2013). In the present work, we have characterized two SUR2 mutations associated with CS.

K_{ATP} channels has been implicated in ischemic tolerance in myocardial cells as in the central neurons system. Through ischemic stress, the concentration of ATP in the cells declines, causing K_{ATP} channel opening, and increasing the K⁺ permeability of the membrane. This favors hyperpolarization and decreases excitability. The change in membrane potential decreases Ca²⁺ influx, shortens action potential duration and reduce

contraction. Previous experiments in Kir6.2 knock-out animals have demonstrated this protective effect (Gumina et al., 2006). Mutations of K_{ATP} channels in the NBD2 of SUR2A, are connected with cardiomyopathy, ventricular arrhythmia and atrial fibrillation.

4.d. K_{ATP} channel pharmacology

K_{ATP} channels are the target of several drugs that can act as potassium channel blockers, which inhibit activity, or as potassium channel openers (KCO), which cause activation of the channels.

4.d.1. K_{ATP} channel inhibitors

K_{ATP} channel inhibitors can be classified in two groups: those that target Kir6.2 (imidazolines) (Mukai et al., 1998), and those targeting SUR (sulfonylureas and benzamido derivatives) (Ashcroft and Gribble, 1999). The sulfonylureas can also interact with the Kir6.2 subunit but with a lower affinity (Gribble et al., 1997a). All these compounds can cause conformational reorganization of the K_{ATP} channel that result in channel closure, and subsequent membrane depolarization. These inhibitors can stimulate insulin secretion, and are used to treat patients with type II diabetes. The hypoglycemic properties of sulfonylureas have long been known, before the identification of the blocking effect on K_{ATP} channels (Sturgess et al., 1985). The sulfonylureas made it possible to clone the SUR1 gene (Aguilar-Bryan et al., 1995).

As shown in Table 2, the SUR isoforms have different levels of affinity for hypoglycemic drugs (Vila-Carriles et al., 2007).

	Tolbutamide	Glibenclamide	Meglitinide
Kir6.2	1.7 mM	40 μ M	> 1 mM
SUR1-Kir6.2	5 μ M	8 nM	0.7 μ M
SUR2A-Kir6.2	1 mM	0.04 μ M	0.3 μ M

Table 2. IC_{50} of K_{ATP} channel blockers (adapted from Vivaudou et al. 2009).

Thanks to this difference in affinities, sulfonylureas can be used to target specific K_{ATP} channels. Tolbutamide at micromolar concentration only targets SUR1 channels, while glibenclamide and meglitinide block both SUR1 and SUR2A channels (Proks et al., 2002).

The affinity difference of SUR1+Kir6.2 and SUR2+Kir6.2 for tolbutamide was used to localize its binding sites in the SUR subunit using a chimeric approach. These experiments identified a first binding site for blocker in SUR1 located in the cytoplasmic

loop linking 15 and 16 helices with residue S1237 being essential. In SUR2, the amino acid equivalent to S1237 in SUR1 is a tyrosine that interferes with the tolbutamide-mediated effect (Ashfield et al., 1999). Using glibenclamide, a second binding site was defined that includes the loop L0 that connects TMD0 to TMD1, and perhaps the Kir6.2 N-terminal region (Mikhailov et al., 2001). This binding site is preserved in both SUR1 and SUR2 receptors.

Considering the chemical structures of the inhibitors (Figure 19), two blocker interaction sites would exist on SUR, site A for the sulfonylurea group and site B for the benzoamido group. Both sites are present on SUR1 while SUR2 has only the A site. This would explain the differential affinities for sulfonylureas of SUR1 and SUR2A isoforms. Indeed, glibenclamide, which possesses both the sulfonylurea group and the benzoamido group, would bind tightly to SUR1 but would not properly bind to SUR2, inducing a lower effect.

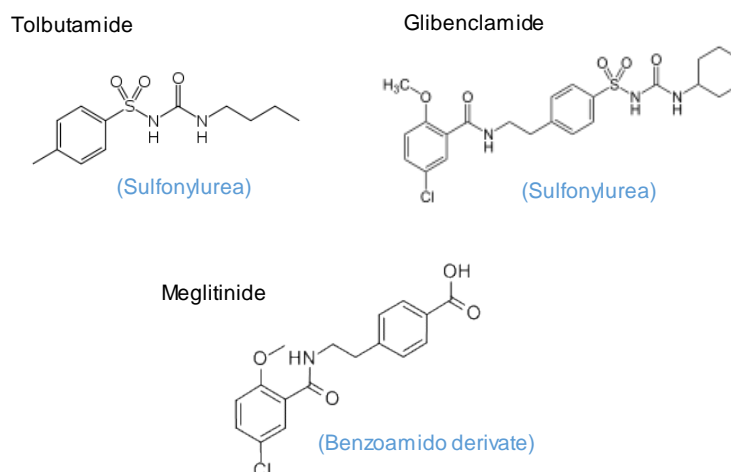


Figure 19. Chemical structures of K_{ATP} channel inhibitors (Principalli, 2015).

Since all inhibitors shown have a superior affinity for SUR1 than for SUR2 isoform, a sulfonylurea termed as HMR1833 was synthesized, which can target the cardiac K_{ATP} channels with a higher affinity for the SUR2 isoform than for the SUR1 (Russ et al., 2001).

Additionally, another K_{ATP} channel blocker was synthesized in order to differentiate between Kir6 isoforms, guanidine U-37883A (imidazoline class). Although its action in fact depends on the SUR isoform present in K_{ATP} channels, it selectively inhibits Kir6.1 isoforms channels like the vascular SUR2B+Kir6.1 channels (Teramoto, 2006).

4.d.2. K_{ATP} channel openers

K_{ATP} channel openers (KCO) make up a large family of molecules that induce the opening of the channel and, consequently, can cause membrane hyperpolarization. Those

INTRODUCTION

molecules are classified depending of their chemical structure (Figure 20), such as the benzothiadiazines (diazoxide), benzopyrans (cromakalim), cyanoguanidines (pinacidil), and nicotinamides (nicorandil).

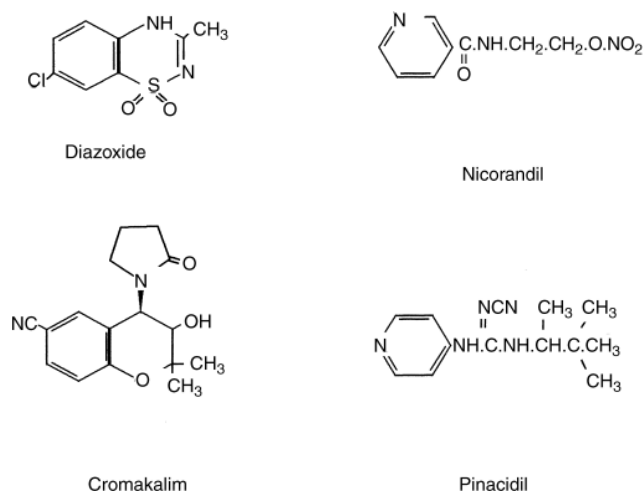


Figure 20. Structures of representative *K*_{ATP} channel openers (Principalli, 2015)

KCOs act through the SUR subunit, and, as shown in Table 3, have different affinities for the K_{ATP} channel, depending on the SUR isoform. Most KCOs have a higher affinity for SUR2A and SUR2B isoforms, although diazoxide has an effect mainly on the SUR1 isoform (Moreau et al., 2005a).

	diazoxide	nicorandil	pinacidil	Cromakalim
SUR1-Kir6.2	30 μ M	unknown	1 mM	> 1 mM
SUR2A-Kir6.2	> 1 mM (100 μ M)	1 mM (100 μ M)	10 μ M	10 μ M

Table 3. Concentrations of *K*_{ATP} channels openers causing half-maximal activation. Values recorded in presence of Mg-ATP and Mg-ADP are reported in parenthesis (adapted from Vivaudou, Moreau and Terzic, 2009).

It has been shown that two residues, L1249 and T1253, located in helix 17 of SUR2A receptor, are implicated in the binding of non-diazoxide openers. Experiments demonstrated that, when these residues are mutated, SUR2A loses the capacity to be regulated by openers (Moreau et al., 2005b). Furthermore, another study has shown the importance of the loop region connecting helix 13 to 14 (Uhde et al., 1999). These two

INTRODUCTION

studies highlight the essential role of the TMD2 domain in the selective binding of KCOs to the SUR2 isoform.

The diazoxide binding site has not been exactly located and the existing data is contradictory, although it seems that the TMD1 domain has a main role in diazoxide binding (Babenko et al., 2000). The activity of KCOs is connected with the presence of Mg-ATP and Mg-ADP. For example, diazoxide, that acts specifically on SUR1, can bind to SUR2 in the presence of Mg-ADP (D'hahan et al., 1999). In addition, it has been observed that KCO binding is positively modulated by Mg-ATP through the NBDs (Schwanstecher et al., 1998).

In this thesis work, the SUR2A opener used is P1075, an analogue of pinacidil.

5. Ion Channel-Coupled Receptors

5.a. Principle of the ICCR concept

The ICCR inspiration comes from the natural intermolecular regulation occurring in K_{ATP} channels. It was hypothesized that the SUR subunit could be swapped with any receptor able to communicate conformational changes produced by ligand binding to the receptor to Kir6.2 gates. The ligand-induced change in current can be easily detected by classical electrophysiological techniques, as shown in Figure 21. The current amplitude produced by the potassium flow through Kir6.2 channel depends on ligand concentration, thus allowing the estimation of apparent affinities by dose-response measurements (Moreau et al., 2008).

Since the G-protein coupled receptors (GPCR) represent the largest family of receptors, and have a huge relevance as drug targets (GPCR overview see section 5.d.4), they were chosen to construct ICCRs.

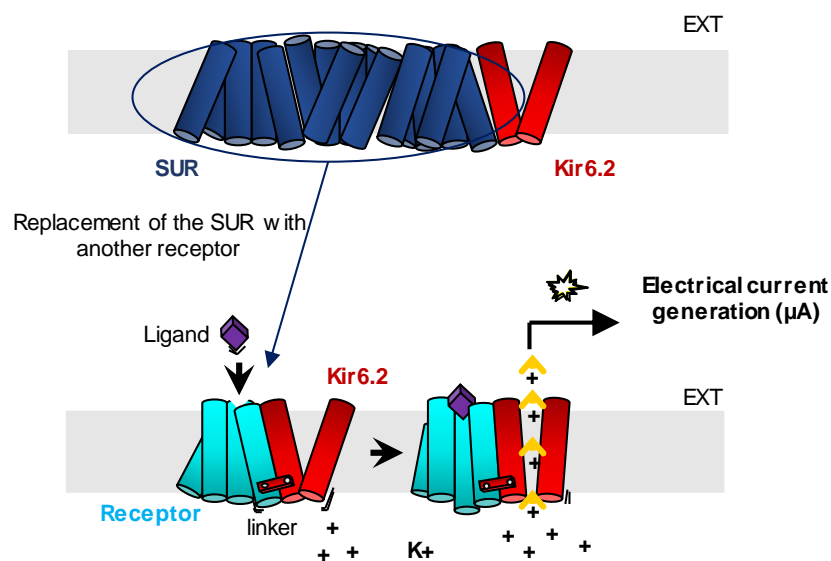


Figure 21. The ICCR concept. The SUR subunit of the natural K_{ATP} channel is replaced by a receptor that is physically linked to the Kir6.2 channel. Receptor and Kir6.2 are linked in such a way that the binding of a ligand to the receptor causes conformational changes that are communicated to the Kir6.2 channel. The Kir6.2 channel responds to these changes by altering its gating. The current generated by the flow of K^+ ions through Kir6.2 channel are detected by electrophysiological techniques (Principalli, 2015).

5.b. ICCR engineering

Ion channel-coupled receptors (ICCRs) are artificial ligand-gated channels formed by the covalent assembly of a GPCR and the Kir6.2 channel. This is achieved by linking the C-terminus of a GPCR to the N-terminus of Kir6.2. This fusion ensures a needed physical link between these two unrelated proteins, and a functional role in the transmission of the GPCR ligand binding events to the Kir6.2 gates (Moreau et al., 2008). The Kir6.2 channel is arranged as homo-tetramer to form a potassium selective pore; this organization leads the assembly of the full ICCR complex of four GPCR-Kir6.2 monomers per channel.

The conformational changes at the GPCR level are reported by the ICCR, by detecting the agonist- and antagonist-bound states of the receptor (Moreau et al., 2008). However, this union between receptor and channel does not assure a functional communication between the two partners. The linker region must be adjusted by specific deletion in the channel N-terminus and the receptor C-terminus. It has been discovered that, for the prototypical human M2 muscarinic and D2 dopaminergic ICCRs, truncation of the Kir6.2 first 25 N-terminal residues results in the most efficient coupling between the receptors and the channel (Moreau et al., 2008). This principle was confirmed for two subsequently constructed ICCRs based on human β 2 adrenergic and bovine rhodopsin receptor (Moreau et al., 2008; Caro et al., 2011, 2012). ICCR engineering depends of the length of the C-terminus of the receptor. As M2-muscarinic and D2-dopaminergic receptors have rather short C-termini, the deletion of this region was not needed. In contrast, for the β 2 adrenergic and rhodopsin receptors which possess longer C-termini, truncation of this domain was a crucial step to get functional ICCRs. When Kir6.2 was fused to full-length receptors, no response was detected in presence of ligands. The explanation of this phenomenon could be that long C-terminus might preclude proper coupling between receptor and channel (Niescierowicz et al., 2014).

Moreover, the achievement of the ICCR technology developed in the 'Channels' group, inspired the creation by another group of an ICCR containing the human olfactory receptor (hOR) (Oh et al., 2015).

5.c. Applications of the ICCR technology

ICCRs were originally designed as electrical biosensors to insert into microelectronic systems for *in vitro* diagnostic or high efficiency drug screenings. ICCRs combine the benefits of both partner proteins: the GPCR acts as a molecular receptor which can identify an extensive range of chemical ligands with high affinity and specificity; while ion

channels produce an electrical signal, large enough to allow the detection of a single molecule. The signal amplitude produced by the channel correlates with the ligand concentration, which allows label-free assays with a high signal-to-noise ratio and fast real-time measurement (Moreau et al., 2008). Since the signal is independent of the downstream intracellular pathway, including the heterotrimeric G proteins, ICCRs are a unique tool for functional characterization of altered GPCRs optimized for crystallographic studies, and thus no longer capable to interact with G proteins (Niescierowicz et al., 2014). ICCRs have been used in another laboratory to develop a platform for the high-throughput screening of the activity of olfactory receptors (Lim et al., 2015).

5.d. G Protein-Coupled Receptors

GPCRs form the largest family of membrane proteins, encoded by approximately 800 genes which cover about 2 % of the human genome. They share a common topology, as shown in Figure 22. They possess seven transmembrane helices that are connected by loops, three extracellular loops (ECL1, ECL2, ECL3) and three intracellular loops (ICL1, ICL2, ICL3). GPCRs have an extracellular N-terminal and an intracellular C-terminal domains. In the GPCR class containing Rhodopsin, the intracellular C-terminus contains a short amphipathic helix called helix VIII, followed by a tail carrying signaling sites for palmitoylation and phosphorylation, (Katritch et al., 2012; Maeda et al., 2010). In spite of this common architecture, GPCRs share low sequence identities, which might relate to their capacity to recognize a large variety of ligands.

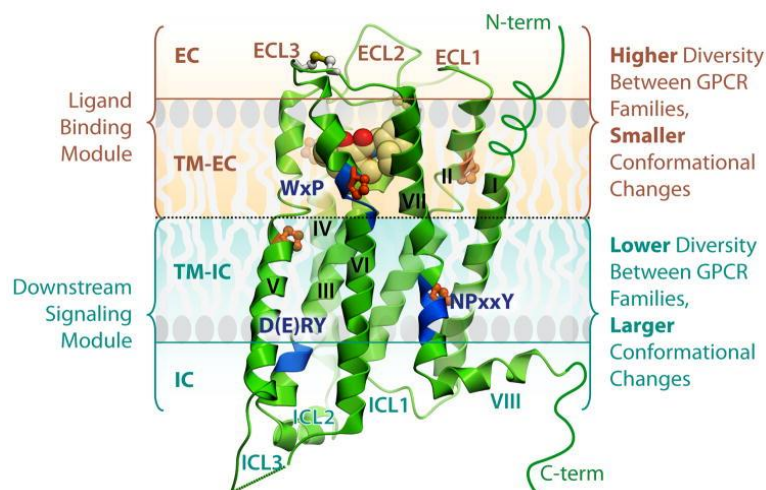


Figure 22. General topology of GPCRs. Major regions and structural features are shown on the crystal structure of the D3 dopamine receptor. The seven transmembrane helices contain a number of proline-dependent kinks (prolines shown in orange) that approximately divide the receptor into two modules. The EC module (EC and TM-EC regions) is responsible for binding diverse ligands and has much higher structural diversity. In contrast, the IC module (IC and IC-TM regions), involved in binding downstream effectors is more conserved between GPCRs, but undergoes larger conformational changes upon receptor activation. Blue ribbon patches highlight highly conserved, functionally relevant motifs in the transmembrane helices of Class A GPCRs. The C-terminus in most GPCRs includes helix VIII (Katritch et al., 2012).

In humans, GPCRs are expressed in all tissues; their role involves the recognition of several ligands, and consequent transmission of the associated message to downstream effectors inside the cell. The precise responses to these ligands are involved in biologically vital processes such as smell, vision, inflammation, pain sensation and mood regulation. Since the GPCRs have the ability to cause cell responses, and have an easy accessible ligand binding site (at the cell surface), it makes them a major pharmaceutical target (Wise et al., 2002).

5.d.1. The GPCR Family

GPCRs form a large family. They have been classified in several ways, the most used ones being based on structure similarities and/or ligand binding mode (classes A-F (Kolakowski, 1994) or on phylogenetic relationship as in the GRAFS nomenclature (Lagerström and Schiöth, 2008). The A-F classification contains all GPCR members in both vertebrates and invertebrates. However, the most used system is the GRAFS, which distributes GPCRs into five central subfamilies: Glutamate (G, 15 members), Rhodopsin (R, 701 members), Adhesion (A, 24 members), Frizzled/taste2 (F, 24 members) and Secretin (S, 15 members).

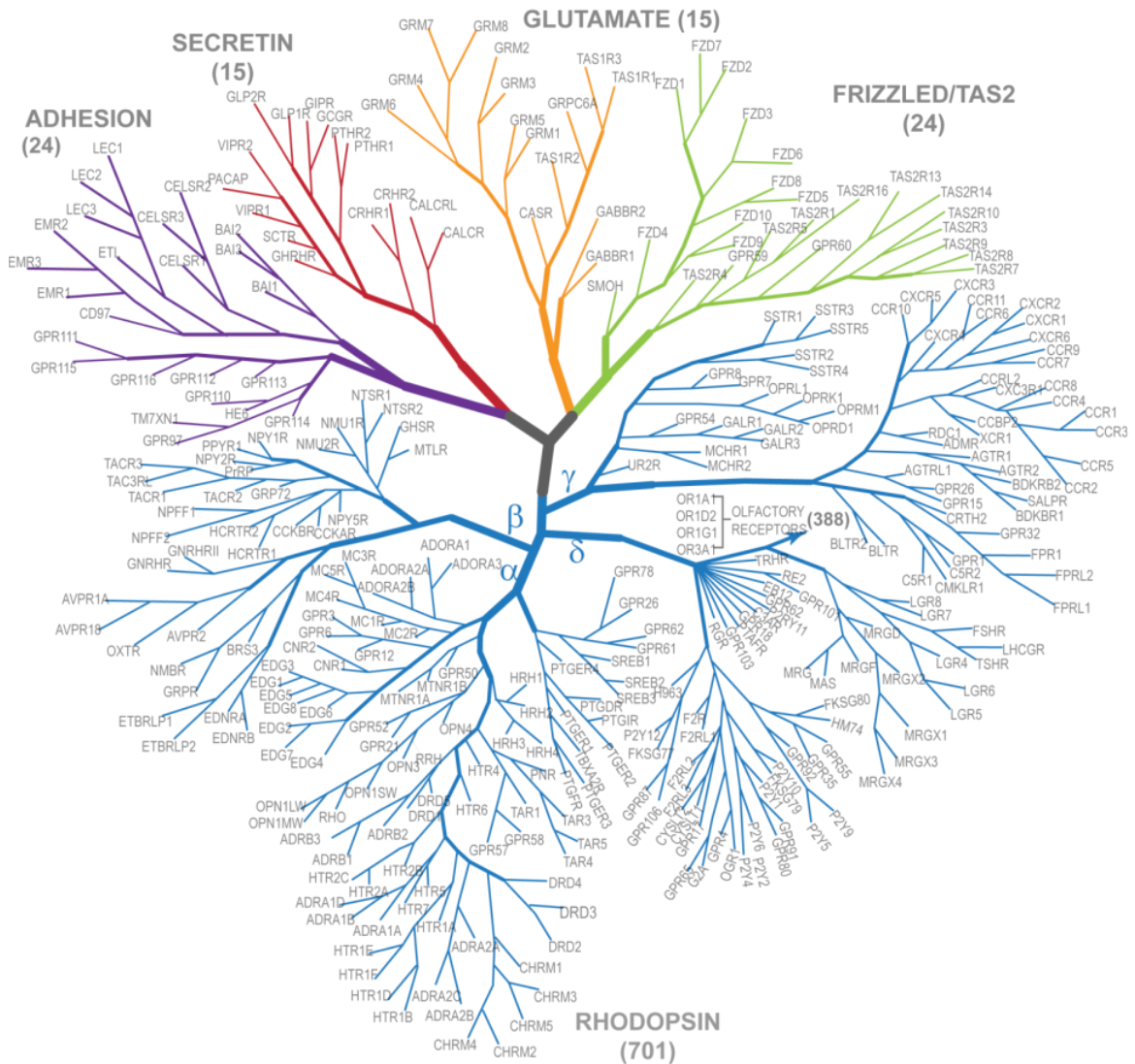


Figure 23. GPCRs phylogenetic tree and the GRAFS (Glutamate, Rhodopsin, Adhesion, Frizzled/Taste 2, Secretin receptors classes) organization. Because the Rhodopsin family comprises the largest number of members, it is further divided into four groups (α , β , γ and δ) (Katritch et al., 2012).

The rhodopsin subfamily

This subfamily has the largest number of members. Due to its diversity and number of members, it is divided into four groups (α , β , γ and δ). It contains the light-activated opsin receptor, the olfactory receptors, and receptors activated either by small molecules (amines, prostaglandins), peptides (hormones), or proteins (chemokines, glycoproteins) (Niescierowicz, 2013). Members of this subfamily have several common characteristics such as NSXXNPXXY motif in the helix VII and the DRY motif between helix III and the ICL2. These signatures play an essential role in receptor stabilization in specific states and in coupling with G proteins. The ligand binding site is commonly located in the TMs

INTRODUCTION

domains, with some exceptions for the glycoprotein binding receptors in which the substrate binding site is at the N-terminus.

The glutamate receptor subfamily

Eight metabotropic glutamate receptors belong to this subfamily. Members of this subfamily are generally characterized by long N- and C-terminal regions. The ligand-binding mechanism of the extracellular region is related to a Venus flytrap mechanism (VFTM), in which two lobes of the region form a cavity where glutamate binds to a conserved ligand binding site (Fredriksson et al., 2003) and activates the receptor.

The adhesion receptor subfamily

These receptors are rich in functional domains. A representative feature of these receptors is the long and diverse N-terminal domain, which is rich in cysteine and proline residues, which are supposed to be highly glycosylated and form a rigid structure. Moreover, the N-terminus of these receptors possess a proteolytic domain that is removed at the level of the endoplasmic reticulum to allow proper addressing of the protein to the plasma membrane (Krasnoperov et al., 2002).

The frizzled/taste 2 receptor subfamily

In this subfamily, we can distinguish two groups of receptors, which are grouped together because of the presence of precise common signatures in the C-terminal region. Frizzled receptors have a long N-terminus of about 200 residues in contrast with the short N-terminus of the related taste 2 receptors group. The Frizzled receptors are implicated in cell proliferation and development, while Taste 2 receptors function remains uncertain. It has been postulated that they are involved in bitter taste sensation as they are expressed in the tongue and in the palate epithelium (Fredriksson et al., 2003).

The secretin receptor subfamily

Members of this subfamily have an extracellular hormone-binding domain that binds peptide hormones. All members of this subfamily share 21 to 67% sequence identity, with most of the differences in the N-terminal region. Additionally, they have a conserved cysteine residue in the ECL1 and ECL2. Practically all of these receptors contain conserved cysteine residues that form disulfide bridges in the N-terminal domain (Fredriksson et al., 2003).

5.d.2. GPCR ligands

GPCR ligands or drugs are classified depending on their action when they bind to the receptor. According to its biological activity, the ligand can be categorized as:

An agonist: A molecule that produces activation of the receptor, and stimulates a specific biological effect;

A neutral antagonist: A molecule that neither activates the receptor nor inhibits its basal activity, and blocks binding of endogenous agonists to the receptor (Tate, 2012);

An inverse agonist: A molecule that inhibits the basal activity of the receptor by stabilizing it in inactive state.

5.d.3. GPCR-mediated signaling through G Proteins

G protein stands for GTP-binding proteins. G proteins can bind and hydrolyze guanine nucleotides. GPCRs interact with heterotrimeric G proteins made up of $G\alpha$, $G\beta$ and $G\gamma$ subunits, which are able to mediate several signal cascades in the cell. The signaling process produced by G proteins starts with the binding of a ligand to the GPCR, which causes receptor conformational changes, and stimulates the exchange of GDP to GTP on the $G\alpha$ subunit leading to the dissociation of the $G\beta\gamma$ dimer from $G\alpha$. Activated $G\alpha$ and $G\beta\gamma$ proteins modulate downstream effectors (ion channels, adenylyl cyclases, and phospholipases) which, in turn, generate secondary messenger molecules (Ca^{2+} , IP_3 , DAG, cAMP) (Principalli, 2015). This process begins a cascade of signals within the cell that influence a wide variety of metabolic functions (Dorsam and Gutkind, 2007).

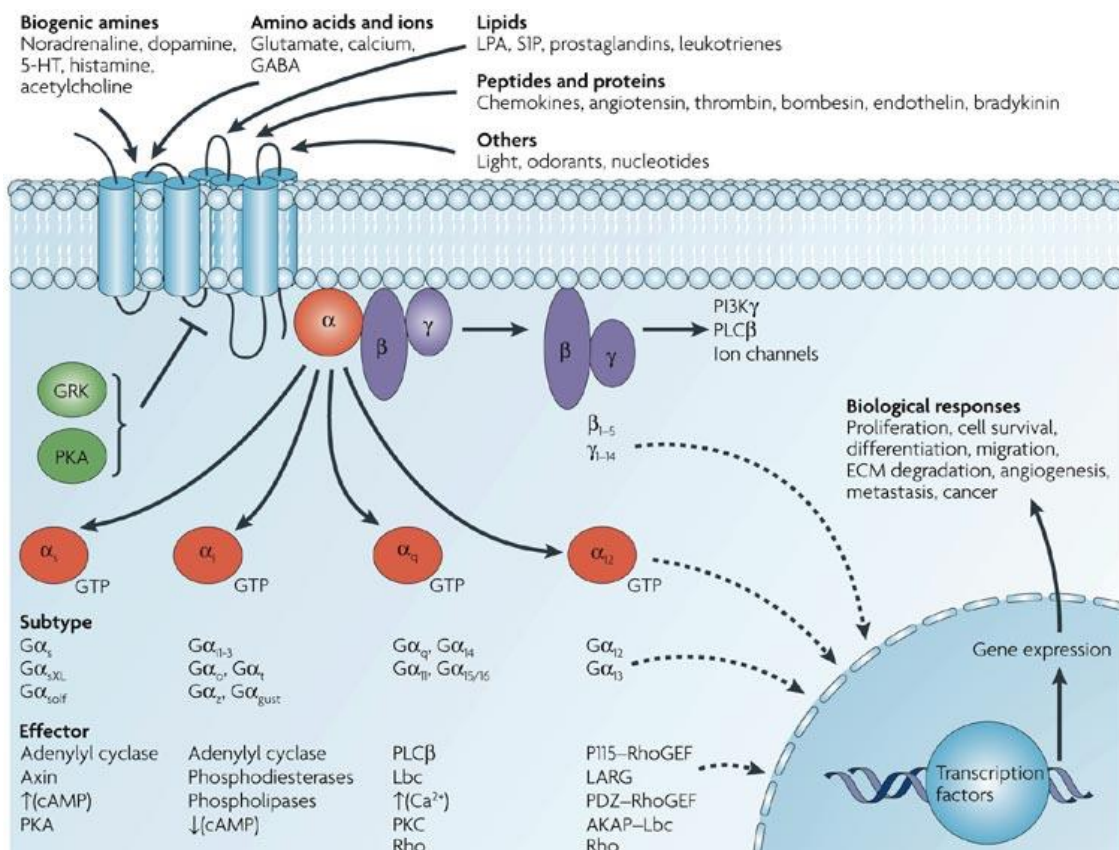


Figure 24. G protein-mediated signaling network (Dorsam and Gutkind 2007).

In its resting state, a GPCR associates with heterotrimeric G proteins which are bound to GDP. As shown in Figure 24, when the agonist ligand binds to the GPCR, it catalyzes GDP dissociation from the α subunit. Consequently, GTP binds to the $G\alpha$ subunit causing dissociation of $G\alpha$ from $G\beta\gamma$ subunits and release from the GPCR.

$G\alpha$ is subcategorized into four groups: $G_{\alpha s}$, $G_{\alpha i}$, $G_{\alpha q}$ and $G_{\alpha 12}$, and a single receptor can interact with one or more groups of $G\alpha$. G proteins can activate several downstream events. For instance, $G_{\alpha s}$ stimulates adenylyl cyclase increasing the levels of cAMP; $G_{\alpha i}$ inhibits adenylyl cyclase and lowers cAMP levels; $G_{\alpha q}$ activates phospholipase C (PLC), which cleaves PIP_2 into diacylglycerol (DAG) and inositol triphosphate (IP_3). $G\beta$ and $G\gamma$ subunits work as a dimer to activate phospholipases, ion channels and lipid kinases. $G\beta\gamma$, $G_{\alpha 12}$ and $G_{\alpha q}$ subunits can control the activity of intracellular signal-transducing molecules which include the small GTP-binding proteins belonging to the Ras and Rho families, members of the mitogen-activated protein kinase (MAPK) family such as extracellular signal-regulated kinases (ERK) and c-jun N-terminal kinases (JNK), through a complex network of signals (Principalli, 2015).

5.d.4. The M2 muscarinic acetylcholine receptor

M2 belongs to the Rhodopsin subfamily of the GPCRs. M2 is endogenously activated by acetylcholine, but also by other exogenous molecules such as muscarine or carbachol. Its activity can be antagonized by atropine. The M2 receptor signaling follows the general scheme described earlier. M2 receptors play an essential role in potassium conductance regulation by released $G\beta\gamma$ subunits of G_i/o proteins. The heterotetrameric cardiac potassium channels Kir3.1/Kir3.4 are activated by the binding of $G\beta\gamma$ (Krapivinsky et al., 1995). Also, the M2 receptor mediates inhibition of adenylyl cyclase via G_i proteins, which result in lower intracellular levels of cAMP (Ockenga et al., 2013). After ligand binding and stimulation, muscarinic receptors are desensitized in a process that is dependent on receptor phosphorylation at serine and threonine residues. Phosphorylation of the receptor allows β -arrestins to bind, which suppresses the G protein interactions and terminates the signal (Hosey et al., 1995).

In humans, the M2 muscarinic receptors are mainly expressed in the heart where they slow the heart rate down by activating G protein-activated K^+ channels thus reducing the rate of depolarization between action potentials. A recent structure of the human M2 receptor in the presence of the antagonist iperoxo provides insights into allosteric and orthosteric regulation of muscarinic receptors. As shown in Figure 25, the binding of the orthosteric agonist causes a conformational reorganization of the TM helices. In particular, helix VI is displaced outward while helix VII moves inward. These motions are

responsible for the formation of the intracellular cavity necessary for G protein binding (Kruse et al., 2013).

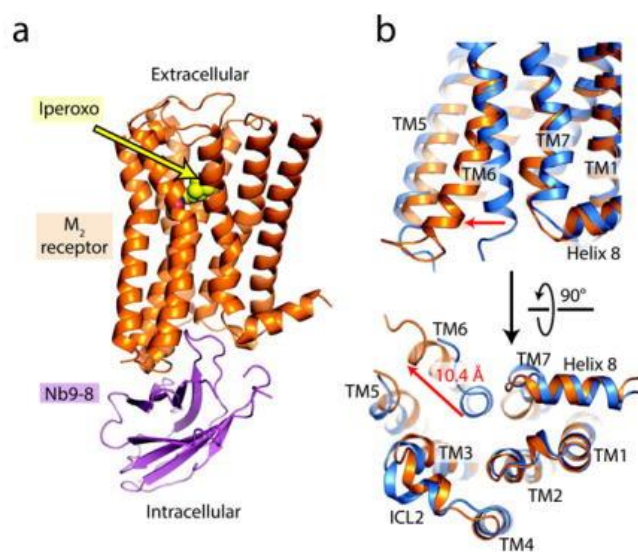


Figure 25. Intracellular changes on activation of the M2 receptor. **A.** Overall structure of the active-state M2 receptor (orange) in complex with the orthosteric agonist iperoxo (yellow) and the active-state stabilizing nanobody (purple). **B.** Compared to the inactive structure of the M2 receptor (blue), transmembrane helix VI (TM6) is substantially displaced outward, and TM7 has moved inward (Kruse et al., 2013).

In 2012, a structure of the inactive M2 receptor demonstrated the existence of a large extracellular vestibule capable of binding allosteric modulators. Situated above the orthosteric site, this cavity displays a significant contraction upon activation of the M2 receptor, due to the rotation of TM6. This motion offers a structural link among three regions of the receptor: the extracellular vestibule, the orthosteric binding pocket, and the intracellular surface. The structural coupling of these three regions suggests that allosteric modulators can affect the affinity and efficacy of orthosteric ligands (Haga et al. 2012; Principalli 2015). Later in 2013, the structure of the M2 receptor in complex with both an agonist and an allosteric modulator is very similar to the structure of the receptor in complex with the agonist only, suggesting that the allosteric binding site is pre-formed in the presence of agonist (Kruse et al., 2013).

In this thesis work, the ICCR used to perform the experiments is a M2-based ICCR.

6. Light as a tool in Biology

In the last decade, light has been used as a “non-invasive” stimulus in order to achieve specific and selective control of ionic pumps, receptors and ions channels.

As is shown in Figure 26, the strategies to use light as a tool in biology can be divided into different groups depending on the way chemistry and/or genetics are combined to accomplish light-induced control such as optogenetics, which involves the expression of exogenous photosensitive microbial opsin-based proteins. Also, there is optopharmacology that covers all the photolabile precursor ligands which can be divided in two subgroups: the “ligand-cage” and chemical photoswitches or “photochromic ligands”. Recently, “optogenetic pharmacology” has emerged as a new method which combines optics, chemistry and genetics (Kramer et al., 2013).

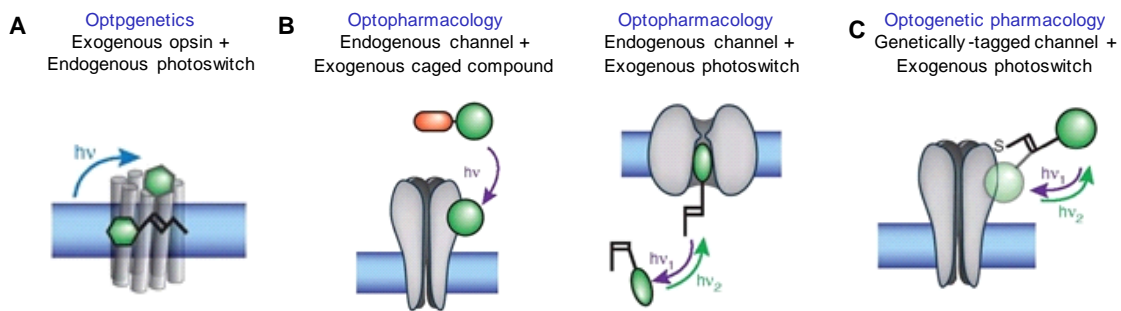


Figure 26. Tools to optically manipulate neural activity. **A.** Optogenetics by exogenous expression of photosensitive proteins (opsins) in the membrane of neurons. **B.** Optopharmacology consists in a photosensitive precursor ligand that can be a “ligand cage” or a “photochromic ligand” **C.** Optogenetic pharmacology involves the attachment of a synthetic photosensitive ligand to a genetically-modified protein (Kramer et al., 2013).

Opsins expressed in mammalian neurons were used for the first time by Boyden et al. 2005, when they demonstrated that neurons could respond to light upon the introduction of a single microbial opsin gene. This type of gene, which is naturally found in microorganisms (prokaryotes, algae and fungi), encodes the production of rhodopsin proteins containing retinal photoswitches (e.g., Channelrhodopsin-2). However, optogenetics using microbial opsins had a few drawbacks, such as the lack of specificity, and the inability to mimic the endogenous behavior of proteins. Most of these issues can be tackled by alternatives approaches such as optopharmacological and optogenetic pharmacology, making use of photoactive synthetic molecules to directly target the endogenous, or slightly genetically modified receptors and ion channels in neurons (Fehrentz et al., 2011; Kramer et al., 2013).

Since optogenetic pharmacology is used in this thesis work, it is discussed in depth in the following section.

6.a. Optogenetics, optopharmacology and optogenetic pharmacology.

The term optogenetics designates as the combination of genetic and optical methods to produce either a gain or loss of function of well-defined events in specific cells of living tissue (Deisseroth, 2011). In the last decade, different strategies have been developed to optically control neuronal activity: optogenetics which involves the use of microbial opsins, optogenetic pharmacology and optopharmacology which involves the use of light-responsive synthetic molecules which may or may not require the genetic modification of native cells, respectively.

6.a.1. Optogenetics: Rhodopsins at a glance

The result of the interaction between opsins with retinal is a complex called rhodopsins. Opsins are divided in two families: Type 1 (Figure 27) containing the microbial opsins, and Type 2 containing the mammalian opsins. Although, both families encode 7 transmembrane helices structures, the main difference between Types 1 and 2 is the capacity or not to transport ions through the plasma membrane, respectively. This characteristics make it possible to use microbial opsins as tools to optically control neuronal activity, and the animal opsins, which are G-protein-coupled receptors, as tools to modify signaling (Zhang et al., 2011).

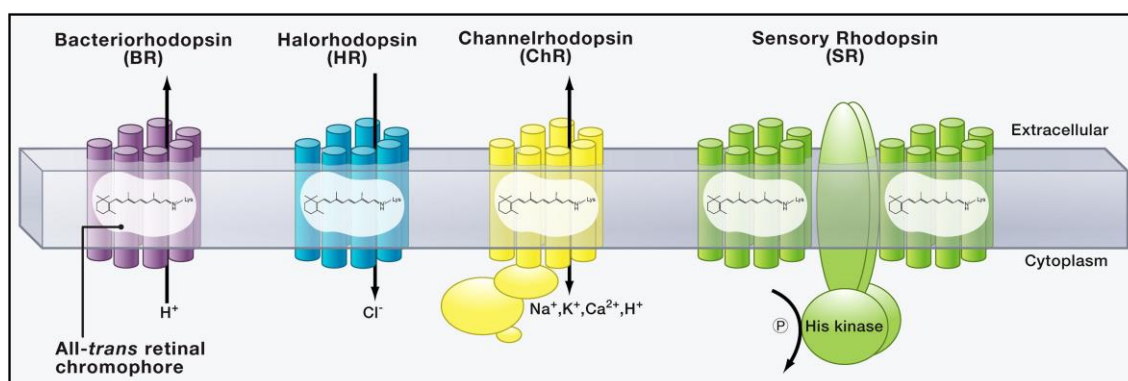


Figure 27. Schematic representation of the different microbial opsins (Type 1) (Zhang et al., 2011).

Retinal, a form of vitamin A, is an essential cofactor that serves as an antenna for photons. When retinal is bound to an opsin, it confers sensitivity to light. After the retinal has diffused into the binding pocket of the opsin, it is covalently attached to a conserved lysine residue, located in helix VII by formation a protonated retinal Schiff-base. The ionic

INTRODUCTION

environment of positive charges determines the spectra and kinetic characteristics of each rhodopsin. Upon photon absorption, the retinal isomerizes (Figure 28) and generates a wave of conformational changes inside the opsin, making possible all the activities that these proteins perform (Yizhar et al., 2011).

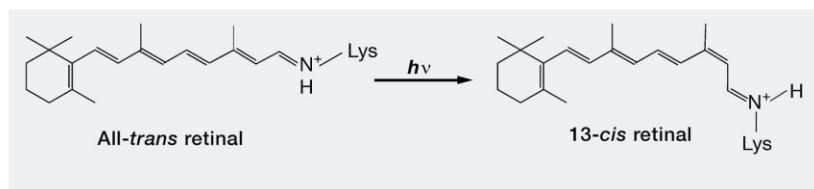


Figure 28. Light-mediated isomerization of the retinal Schiff base. Retinal in the all-trans state is found in the dark-adapted state of microbial rhodopsins. The absorption of a photon converts the retinal from the all-trans to the 13-cis configuration (Zhang et al., 2011).

Three members of the microbial opsins family have been found to be useful in optogenetics: the bacteriorhodopsins (BR), the halorhodopsins (HR) and the channelrhodopsins (ChR). The first discovered member of this family is BR, which pump protons out of the cell. Like HR that pumps chloride ions into the cell, BR is normally inhibitory in neural systems, as both proteins hyperpolarize the membrane, making it harder for neurons to fire action potentials. ChR which is cation-selective and allows positively-charged ions to flow freely through the opsin pore tends to be depolarizing and excitatory (Zhang et al., 2011).

In 2014, the determination of a the high-resolution structure of ChR allowed the rational design a chloride-conducting anion channel by mutagenesis of the original cation-conducting ChR (Berndt et al., 2014; Kato et al., 2012). Subsequently, in 2015, a natural chloride-conducting ChR was identified (Govorunova et al., 2015).

In neurons the expression of ChR2 has allowed the optical control of hippocampal neurons from rat (Boyden et al., 2005). The strong advantage of ChR is that retinal, necessary cofactor for light sensitivity, is naturally present in vertebrate tissues and incorporates into exogenous opsins. Living organisms have biological systems that can identify β -carotene, an inactive form of vitamin A, and convert it into retinal, an active form. This system can allow the study of a specific population of neurons through targeted illumination. Despite this advantage, studies in neuronal systems using microbial opsin have several weaknesses: expression is low and cannot be controlled, conductance is very small, and ion selectivity does not permit inhibitory action. An alternative would be to use mammalian channels, especially potassium channels. Such a light-sensitive K⁺ channel was designed in the Channels group in 2012 using ICCR

technology. As shown in Figure 29, a light-gated potassium channel was constructed by physical coupling of rhodopsin to the Kir6.2 channel. When the rhodopsin is exposed to light, it changes its conformation, and this change is directly transmitted to the channel and results in gating alterations of the Kir6.2 channel (Caro et al., 2012).

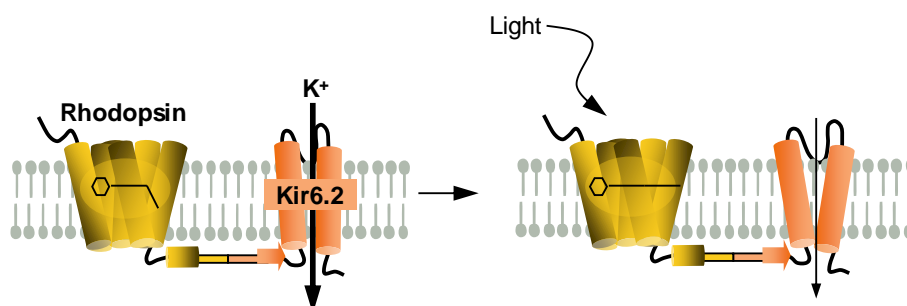


Figure 29. Rhodopsin-based ICCRs and functional coupling (channel group)

However, the rhodopsin-based ICCR remains a proof-of-concept and would require improvement in terms of expression and light-dependent signal amplitude to become a useful tool. In this work, we designed a light-dependent K_{ATP} channel using optogenetic pharmacology.

6.a.2. Optopharmacology and optogenetic pharmacology.

Optopharmacology and optogenetic pharmacology are alternative light-based strategies to optogenetics. They exploit the combined use of an intrinsic receptor or ion channel and synthetic photoactive molecules. As mentioned above, such proteins can be endogenous or genetically modified, thus giving rise to the fields of optopharmacology and optogenetic pharmacology. In both cases, however, the basic strategy remains the same, to use light-responsive pharmacologically active substances whose interaction with the target proteins can be modulated upon irradiation. In this way, cell signaling processes can be triggered (by photoactive receptor agonists) or blocked (by photoactive receptor antagonists and channel blockers) without the need of introducing exogenous opsins in the cell membrane.

With regard to the optopharmacology and optogenetic pharmacology approaches, there are three main methods for optical remote control of cell signaling with photoactive synthetic molecules: caged ligands, photochromic ligands, and photoswitched tethered ligands. Whereas the two first types of systems are strictly optopharmacological, photoswitched tethered ligands are used both in optopharmacology and optogenetic pharmacology.

INTRODUCTION

The caged ligand (CL) method involves a biologically active molecule or ligands such as an ion, a neurotransmitter or an intracellular signaling molecule that is equipped with a photolabile protecting group (caging group) which silences its pharmacological activity. Upon exposure to light, photocleavage of the protecting group releases the active substrate and causes the wanted biological effect (Wieboldt et al., 1994; Gorostiza and Isacoff, 2007). However, the CLs have a main drawback: uncaging is an irreversible process, and the released ligand is free to diffuse and act on non-targeted areas where its pharmacological activity is unwanted. The disadvantage of CLs can be overcome with the use of photochromic ligands (PCLs) and photoswitched tethered ligands (PTLs) methods. In both cases, a biologically active ligand is attached to a photoswitch, a photoisomerizable group that can change its conformation rapidly and reversibly between two different states upon illumination with different wavelengths. However, as with caged ligands, photochromic ligands are free to diffuse away from the illuminated area. This difficulty can be overcome if the photoisomerizable molecule with optopharmacological activity is directly attached to the protein of interest. This is the main idea behind the use of photoswitched tethered ligands, which require at least three different functional parts: the biologically active part, a photoisomerizable moiety and a reactive group with which the whole molecule can be covalently tethered to the target protein. Provided the attachment point is correctly selected, the geometrical changes induced by the reversible isomerization of the photoswitch moves the ligand closer to or further from the binding site, thus allowing the ligand-receptor interaction to be light-controlled selectively on the functionalized proteins.

Another approach, a derivative of the PTL method was developed by Lemoine et al. 2013, termed as "optogating". This differs from the current optogenetic approach in that it only targets the transmembrane gate of the channel by using photoswitchable molecules that do not target an active site. In order to apply the optogating approach to the P2X2 receptor, a photoswitchable compound was synthesized: the sulfhydryl reactive, maleimide ethylene azobenzene trimethyl ammonium derivative (MEA-TMA) that is similar to the maleimide azobenzene quaternary ammonium (MAQ), a compound initially developed to optochemically control K⁺ channels activity. The covalent attachment of this compound in the transmembrane (TM) pore region, allows the reversible optical manipulation of its gate (Lemoine et al., 2013). Moreover, recent studies on the P2X2 receptor demonstrated its activation by attaching photoswitchable tweezers, termed as MAM (4,4'-bis(maleimido-glycine) azobenzene). MAM contains a photoswitchable azobenzene cross-linker carrying two reactive maleimides at each end. This molecule is attached to two engineered cysteines located at the outer ends (horizontal cross-linking)

or between the inner and outer ends (vertical cross-linking) of adjacent TM2 helices. When MAM is switched to its longer conformation, it provokes a lateral expansion between TM1 and TM2 helices which drives channel opening. Additionally, this study provided the first application of photoswitchable derivatives to investigate the mechanism of pore gating in P2X receptors (Habermacher et al., 2016).

In this work, we used the PTL method as a tool to optically control the K_{ATP} channel.

6.b. PTL approach in membrane proteins

Thanks to the determination of crystal structures of channels and receptors, and advances in pharmacology, it has become possible to design tethered ligands and azobenzene linkers of defined geometry, that can photoisomerize in a fast, reversible, and predictable way so that the photoswitchable compound can bind or pull out the ligand from its binding site. The ligand in these photoswitches can be used either as a pore blocker (Banghart et al., 2004) or as an allosteric ligand for an ionotropic receptor (Volgraf et al., 2006).

6.b.1. Ionotropic glutamate receptor (iGluR)

Based on previous structure-function studies and the identification of the ligand-binding domain (LBD) (which provides the binding site for agonists and antagonists for the individual iGluR subunits), a detailed understanding of agonist recognition in the diverse family of ionotropic glutamate receptors has been possible.

In 2006, the first light-controlled ionotropic glutamate receptor was developed, with the PTL strategy. The design of the tethered agonist was based on the extensive pharmacology of iGluR and on the structure of the ionotropic glutamate receptor subtype 6 (iGluR6) containing the agonist (2S,4R)-4-methyl glutamate bound. In order to perform the PTL method, the photoswitchable molecule MAG was used. As shown in Figure 30A, MAG contains three different parts: a maleimide group for attachment to an engineered cysteine on the exterior of the LBD (M); an azobenzene photoswitch undergoing *trans-cis* photoisomerization (A); and a glutamate analogue as ligand (G). Then, by cysteine screening on the perimeter around the exit channel of the receptor, the suitable position to attach the MAG is selected, (just upon ligand-binding site where the *cis* state of MAG can interact).

As shown in Figure 30B, once the MAG is attached to the engineered cysteine on iGluR, the change between the two states of this photoswitchable compound allowed light control of the glutamate-binding site interaction, which was only observed to take place for the *cis* isomer of the photoswitch. This resulted in a clamshell-like movement of the

LBD around the tethered agonist upon illumination, which was demonstrated to allosterically trigger the opening and closing of the channel pore. This association of the cysteine mutated iGluR and the tethered MAG ligand was designated the light-gated ionotropic glutamate receptor (LiGluR) (Volgraf et al., 2006).

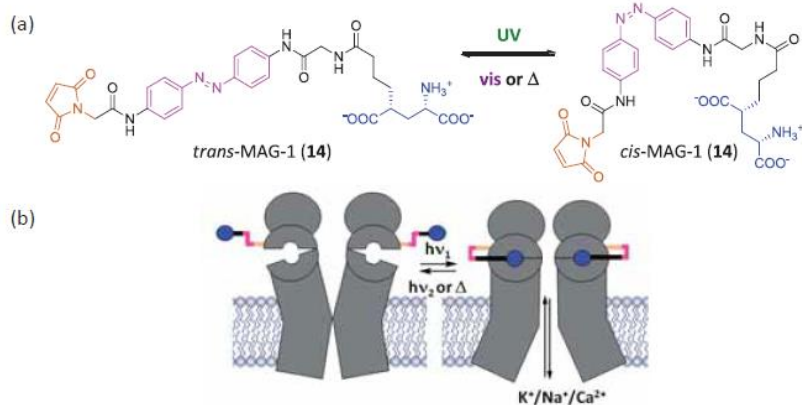


Figure 30. A. *Trans-cis* isomerization of MAG. **B.** Schematic representation of the light-induced operation of LiGluR (Volgraf et al., 2006).

6.b.2. Nicotinic acetylcholine, GABA and metabotropic glutamate receptors

The first optically-modulated nicotinic acetylcholine receptor (nAChR) was developed before genetic manipulation of the protein was possible, by using an endogenous disulfide bridge which is localized in the pocket of the ligand binding site of acetylcholine. When this bridge is broken, the free cysteine can interact with Q-Br, a derivative of azobenzene that contains, at one end, an electrophilic bromomethyl and, at the other, a quaternary ammonium. However, this approach did not allow specific optical control of the nAChR (Lester et al., 1980). In 2012, the PTL approach on this receptor was developed in order to optically activate and inhibit the $\alpha 3\beta 4$ and $\alpha 4\beta 2$ nAChR heteromers. Based on the extensive pharmacology and structural data of nAChR, photoswitchable compounds were synthesized: Maleimide azobenzene acetylcholine (MAACh) as an agonist, and Maleimide azobenzene homocholine (MAHoCh) as an antagonist. These two photoswitchable compounds were able to interact with the engineered cysteine located in the α subunit near the acetylcholine binding site located in the β subunit. The *Cis* isomer states of MAACh and MAHoCh allowed optical activation and inhibition of nAChR, respectively. The resulting engineered light-sensitive nAChR was called LiAChR (Tochitsky et al., 2012).

Similarly, the GABA receptor was optically controlled using the PTL approach, based on a photoswitchable compound which involves a sulfhydryl-reactive maleimide group, a photoswitchable azobenzene core, and a ligand for the GABA-binding site creating a light-regulated GABA receptor (LiGABAR) (Lin et al., 2014).

Photoswitchable compounds were also synthesized in order to apply the PTL approach to metabotropic glutamate receptors (mGluRs), resulting in light-activated and light-antagonized “LimGluRs” and light-activated “LimGluR2” receptors (Levitz et al., 2013).

6.b.3. Potassium channels

The Shaker voltage-dependent potassium channel was the first potassium channel to be modified to be modulated by light. The photoswitchable compound used to optically modulate the channel by PTLs was called MAQ. As shown in Figure 31A, MAQ contains a maleimide group (M), a photoisomerizable azobenzene linker (A), and a pore-blocking quaternary ammonium group (Q). Studies using MAQ were based on the use of blockers covalently linked at different distances to the pore (Blaustein et al., 2000), and it was originally used to optically modulate the Synthetic Photoisomerizable Azobenzene Regulated K⁺ (SPARK), an engineered light-gated potassium channel derived from Shaker (Banghart et al., 2004). As shown in Figure 31B, MAQ is covalently attached to an engineered cysteine located in the extracellular loop of the channel. The MAQ *trans* state allows the quaternary ammonium to reach the pore and block the channel. The *cis* state shortens the MAQ, preventing the quaternary ammonium block. It has been shown that SPARK allows the optical modulation of rat embryonic hippocampal neurons (Figure 32) (Banghart et al., 2004).

INTRODUCTION

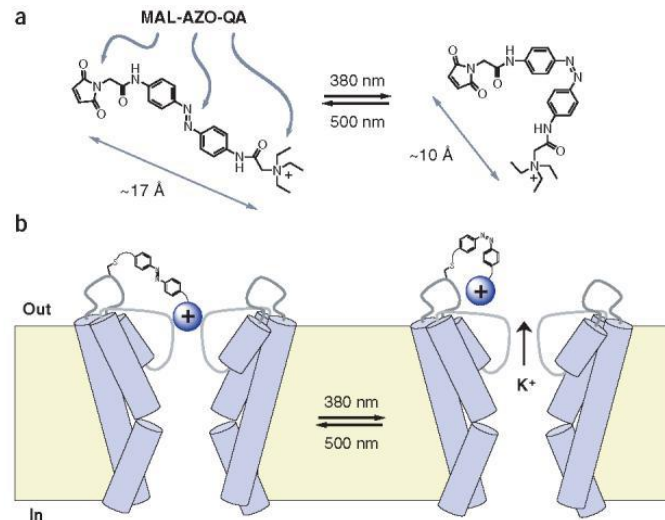


Figure 31. Photoisomerization of MAQ. **A.** The rigid core of MAQ (between the α carbons flanking the azobenzene moiety) changes by about 7 Å upon photoisomerization. **B.** MAQ blocks ion flow in the trans configuration but is too short to block effectively after photoisomerization to the cis configuration (Banghart et al., 2004).

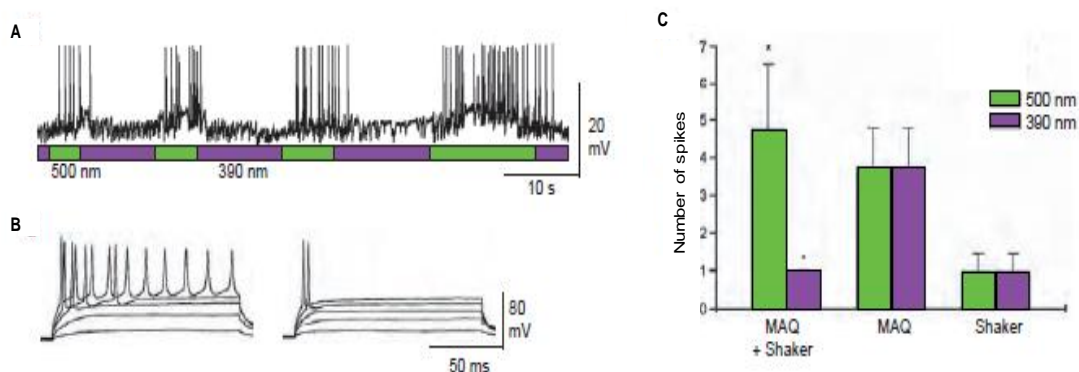


Figure 32. Expression of light-modulated channels confers light sensitivity to hippocampal pyramidal neurons. **A.** Spontaneous action potentials are silenced and revived by exposure to 390-nm and 500-nm light, respectively. Neurons, transfected with the mutated Shaker channel, were treated for 15 min with MAL-AZO-QA before recording. The frequency of spontaneous synaptic potentials generated by untransfected presynaptic neurons is not affected by light. **B.** Depolarizing current steps elicit repetitive firing in 500-nm light (left) but only single action potentials in 390-nm light (right). Neurons were held under current clamp at -55 mV and were depolarized to -15 mV. **C.** Histogram of number of spikes resulting from a supra threshold depolarization to -15 mV is significantly modulated by light in the mutated Shaker-transfected neurons treated with MAQ. Neurons expressing the channel without MAQ treatment or treated with MAQ without channel expression were unaffected by light (Banghart et al., 2004).

INTRODUCTION

As shown in Table 4, potassium channels optically modulated by MAQ now include different sets of mammalian potassium channels, including channels in the voltage-gated and K_{2P} families (Sandoz and Levitz, 2013).

Channel	Family	Cysteine	<i>cis</i> or <i>trans</i> block?	Properties	Potential neuronal applications	Reference
<i>Drosophila</i> Shaker Δ6-46 L366A T449V "SPARK"	K_v	E422C	<i>trans</i>	A-type current Voltage-gated $V_{1/2} = -36$ mV Weak inactivation	Photocontrol of V_m	Banghart et al. (2004)
"D-SPARK" V443Q	K_v	E422C	<i>trans</i>	Non-selective cation channel Voltage-gated $V_{1/2} = -36$ mV	Photocontrol of V_m	Chambers et al. (2006)
Kv1.3-H401Y	K_v1	P374C	<i>trans</i>	Voltage-gated $V_{1/2} = -30$ mV	Photocontrol of Accomodation	Fortin et al. (2011)
Kv3.1	K_v3	E380C	<i>trans</i>	Weak inactivation $V_{1/2} = -40$ mV	Photocontrol of V_m	Fortin et al. (2011)
Kv7.2	K_v7	E257C	<i>trans</i>	M-type current $V_{1/2} = -30$ mV	Photocontrol of V_m Photocontrol of M-current	Fortin et al. (2011)
SK2	SK	Q339C	<i>trans</i>	Ca^{2+} -activated	Photocontrol of afterhyperpolarization	Fortin et al. (2011)
TREK1/ $K_{2P}2.1$ "TREKlight"	K_{2P}	S121C	<i>cis</i>	Leak current pH-sensitive Extensive regulation	Photocontrol of V_m	Sandoz et al. (2012)
TREK1/ $K_{2P}2.1$ "SRARK-like"	K_{2P}	K231C	<i>trans</i>	Leak current pH-sensitive Extensive regulation	Photocontrol of V_m	Sandoz et al. (2012)
TREK1 ΔC "TREK1-PCS"	K_{2P}	S121C	<i>cis</i>	Leak current pH-sensitive Extensive regulation	Photocontrol of native TREK1 Conduction	Sandoz et al. (2012)
TASK3/ $K_{2P}9.1$	K_{2P}	R73C or A74C	<i>trans</i>	Leak current pH-sensitive Extensive regulation	Photocontrol of V_m	Sandoz et al. (2012)

Table 4. PTL-mediated photoswitchable ion channels (Sandoz and Levitz, 2013).

In this work we used the PTL approach in order to enable optically-dependent block of the K_{ATP} channel. As in other potassium channels, the photoswitchable compound used was MAQ. Suitable engineered cysteine positions were selected based on structural models.

MATERIALS AND METHODS

The main objective of this project is the study and design of an optogenetic potassium ion channel. Two other side projects concerned investigation of the mechanics of Kir6.2 gating and the molecular mechanisms of Cantù syndrome mutations in SUR2A. In order to accomplish the work, the following techniques have been used.

1. Molecular biology

1.a. Genes and expression vectors

Gene	Organism	Source
Kir6.2	Mouse	GenBank: accession number: D50581 Dr. S. Seino (Chiba University School of Medicine, Japan)
SUR2A	Rat	GenBank: accession number: D83598 Dr. S. Seino (Chiba University School of Medicine, Japan)
Kir3.4	Human	Dr. D. Logothetis (Virginia Commonwealth University)
M2	Human	GenBank: accession number NM_000739 Dr. D. Logothetis (Virginia Commonwealth University)
M2=K-9-25 (ICCR)	Human (M2) Mouse (Kir6.2)	Constructed by Christophe Moreau

Table 5. Genes used in this work.

Each gene was cloned into a vector appropriate for the desired expression host (Table 6).

Vector	Expression system	Source	Promoter	Resistance
pGH	<i>Xenopus</i> oocytes	Dr. D. Logothetis	T7/SP6	Ampicillin
pGH2	<i>Xenopus</i> oocytes	Dr. F. Pages	T7/SP6	Ampicillin
pXOOM	<i>Xenopus</i> oocytes and mammalian cells	Dr. D. Logothetis	T7/SP6/CMV	Kanamycin Neomycin

Table 6. Vectors used in this work.

All vectors contain a bacterial origin of replication (ORI), a bacterial resistance gene (ampicillin or kanamycin), and a poly-A tail at the 3' end of the cDNA to stabilize mRNA transcripts. The pXOOM vector contains an enhanced GFP gene (neo-EGFP) fused to

a neomycin resistance gene to visualize transfected cells by fluorescence microscopy (excitation of ~500 nm).

1.b. Site-directed mutagenesis

Site-directed mutagenesis is an *in-vitro* method to create specific, targeted changes in double stranded plasmid DNA. This technique can be used to carry out specific DNA alterations (insertions, deletions and substitutions).

In our experiments, we used the QuikChange Lightning Site-Directed Mutagenesis Kit (Agilent Technologies). This method is based on a PCR reaction in which *Pfu* Ultra high-fidelity DNA polymerase uses complementary mutagenic primers to direct replication of the plasmid. The principle of this method is illustrated in Figure 33.

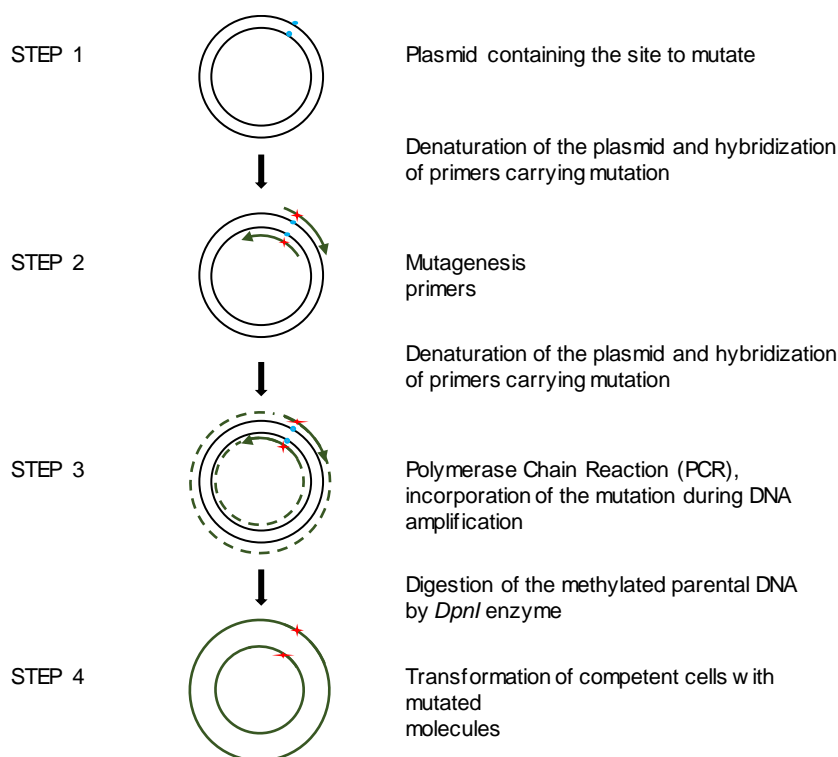


Figure 33. Principle of the site-directed mutagenesis carried out with Quick-change Site-Directed Mutagenesis Kit (Agilent Technologies). Complementary primers (forward and reverse) hybridize with a specific region of the DNA and are elongated by the polymerase.

Complementary mutagenic primers (forward and reverse), designed to hybridize with a specific region of the DNA strand, are elongated by the polymerase to generate a new mutated plasmid. The resulting PCR product is subjected to digestion with *DpnI* endonuclease with the purpose of eliminating the parental (methylated) template DNA, leaving only the new mutation-containing synthesized DNA. Finally, the mutated DNA molecules are transformed into *E.coli*.

1.c. Subcloning

This technique is used to transfer a particular gene of interest from a parent vector to a recipient vector. This method was used to transfer the Kir6.2 gene from pGH vector (for expression in *Xenopus oocytes*) and SUR2A from pGH2 (for expression in *Xenopus oocytes*) to pXOOM vector (for expression either in *Xenopus oocytes* or mammalian cells).

Subcloning was performed in two different ways.

The classic restriction method, was preferred for long genes such as the SUR2A gene. Using the same unique restriction sites present at both the 5' and 3' ends of the SUR2A gene and the recipient pXOOM vector, the SUR2A gene was excised from the pGH2 vector and inserted into the pXOOM vector, as illustrated in Figure 34. In order to identify and subsequently separate the SUR2A gene from the parent pGH2 vector, the SUR2A-pGH2 digestion product was loaded onto a 0.8% agarose gel. The DNA band corresponding to the SUR2A gene was cut out from the gel and purified using the GeneClean kit (MP Biomedicals). The SUR2A gene and recipient pXOOM vector were then ligated together with DNA ligase (rapid DNA ligation Kit, Roche).

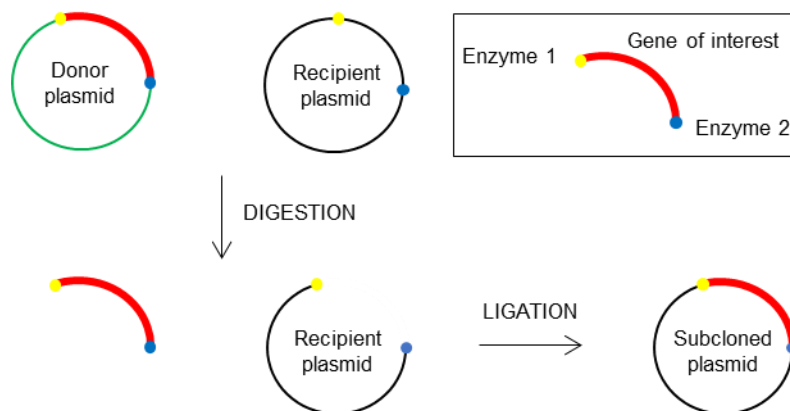


Figure 34. Subcloning by restriction enzymes.

The PCR method, was often more successful than the classical method. Forward and reversible flanking primers, 25 to 30 bases long, were designed as hybrids, matching the Kir6.2 gene at one end and the recipient pXOOM vector at the other. A first PCR is performed in order to generate megaprimers (primers covering the whole sequence of the gene). This PCR product is loaded onto a 0.8% agarose gel in order to identify and isolate the megaprimers from the template DNA. The megaprimers are then purified using the GeneClean kit (MP Biomedicals) and subsequently used in a second PCR

reaction to incorporate the megaprimers into the recipient pXOOM vector as illustrated in Figure 35.

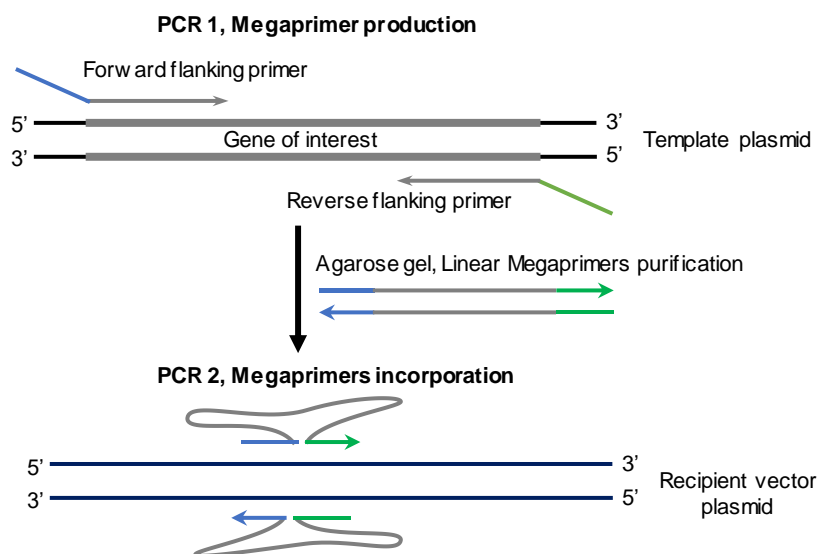


Figure 35. Subcloning using megaprimers. The DNA template plasmid containing the gene of interest is first amplified in PCR 1, using primers with 5' tails (blue and green) carrying homology to the site of insertion of the recipient vector plasmid.

1.d. Amplification of the genetic material

1.d.1. Transformation of competent bacteria

After genetic engineering, the DNA of interest is amplified and selected by transforming into “ultracompetent” bacteria (*epicurian coli* XL-10 Gold) provided by the Quick-change Lightning Site-Directed Mutagenesis kit (Agilent Technologies). Approximately 50 μL of competent bacteria are mixed with the DNA and incubated on ice for 30 min. This is followed by a thermal shock of 45 seconds at 42°C followed by 2 minutes on ice, in order to induce transport of the DNA across the bacteria cell wall. Finally, 500 μL of SOC media is added and the cells are incubated at 37°C for at least 60 min to allow expression of the antibiotic resistance gene. Subsequently, recombinant bacteria are selected by plating on LB agar plates containing either ampicillin or kanamycin and incubating at 37°C overnight.

1.d.2. Amplification and purification of DNA

The extraction of plasmid DNA from bacteria cells is based on the alkaline lysis method. Cells grown overnight were pelleted by centrifugation and re-suspended in a solution containing: Tris, EDTA, glucose and RNase A (RNase A is included to degrade cellular RNA). SDS detergent (Sodium Dodecyl sulfate) is used for cell lysis and protein denaturation, followed by the denaturation of genomic DNA, plasmid DNA, and proteins

with sodium hydroxide. This method is based on the different physical-chemical characteristics of the linear genomic DNA and the supercoiled plasmid DNA. Once the neutralizing solution of potassium acetate is added to the cell lysate, only the plasmid DNA will renature while genomic DNA, which is too long to re-anneal properly, will become tangled causing the complementary strands to stay separated resulting in precipitation. The precipitate containing membranes, proteins and genomic DNA is separated from the plasmid DNA by high-speed centrifugation (14000 rpm at 4°C for 15 minutes) or with purification columns (MidiPrep Qiagen kit). The supernatant containing the plasmid DNA is recovered, and then precipitated with isopropanol (14000 rpm at 4°C for ≥ 30 min). Subsequently, purification is performed using 70% ethanol to remove any remaining contaminants. Finally, the DNA pellet is allowed to dry to eliminate ethanol, and dissolved in distilled water.

Two variations of this method have been used in our experiments: “Miniprep” for screening a high number of clones and ‘Midiprep’ used to scale up DNA after selecting a positive clone from the miniprep step.

1.d.3. Miniprep and midiprep methods

Miniprep is used in order to select positive clones. Bacteria were grown on agar plates are transferred to 5 mL of LB medium containing antibiotic. After overnight growth, the cultures are treated with solutions provided by the Qiagen kit as described above. Miniprep allows us to recover enough plasmid DNA to perform the selection of positive clones. Selection is done by digestion with restriction enzymes and analysis of the restriction profile. Selected clones are then sequenced. Selection can also be done directly by sequencing, a solution which avoids the need of adding restriction sites and which is now becoming cost-effective.

Midiprep is used to scale up the amount and quality of the plasmid DNA selected in the Miniprep step. Bacteria were grown in 50 mL of LB medium supplemented with antibiotic, which results in a larger quantity of genetic material compared to Miniprep. The Qiagen Plasmid Purification kit provides all solutions required. The purity of the obtained DNA increases due to the filtration step enabling the elimination of all bacteria remnants, and the anion-exchange column, that selectively binds the plasmid DNA. Purified DNA concentration is estimated using the NanoDrop 2000 (Thermoscientific) spectrophotometer by measuring the optical density at a wavelength of 260 nm.

1.e. Sequencing

A volume of 20 μL of DNA plasmid at a concentration of 100 $\text{ng}/\mu\text{L}$ is sent to Beckman Coulter Genomics for sequencing. This company uses the Sanger sequencing method (1977), which requires a single-stranded DNA, a DNA primer, deoxynucleosidetriphosphates (dNTPs) and modified nucleotides (ddNTPs) labelled with fluorescent probes. The DNA sample is divided into four separate reactions which run simultaneously. Each reaction contains all four standard kinds of dNTPs and the DNA polymerase. Only one of the four ddNTPs is added, labelled with a fluorescent probe. ddNTPs are a particular kind of nucleotides that have the ability to terminate the synthesis of the new strand of DNA. PCR products are then loaded into a capillary gel electrophoresis to allow the separation of DNA fragments of different lengths and the presence of fluorochromes facilitates the reading in an optical system. Depending on the size of the synthesized fragments it is possible to rebuild the whole sequence of the DNA.

1.f. In vitro transcription

RNA is very susceptible to contamination; its manipulation requires 'RNase-free' conditions. In order to maintain RNase-free conditions all manipulations are performed in the fumehood, wearing gloves, using dedicated pipettes, tips, tubes, and water treated with diethyl pyrocarbonate (DEPC) which deactivates RNases.

The plasmid DNA is linearized using restriction enzymes which cut once at a specific site of the plasmid, located downstream of the 3' UTR sequence (linearization site). Twenty units of enzyme are used to digest 10 μg of DNA during overnight digestion at 37°C. Subsequently, linearized DNA is purified and extracted using phenol/chloroform/isoamyl alcohol. Quantity and quality of the linearized DNA is estimated on a 0.8% agarose gel.

Transcription is performed by RNA T7 polymerase, whose promotor is localized upstream of the sequence to be transcribed. The mMessage mMachine T7 kit (Ambion) provides all reagents used for transcription. The kit enables a large quantity of RNA capped at the 5' end with a methylated guanosine to be produced. This is crucial for the initiation of the transcription and protection against RNA degradation. After four hours of transcription, synthesized mRNA is purified by extraction with phenol/chloroform mixture. Quantity and quality of the purified mRNA is estimated using both NanoDrop2000 analysis and a 0.8% agarose gel. At the final stage of manipulation, mRNA is diluted to obtain the final concentrations used for injections (Table 7) and stored at -80°C .

mRNA	Concentration ($\mu\text{g}/\mu\text{L}$)
SUR	0.36
Kir6.2	0.12
Kir3.4	0.15
M2	0.15
ICCR	0.24

Table 7. RNA stock concentrations for preparation of oocyte injection mixes.

2. Heterologous expression in *Xenopus laevis* oocytes

2.a. *Xenopus laevis* oocytes

Xenopus oocytes are big spherical cells with a diameter of 1-1.3 mm at stage VI of development. These cells can be handled at room temperature in non-sterile conditions. Their cytoplasm is rich in proteins, ribosomes, tRNA and enzymes essential for protein expression and function. Oocytes have little background channel activity and therefore offer a very high signal-to-noise ratio. For these reasons, *Xenopus* oocytes are an ideal single-cell expression system that is widely used in electrophysiology as a tool for functional characterization of ion channels and transporters.

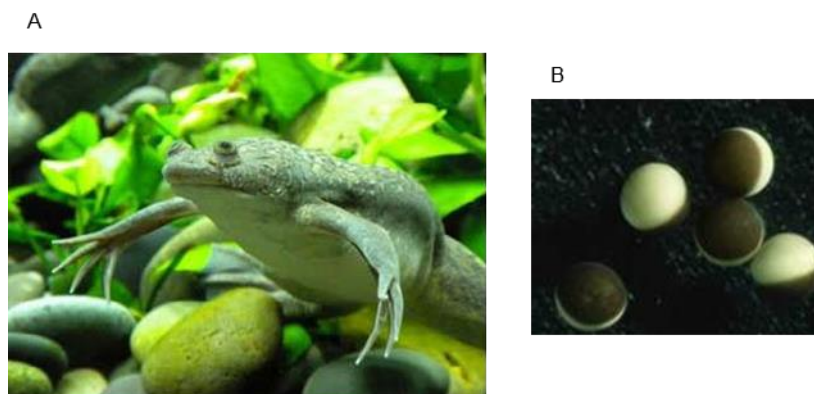


Figure 36. **A.** A fully developed *Xenopus laevis*. **B.** *Xenopus laevis* oocytes at stage VI of development

A *Xenopus* oocyte is divided in two main regions: a well-defined brown hemisphere, the ‘animal pole’, which contains the nucleus, and a yellow hemisphere, the ‘vegetal pole’, containing the majority of the yolk platelets. These two regions are separated by a thin, unpigmented ring called the equatorial belt. Oocytes are encased in a vitelline layer

made of a glycoprotein matrix, which protects the cell against mechanical and pressure shocks, and a follicular layer which protects the oocytes from the outside environment.

Oocytes are localized in the abdomen of the *Xenopus laevis* inside ovaries. Each ovary is subdivided into multiple lobes which contains hundreds of oocytes at different stages of development as well as blood vessels and connective tissue.

2.b. Extraction and preparation of oocytes

The *Xenopus laevis* frogs used for our experiments were provided by the Xenopus Express Company (Vernassal). Animals are raised in water tanks at 22°C with a 12h/12h night cycle. To perform the extraction of the oocytes, animals are first anesthetized with a solution of acid aminobenzoic ethyl ester (1g/L). After 20 minutes, the *Xenopus* are placed on ice. An incision of approximately 8 mm is performed on the skin, and the muscles are incised to enable access to the ovarian lobes. Oocytes are extracted and transferred to Barth's isotonic solution (NaCl 88 mM, KCl 1 mM, NaHCO₃ 2.4 mM, HEPES 16 mM, MgSO₄ 0.82 mM, Ca(NO₃)₂ 0.3 mM, CaCl₂ 0.41 mM, pH 7.4). After oocyte extraction, both incisions are stitched with absorbable thread (5-0, tip 16 mm 3/8c, 75 cm VICRYL Ethicon). The animal is then rinsed and placed into a small container filled with water in order to recover. After a few hours, the awakened animal is transferred to the post-surgery tank.

Oocytes are isolated by enzymatic defolliculation (Type 1A Collagenase, Sigma-Aldrich). Digestion, is performed for 2 hours at 19°C under gentle shaking. After digestion isolated oocytes are rinsed with Barth's solution. The oocytes in stages V-VI of development are selected individually based on visual criteria, choosing those with the best shape and homogeneity of pigmentation. Finally, selected oocytes are stored in Barth's solution supplemented with penicillin and streptomycin.

2.c. mRNA Microinjection

Oocytes are injected the day after surgery. Before injection a reselection is performed, in order to inject only the best oocytes. Micro-injections are performed manually using a Nanoject machine (Drummond). Glass microcapillary (3.5" Drummond # 3-000-203-G/X), pulled horizontally (Micropipette puller P-97, Sutter Instruments Co.) and then broken to a tip diameter of approximately 0.5 µm, are filled with incompressible mineral oil (Sigma-Aldrich) and placed on the Nanoject piston. The glass pipette is then filled with the purified RNA obtained after *in-vitro* transcription.

Oocytes are pricked one by one with the micropipette (micro-injector is set to release a volume of 50 nL per each injection). The amount of RNA injected for each construct is

shown in Table 8. Injected oocytes are then transferred to a 96-well plate filled with Barth's solution supplemented with antibiotics. Plates are incubated at 19°C for 48/72 hours to allow RNA translation.

mRNA	Quantity per oocytes (ng)
SUR	6
Kir6.2	2
Kir3.4	2.5
M2	2.5
ICCR	4

Table 8. Quantity of mRNA encoding indicated constructs injected per single oocyte. This quantity is obtained by adding to the injection mix of 3 μ L, 1 μ L of the mRNA solution indicated in Table 7, and by injecting 50 nL of that mix.

3. Expression in mammalian cells

Mammalian cells are isolated from specific tissues (skin, liver, glands, etc.) and then cultured and reproduced in an artificial medium. The use of mammalian cells allows the analysis of endogenous channels in their native tissues and thus are widely used for biophysical and pharmacological studies of proteins.

In our experiments we used two kind of cell lines: HEK293 cells originally derived from human embryonic kidney cells and INS-1 cells originally from rat pancreas.

3.a. Transfection DNA mammalian cells

Mammalian cell transfection is a method widely used to introduce genetic material into a host cell. There are different ways to transfect mammalian cells, depending on the cell line characteristics. In our experiments, we used the Lipofectamine method and the precipitation with calcium phosphate method to transfect cells with DNA containing the Kir6.2 and/or SUR2A genes.

3.b. Calcium Phosphate Transfection

This technique was performed on HEK293 cells in order to co-transfect SUR2A and Kir6.2. The principle of this transfection method is based on the precipitation of genetic material by a formation of a complex with calcium-phosphate. A calcium-phosphate-DNA complex is obtained by mixing approximately 3 μ g DNA with 6 μ L of calcium chloride at 2M in presence of a buffered saline/phosphate solution. Subsequently, this mixture is

dispersed onto cultured cells. Calcium phosphate helps the binding of the condensed DNA in the co-precipitate to the cell surface, and allows DNA to pass through the cell membrane by endocytosis. The transfected HEK293 cells are maintained in Dulbecco's Modified Eagle Medium (DMEM) with 5% FBS on Poly-L-lysine-coated glass coverslips at 37°C.

3.c. Lipofectamine transfection

In order to analyze Kir6.2 mutants in a native tissue, mutated Kir6.2 plasmid DNA was transfected in INS-1 cells. Since these cells already have endogenous Kir6.2 and SUR1, only mutated Kir6.2 DNA plasmid needed to be transfected.

Lipofectamine (Lipofectamine® 2000, ThermoFisher) is a cationic lipid reagent consisting of a positively charged head group and hydrocarbon chains that facilitate genetic material delivery into the cell. When plasmid DNA is mixed with lipofectamine, the backbone of the nucleic acid interacts with the positive charge of the head group of the lipofectamine and facilitates DNA condensation by forming a liposome/nucleic acid transfection complex. The positive surface charge of the liposomes mediates the interaction of the nucleic acid and the cell membrane, allowing the transfection complex to enter the cell through endocytosis.

4. Electrophysiological characterization of ion channels

Ion channels are membrane proteins that transport ions across the plasma membrane. The ion flow intensity and direction depend on two influences: diffusion force which depends on the concentration gradient and the electric force which depends on the membrane potential. The movement of ions across the membrane translates in an electric current which can be detected by electrophysiological techniques.

4.a. Patch Clamp Technique

The patch clamp technique was invented in 1976 by Neher and Sakmann (1991 Nobel Prize for Medicine and Physiology). This technique and its different configurations (Figure 38), allow the study of a single channel or multiple ion channels. The patch clamp technique is based on the isolation of a patch of membrane with a glass pipette.

In order to get this patch, a contact is obtained by positioning a glass pipette against the plasma membrane of the cell, suction is then applied to help formation a seal which electrically and mechanically isolates a little piece of cell membrane ('patch'). Obtaining a good seal requires a clean and accessible lipid membrane. This implies prior enzymatic

treatment of cells to remove the extracellular matrix or, in the special case of *Xenopus* oocytes, manual removal of the protective vitelline.

During recording, a constant potential value is imposed to the cell membrane ('voltage clamp'). To cancel differences between the measured membrane potential (V_m) and the expected membrane potential (V_i), the amplifier injects a current using a negative feedback loop. This current reflects the ionic current through the membrane patch. Several parameters dictate the properties of the ionic current through an ion channel.

The equilibrium potential or reversal potential (E_{ion}) represents the membrane voltage at which the electrical and diffusive forces counterbalance, meaning that there is no net ion flow across the membrane. E_{ion} depends on the concentrations of the ion (K^+ in our case), on both sides of the membrane. It is given for a given ion by the Nernst equation:

$$E_{ion} = \frac{RT}{zF} * \ln \frac{[ion]_e}{[ion]_i}$$

Where $R = 8.315 J.K^{-1}.mol^{-1}$ (ideal gas constant), T is the absolute temperature, Z is the valence of the ion and $F = 96489 C.mol^{-1}$ (Faraday constant).

The membrane potential (V_m) is imposed by the user in voltage clamp mode.

The conductance of the channel (g_{ion}) corresponds to the ease with which an ion can travel through the channel.

The unitary current i can be calculated using Ohm's law:

$$U = r_{ion} * i$$

where the driving force $U = V_m - E_{ion}$ and $r_{ion} = \frac{1}{g_{ion}}$.

The current through an open channel is therefore given by:

$$i = g_{ion} \cdot (V_m - E_{ion})$$

In voltage clamp, V_m is constant. In our conditions E_K is zero because the concentration of K^+ ions is the same on both sides of the membrane excised patch. Therefore, i is proportional to g which is a characteristic of a given channel (50-80 pS for the K_{ATP} channel).

The opening probability (P_o) is the fraction of time a channel is open, and thus reflects channel activity. If many identical channels are present in the membrane patch, P_o represents also the fraction of channels that are open at any given time. In that case, the recorded current is:

$$I_{ion} = G_{ion}(V_m - E_{ion})$$

Where G_{ion} is the overall, or macroscopic, conductance.

If N is the number of channels present in the patch, G_{ion} is given by:

$$G_{ion} = NP_o g_{ion}$$

Because N , g_{ion} , V_m , E_{ion} are all constant, the macroscopic current I_{ion} is proportional to P_o , and can therefore be used to follow change in channel activity during an experiment. The absolute value of P_o can only be known if N is known, which is rarely the case.

4.b. Patch clamp Instrumentation

The patch clamp setup is described in Figure 37:

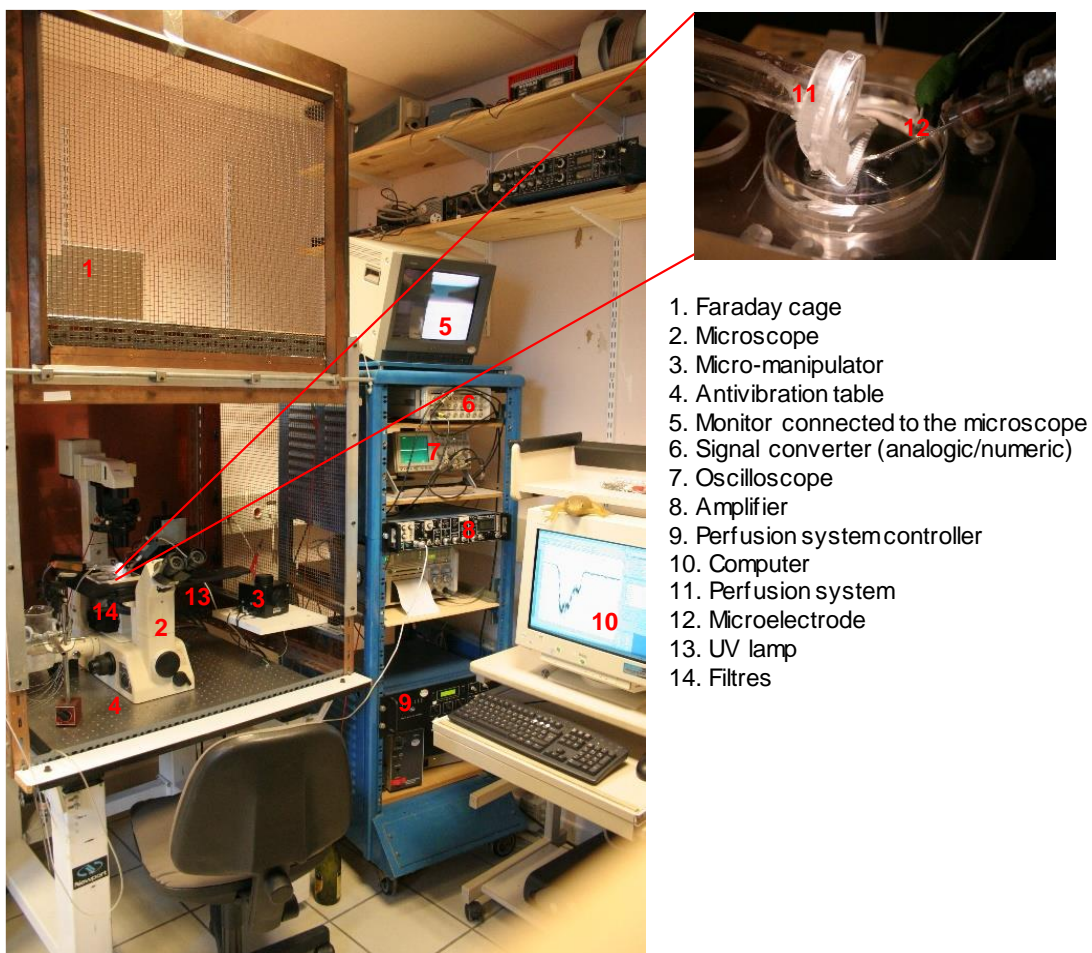


Figure 37. Patch clamp set-up at "Channels" group

Faraday cage: is used in order to protect the experimental area from electromagnetic disturbance.

Microscope: a Nikon diaphot 300/200 with three lenses X 4, X 10, X 40.

Micro-manipulator: an instrument to allow a micrometric displacement of the micropipette in three dimensions.

Anti-vibration table: a damper for mechanical vibrations which must be minimized during any experiment.

Video monitor: connected to the microscope.

Signal converter (analogic/digital): Digidata 1322a to transfer the bidirectional signals between the patch clamp amplifier and the computer station.

Oscilloscope: HM407 (Hameg) enables visualization of the recorded current in real time.

Patch-clamp amplifier RK-300 (Bio-Logic): is used to measure currents as small as pico-ampere (pA). It converts current to voltage using a resistance of 10 G Ω or 100 M Ω and imposes a membrane potential through the patch micropipette.

Perfusion system: is connected to the syringe bodies containing the test solutions.

Perfusion system controller: is a RSC-100 (Rapid-Solution-Changer, Bio-Logic) which is connected to the perfusion system. It enables a rapid and automatic exchange of solutions to test. This system is controlled with a software developed by Michel Vivaudou (Perf).

Computer: allows to manage and follow the experiment.

Microelectrode: is a glass micropipette which contains a silver electrode in the presence of an electrolytic solution. Through this pipette, the patch excision is performed. The microelectrode imposes a voltage (voltage clamp) on the patch and measures the current induced by the ionic flow through the ion channels present in the patch.

UV Lamp a Nikon super high pressure mercury lamp power (model HB-101034AF HB-10104AF), UV-lamp is used as the light source which is directly coupled to the microscope.

Filters are 19000 and 39003 Nikon Eclipse that allow switching between 380 nm and 500 nm excitation wavelengths.

4.c. Patch Clamp configuration

The patch clamp technique can be used in different configurations (Figure 38). The configuration is chosen depending on where the ligand acts. For example the whole-cell configuration is used if we want to study the action of the ligand at the extracellular part of the channel; and the inside-out configuration is used to study the action of the ligand at the intracellular part of the channel. In our experiments with the K_{ATP} channel, we used the “inside-out” configuration.

The inside-out configuration allows the isolation and extraction of a little piece of membrane containing the expressed channels, leaving the intracellular face exposed to different solutions. This kind of configuration is suitable for K_{ATP} channel studies because its regulation depends mostly on ATP and ADP which bind to the intracellular side of the protein, *i.e.*, the site which is exposed to the external solution.

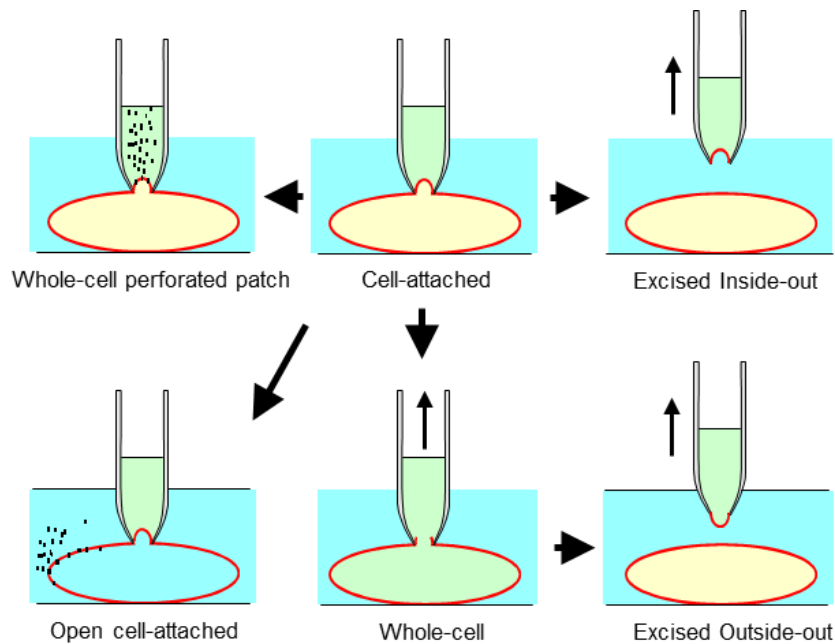


Figure 38. Patch-clamp configurations. « Cell-attached » conserves the cytoplasm integrity. « Whole-cell » allows to measure the total current in the cell. « Inside-out » and « outside-out » allows access to the intra and extracellular side of the membrane, respectively (Channels group).

4.d. Experimental procedure

Oocytes preparation

After 48 to 72 hours of incubation at 19°C (time enough to have a detectable K_{ATP} current, of at least 0.3 μA) an oocyte is placed in a hyperosmotic solution for a few minutes to make it shrink so that the vitelline layer can be removed easily with the help of tweezers.

MATERIALS AND METHODS

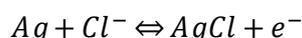
Once the vitelline layer is removed, the oocyte is very fragile and must be immediately transferred to the patch clamp set-up.

Mammalian cells preparation

After 24 to 48 hours of incubation at 37°C (enough time to have a detectable K_{ATP} current induced by P1075 application), the cell culture medium is exchanged for an extracellular solution. The cells are then transferred directly to the patch clamp set-up.

Microelectrodes and solutions

The micropipettes used are made from borosilicate capillaries (Kimax-51, Kimble products), which are exposed to a high temperature and stretched with a controlled tension, using a micropipette puller (P97 Micropipette Puller, Sutter Instrument Co.) resulting in a micropipette with a tip diameter of ~1 μm . Micropipettes are filled with a solution containing a high concentration of potassium ions (150 mM for oocytes and 140 mM for mammalian cells). The concentrations of potassium ions are equal on both sides of the membrane, so that the reversal potential for potassium is zero. A chloride-silver filament allows the conversion of ion flow to electronic current, according to the following reversible reaction:



The current is then amplified, sampled at a rate of 1 kHz and stored and visualized on a computer.

Seal formation

In order to isolate and extract a patch of membrane, it is necessary to pass through a first step called Gigaohm seal formation. This is performed by gently resting the pipette on the oocyte membrane. Once the contact is established, a soft negative pressure is applied by gentle sucking into a tube directly connected to the pipette interior. Negative pressure continues until the connection between the cell membrane and the glass pipette is so strong that the seal resistance reaches a value higher than 1 Gigaohm. The membrane patch is then excised by quick removal of the pipette from the membrane surface and placed in front of the outlets of an automated perfusion system which contains the testing solutions.

Since the only cations present are K^{+} , the only endogenous current that can be detected in the cell membrane is through Ca^{2+} -activated chloride channels and stretch-activated channels. Since $Cl_{(Ca)}$ channels are activated by calcium, these currents can be inhibited

by adding a chelator (Ethylene Glycol Tetra-acetic Acid, EGTA) which removes any activating calcium ions.

In the absence of applied pressure, stretch-activated channels remain mostly closed.

As discussed above, the potassium current (I_K) through ion channels present into the patch is given by the follow equation:

$$I_K = G_K(V_m - E_k)$$

Where,

V_m is the membrane potential (-50 mV, in our condition)

E_k is the K⁺ ions reversal potential (with equimolar potassium, $E_k = 0$),

G_K is given by: $G_k = P_o N g_k$

Where P_o is the channel open probability, N is the number of channels present in the patch, g_k is the unitary conductance of each channel (approximately 70 pS for K_{ATP} channels).

4.e. Optogenetics experiments

4.e.1. Photoswitchable molecule attachment

In our experiments we used the Photoswitchable tethered ligands (PTLs) method for optical control of ion channels. Some potassium channels have been already optically controlled using this method; here a photoswitchable molecule called maleimide-azobenzene-quaternary ammonium (MAQ), which contains a maleimide (M) to tether the molecule to a genetically engineered cysteine, a photoisomerizable azobenzene (A) linker and a pore-blocking quaternary ammonium group (Q) (Banghart et al., 2004; Sandoz and Levitz, 2013; Fortin et al., 2011) was used. The photoswitchable molecule MAQ (200 mM) was provided by Guillaume Sandoz. It was dissolved in dimethyl sulfoxide (DMSO) at a concentration of 20 mM and stored at -80 °C.

In order to attach the photoswitchable molecule to the engineered cysteine, we followed different procedures depending of the expression system.

Photoswitchable molecule attachment in oocytes

To perform the photoswitchable molecule attachment, we used a 96-well plate, as shown in Figure 39. The first well contains 200 μ L of 1 mM dithiothreitol (DTT) in extracellular solution. DTT is used to break all extracellular cysteine bonds to other molecules, mainly extracellular disulfide bridges in the channel. The second well contains 400 μ L of extracellular solution to wash the oocytes after DTT incubation. The third well is first filled

with 150 μL of agarose gel to prevent the oocytes from sticking to the bottom of the well during MAQ incubation. Once the agarose solidifies, the well is washed with 500 μL of extracellular solution, and then filled with 0.2 μL of 20 mM stock of MAQ mixed with 399.8 μL of extracellular solution, for a final volume of 400 μL at 10 μM MAQ. The last well is filled with 200 μL of extracellular solution to wash out any unattached photoswitchable molecule after the MAQ incubation.

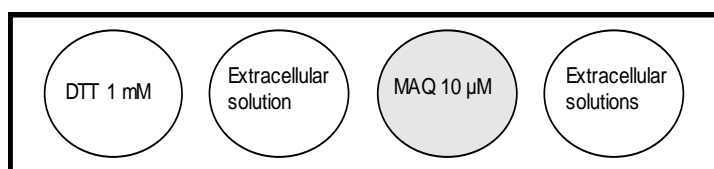


Figure 39. Schematic representation of MAQ attachment incubation sequence. Incubation time in each well (left to the right) : 1 min in 1 mM DTT, 3 mins in extracellular solution, 40 mins in 10 μM MAQ, 5 sec in extracellular solution.

After 48 to 72 hours of incubation at 19 $^{\circ}\text{C}$, oocytes are labelled with MAQ at room temperature using the following sequence:

- 1) Incubation in the DDT well for 1 min.
- 2) Incubate in the second well for 3 min to wash out DTT.
- 3) Incubate in the MAQ well for 40 min in the dark. During MAQ incubation oocytes are turned every 10 min with the help of a glass pipette to ensure uniform MAQ labeling of the entire oocyte surface.
- 4) Incubate in the last well for a few seconds to wash out free MAQ.
- 5) Remove the oocyte vitelline layer and transfer oocyte to the recording set up.

Photoswitchable molecule attachment in mammalian cells

After 24 to 48 hours of incubation at 37 $^{\circ}\text{C}$, coverslips carrying the transfected cells are labeled with MAQ using a 24-well plate. The protocol is similar to the oocyte MAQ labeling, using double volumes of each solution.

4.f. Data processing and analysis

Signals recorded during the experiments are filtered at 300 Hz and sampled at 1 kHz. They can be later digitally filtered at lower frequencies to reduce noise and under-sampled to reduce file size. Sampling, filtering, analysis and data presentation are performed using various software developed by Michel Vivaudou.

The K_{ATP} currents measured in each patch are normalized using as the zero-current baseline the current measured in the presence of 2 mM ATP (where K_{ATP} channels are

closed), and as the open-channel limit the current measured in absence of ATP (where K_{ATP} channels are maximally open). This normalization enables the calculation of statistics in spite of patch-to-patch variability of current amplitudes (Figure 40).

SUR2A+Kir6.2

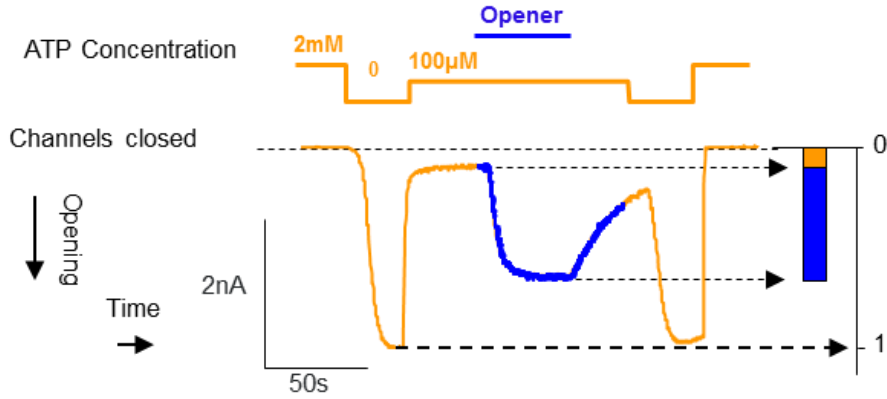


Figure 40. Typical patch-clamp recording in the excised inside-out configuration of wild-type K_{ATP} channels and their response to the pharmacological opener P1075 (10 μ M). The membrane potential is -50 mV. The histogram represents the normalized current, which is 0 when channels are completely closed in 2 mM ATP and 1 is when current is maximal in absence of nucleotides.

The following standard Hill equations were used for fitting:

Activation by openers

$$F(|X|) = i_o + \frac{i_{max}}{[1 + (K_{1/2}/|X|)^h]}$$

Where $|X|$ is the concentration of activator, i_o is the control current (in absence of activator), i_{max} is the maximal current induced by the activator, $K_{1/2}$ is the concentration for half-maximal activation, and h is the Hill coefficient.

Inhibition by nucleotides and glibenclamide

$$F(|X|) = \frac{i_o - i_{min}}{[1 + (|X|/K_{1/2})^h]} + i_{min}$$

Where $|X|$ is the inhibitor concentration, i_o is the control current (in absence of inhibitor), $K_{1/2}$ is the concentration for half-maximal inhibition, i_{min} is inhibitor-insensitive current, and h is the hill coefficient.

Results are displayed as mean \pm standard error of the mean (s.e.m.). Error bars in figures represent s.e.m. and are only shown if greater than the symbols.

5. Two-Electrode Voltage Clamp (TEVC)

The TEVC is a technique used to analyze ion channels in large cells. In the TEVC technique, the membrane of the cell is penetrated by two microelectrodes: one to monitor the membrane potential (which is held at -50 mV) and the other to inject the current necessary to reach the desired voltage that is equal to the membrane current (Baumgartner et al., 1999).

5.a. Experimental procedure

The TEVC technique experimental protocol involves the preparation of ligand solution and microelectrodes. Ligand solutions are prepared in TEVC bath (91 mM KCl, 5 mM HEPES, 1.8 mM CaCl₂, MgCl₂, 1 mM, 0.3 mM niflumic acid, pH adjusted to 7.4 with KOH). Then, microelectrodes are made with two micro-pipettes pulled from borosilicate capillaries (Kimble Product Inc.) in order to obtain a diameter of approximately 10 μm and a resistance between 0.2-0.8 MΩ. Pulled pipettes are subsequently filled with 3 M KCl solution and chloride-silver electrodes are placed inside.

To perform TEVC recordings, we used the HiClamp robot (MultiChannel Systems). As shown in Figure 41, the robot (1) has a table with two 96-well plates, the right side contains a plate with oocytes (8) and the left side contains a plate with the compounds to test (7). With the help of a suction pump the oocyte is transferred from the plate into a silver wire basket (5) which also serves as a reference electrode. Microelectrodes are automatically lowered to impale the oocyte (4) and the membrane potential is clamped to -50 mV. Then, before testing any ligand (in Bath TEVC solution), the oocyte inside the basket is placed in the washing station (localized between the plates, 6), the oocyte is perfused with ND96, Low-K⁺ solution (2) (NaCl 91 mM, KCl 2 mM, CaCl₂ 1.8 mM, MgCl₂ 1 mM, HEPES 5 mM, pH adjusted to 7.4 with NaOH). This step is crucial to choose healthy oocytes. A healthy cell being assumed to have a current that is less than 15 μA, any cell displaying a current higher than 15 μA is discarded (leaky oocyte). This parameter can be adjusted to the channel studied. In addition, the membrane resistance of the cell is tested, and the cell is discarded if it has a low membrane resistance (dead oocyte). An oocyte is considered alive when its measured membrane potential is equal or lower than -10 mV. Subsequently the chosen oocyte is washed with TEVC bath solution (High-K⁺ solution) which produces an electrochemical gradient at -50 mV that force K⁺ ions to enter the cell, creating an inward current. The robot will discard the oocyte if the high-K⁺-induced current is lower than 0.1 μA (this parameter is adjustable) indicating poor expression of potassium channels. Once an oocyte is validated, the robot

follows the pre-defined recording protocol. The basket containing the oocyte is automatically transferred to the compound plate and the basket is moved from one compound to the other in order to investigate channel responses. The protocol usually ends with a 3-mM Barium (Ba^{2+}) application, in order to block K^+ channels and establish the K^+ -current baseline. All liquids coming from the wash station are trashed into a bin (3). Experiments are visually followed with a camera (10) and a light source (9).

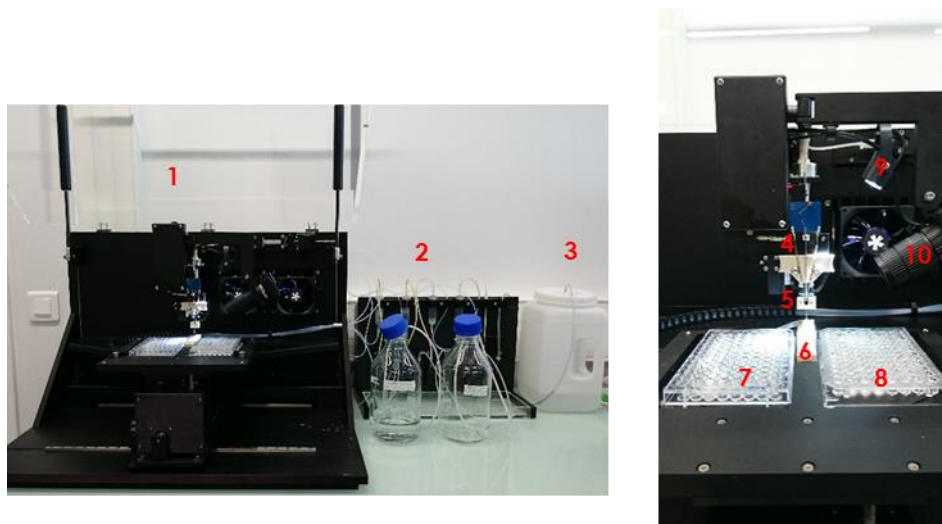


Figure 41. HiClamp Robot (MultiChannel Systems).

5.b. Data processing and analysis

Data is processed with the software HiClamp DataMining and subsequently exported to an Excel file. Software developed by Michel Vivaudou is used to calculate current values in each applied solution. The normalized current is calculated with the following equation:

$$I_{normalized} = \frac{I - I_{\text{Ba}^{2+}}}{I_{\text{bath}} - I_{\text{Ba}^{2+}}}$$

Where I is the current recorded upon application of a specific ligand (agonist/antagonist), $I_{\text{Ba}^{2+}}$ is the current measured in the presence of barium, and I_{bath} is the measured current present in the TEVC bath solution before ligand application.

The percent change in current (activation or inhibition) induced by the applied compound is calculated with respect to “1” (Control current in the TEVC bath solution) and “0” (current in presence of the 3 mM Ba^{2+} solution). Percent change is given by:

$$\%change = (I_{normalized} - 1) * 100$$

where $I_{normalized}$ is the value obtained upon the application of a specific ligand. The data is then fitted according to a standard Hill equation (Figure 42).

MATERIALS AND METHODS

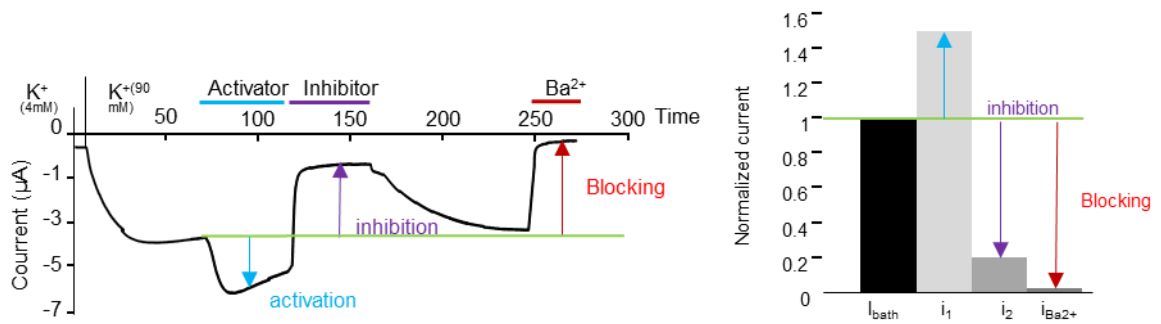


Figure 42. Typical TEVC recording. Blue arrow shows response to an activator, violet arrow shows response to an inhibitor and red arrow represents block by Ba^{2+} . Membrane potential is -50 mV. The histogram at right represents the normalized current, 0 when channels are completely closed ($i_{\text{Ba}^{2+}}$) and 1 in control (i_{bath}), i_1 represents activations and i_2 represents inhibition.

RESULTS

1. Identification of the gates of Kir6.2 controlled by regulatory membrane proteins.

1.a. Relevance of the study

The gating of the Kir6.2 channel alone is mainly controlled by intracellular nucleotides and, like other Kir channels, is also partially controlled by other factors such as pH, Na⁺ ions, or indirectly by G proteins through proteins kinase phosphorylation (PKA and PKC) (Vivaudou et al., 2009). Most of the Kir channels, including Kir6.2, are also dependent on the presence of phosphatidylinositol-(4,5)-bisphosphate (PIP₂) for their activity (Baukrowitz et al., 1998; Shyng and Nichols, 1998). The K_{ATP} channel results from the interaction of two proteins, the Sulfonylurea Receptor (SUR) subunit, an ABC protein, and the inward rectifier K⁺ channel Kir6.2, the pore-forming subunit. The SUR subunit modulates channel gating in response to the binding of intracellular nucleotides or drugs, and the co-assembly of SUR with Kir6.x can affect its sensitivity to ATP by increasing its apparent affinity (Fürst et al., 2014). The full mechanism of how the propagation of molecular motions by regulatory membrane proteins are able to modulate the Kir6.2 channel gate(s) still remains unclear.

The complex regulation by the SUR subunit makes it very difficult to identify the gates of Kir6.x that it modulates. A site-directed mutagenesis of a potential 'gate' residue can either result in actual opening/altering of gate or it can indirectly alter the protein-protein interaction between SUR and Kir6.x. Therefore, straightforward interpretation of mutant phenotypes is limited by possible effects on the SUR/Kir6.2 associations.

Here, we used an artificial and minimal K_{ATP} channel, the "Ion Channel-Coupled Receptors" (ICCRs) (Figure 44), to identify the Kir6.2 gate(s) controlled by regulatory proteins. In ICCRs, Kir6.2 is fused to the C-terminus of a G Protein-Coupled Receptor (GPCR) by a covalent link as the two proteins do not spontaneously associate in physiological conditions. Unlike with SUR, this association of GPCR-Kir6.2 does not affect the intrinsic activity of the channel, the only functional link between the fused GPCR and Kir6.2 being the channel N-terminus (Niescierowicz, 2013).

The objective of this study is to use ICCRs as a tool to functionally map the Kir6.2 gate(s) directly regulated by an interaction at the channel N-terminus with other regulatory subunits, such as SUR or fused GPCRs.

1.b. Project background and experimental approaches

The precise molecular mechanisms of the allosteric regulation of Kir6.2 by SUR are still unknown due to the complex relationship of the physical and functional interaction of the two proteins. Thus the gate(s) regulated by SUR are not identified. Crystallographic structures and functional characterizations of other potassium channels demonstrate the presence of two gates in the transmembrane domains, one in the selectivity filter (Sauer et al., 2011; Cordero-Morales et al., 2006; Proks et al., 2003) and another in the "A" gate at the cytoplasmic interface (Nishida et al., 2007; Pegan et al., 2005). A third gate is present in the cytoplasmic domain of Kir channels, the G loop gate (Jiang et al., 2002; Whorton and MacKinnon, 2011). The molecular identity of the residues implicated in the gate mechanism, according to crystallographic structures data, are shown in Figure 43 (Niescierowicz, 2013). In the selectivity filter, the KcsA E71 (equivalent to Kir6.2 E126) constitutes part of an intricate hydrogen bonding network and can function as a gate (Cordero-Morales et al., 2006). In the second region, the inner helix "A", two constrictions in the ion permeation pathway were found, caused by the two Kir6.2 residues, F168 and L164, which form two hydrophobic seals that close off the pore at the membrane/cytoplasm interface (Loussouarn et al., 2001). In a third region, the G loop, the Kir6.2 I296 residue creates the narrowest section of the cytoplasmic region (Proks et al., 2005). In addition, the T297 residue, located just below the I296 residue, has a hydroxyl group that lies in the cytosolic pore and exposes the oxygen atoms to K⁺ ions. This architecture suggests that K⁺ ions could interact with T297 that could act as a gate (Niescierowicz, 2013).

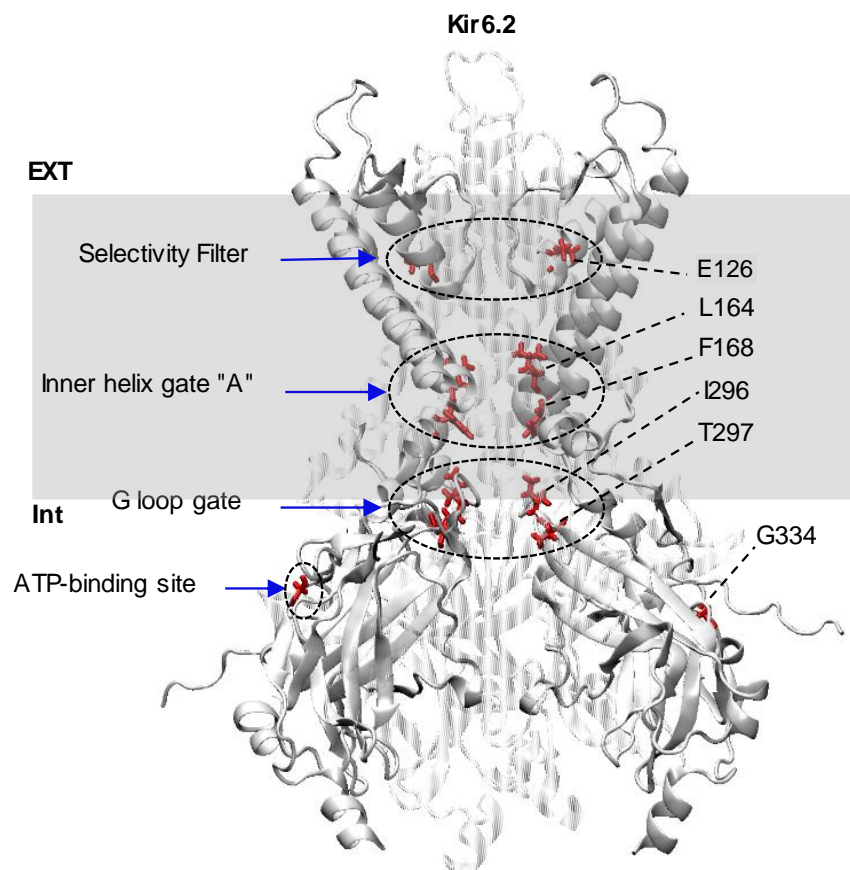


Figure 43. Homology model of Kir6.2, generated by using sequence alignment and crystallographic coordinates of the structure of the Kir3.2 channel. The three proposed gating regions are marked with oval dashed lines. The residues in red are potential gates and G334 is part of the ATP binding site, its mutation in Asp directly impairing ATP binding without affecting the open probability of the channel.

To identify the gate(s) residues controlled by the Kir6.2 N-terminal domain, we developed an original approach based on a functional mapping of the gate(s) under control of the fused GPCR in an agonist-inhibited ICCR.

1.c. Gate scanning approach by site directed mutagenesis.

In earlier studies a M2-based ICCR (M2-K-9-25) was developed where M2 agonists cause channel inhibition (Figure 44) (Moreau et al., 2008). In order to identify the gate(s) regulated by the fused M2 receptor, we used a gate-scanning approach by site-directed mutagenesis (Figure 45). This approach is based on the principle that in a multi-gate system like Kir6.2, closing one gate is enough to close the entire system. Consequently, mutations of gate residues to a short side-chain residue (alanine) should constitutively open the gates and abolish the inhibition by ACh if the mutated residue is the gate

RESULTS

regulated by M2. By mutating one by one the known gate residues, the identification of mutants lacking the ligand-evoked inhibition will reveal the gate under control of the receptor.

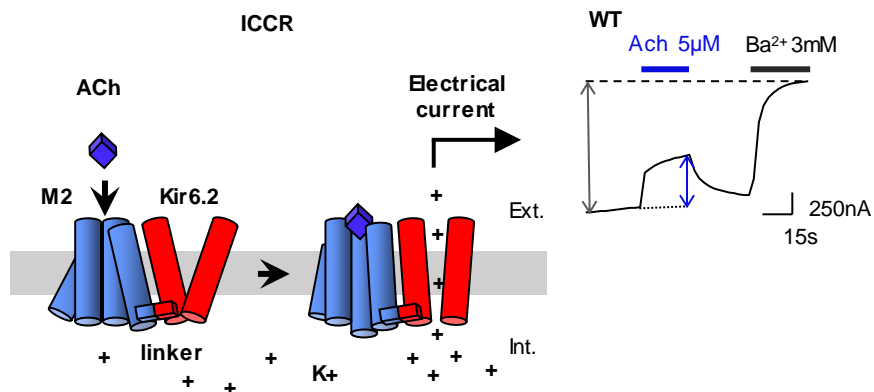


Figure 44. The ICCR principle. Cartoon of ICCR to the left is the GPCR fused to the N terminal of the Kir6.2 channel. Receptor and Kir6.2 are linked in such a way that the binding of a ligand (ACh) to the receptor triggers conformational changes that are transmitted to Kir6.2. The Kir6.2 channel responds to these changes by modifying its gating. The current generated by the flow of K^+ ions through Kir6.2 is detected by electrophysiological techniques. To the right, TEVC representative trace from *Xenopus oocytes* expressing ICCR. Current amplitude was recorded at -50 mV. Dashed line indicates the Ba^{2+} -sensitive current baseline.

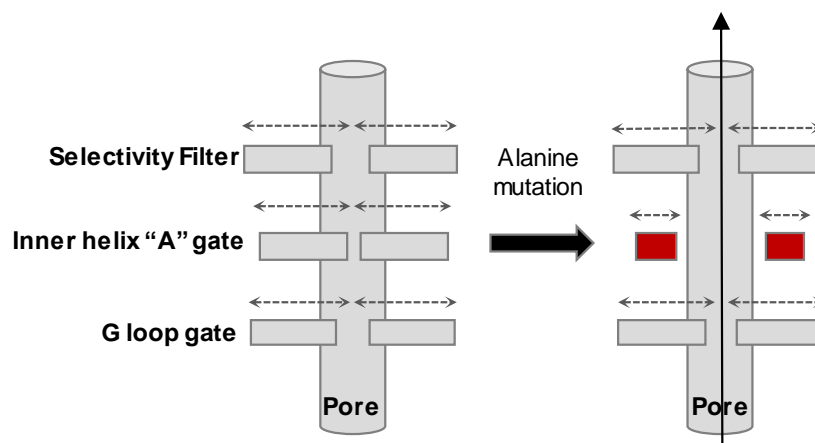


Figure 45. Gate-scanning strategy. This approach is based on the principle that, in a multi-gate system like Kir6.2, closing of one gate is enough to close the entire system. Consequently, mutations of gate residues in short-chain residues (represented by red rectangle) should constitutively open the gates one by one. Identification of the mutants lacking the ligand-evoked inhibition will reveal the gate under control of the receptor.

Oocytes expressing the WT and mutants ICCR were tested in TEVC at -50 mV in symmetrical K^+ concentration, as shown in Figure 44. Results demonstrated that, in the

RESULTS

“selectivity filter” region, E126A did not show any detectable surface expression; the amplitude of the basal currents being equivalent to those generated by non-injected oocytes (Figure 46). In the “inner helix A” region, L164A showed a basal current higher than that produced by the WT ICCR (Figure 46). This could be due to a stabilization of the open state of the channel. Moreover, the inhibition induced by ACh was only 12 (Figure 46). On the other hand, the basal current recorded from the F168A mutant was comparable to that of WT ICCR, but its response to ACh showed a dramatic loss of ligand inhibition of the channel (7%). These results suggest that both L164 and F168 constitutes potential gates in Kir6.2 that are under control of the fused receptor.

In the G loop region, the I296A mutant did not show any detectable surface expression. We then decided to investigate another well-characterized pathophysiological mutant (I296L) that produced basal currents larger than that of the WT (Proks et al., 2005) (Figure 46). Functional characterization by ACh application revealed a complete loss of channel regulation by the GPCR ligand (Figure 46) despite the similarity of size and hydrophobicity of Isoleucine and leucine. This lack of M2-evoked modulation suggests that I296 is a physical gate under control of the fused receptor.

T297A did not change the basal current (Figure 46), compared to the WT ICCR. Also, ACh application induced a strong inhibition of the channel (45 %) similar to its effect in WT ICCR (Figure 46) indicating that this residue is not involved in gating regulation.

In order to rule out the hypothesis that M2 closes Kir6.2 by stabilization of ATP binding, we mutated G334 to an aspartate (G334D), which has been shown previously to directly impair ATP binding without affecting the open probability of the channel, and consequently, without affecting gating (Drain et al., 1998). The basal current of G334D was higher than the WT ICCR and application of ACh resulted in a similar inhibition of the channel (43 %) compared with the WT ICCR. Thus, the inhibition of Kir6.2 by M2 receptor is independent of ATP binding, indicating that the GPCR is able to stabilize the closed state of Kir6.2 in the absence of ATP, reinforcing the hypothesis of direct actuation of gate residues by M2 conformational changes.

RESULTS

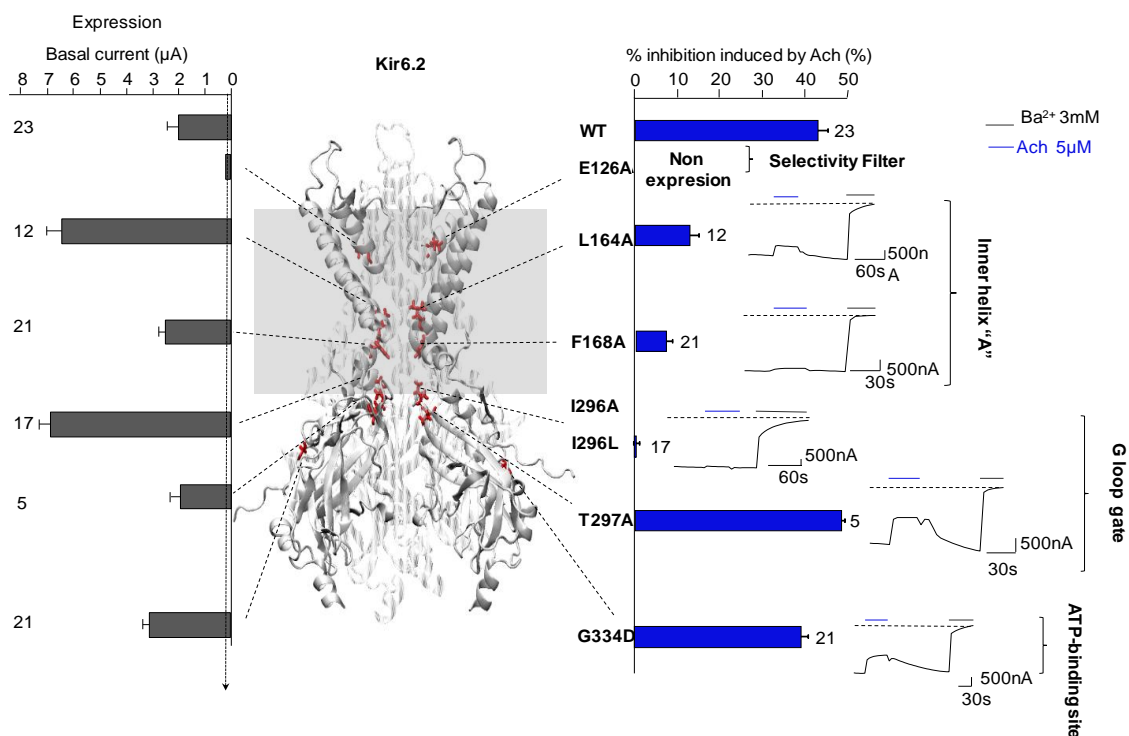


Figure 46. The functionality of the ICCR WT and mutants were measured by Two-Electrode Voltage Clamp using a HiClamp robot. The oocyte is impaled by 2 glass pipettes containing 3 M KCl and an Ag/AgCl electrode. The TEVC bath has a potassium concentration similar to the intracellular K^+ concentration, Current amplitude was recorded at -50 mV. To the right representative TEVC traces from oocytes expressing WT and mutant ICCR. Dashed lines indicate the Ba^{2+} -sensitive current baseline. Histogram on the left shows basal currents; Histogram on the right shows the change in basal current upon application of ACh.

These experiments were done by Katarzyna Nieścierowicz at the institute of structural biology (IBS), Channels team, Grenoble, France (Niescierowicz, 2013).

1.d. Effect of I296L mutation of the G loop gate

To further examine the strong effect of the G loop gate I296L mutation, we extended the study to a molecular level. Taking into account that the leucine side chain is similar in terms of length and hydrophobicity to the isoleucine side chain, we decided to mutate to a valine and a methionine in order to test the effect of a β -branched and a long side chain, respectively. It should be noted that the equivalent of Kir6.2 I296 residue in other Kir channels is a Methionine.

Oocytes expressing the ICCR WT and I296 mutants were tested by TEVC at -50 mV. As shown in Figure 47, ACh application induced an inhibition of around 30% of the I296M mutant, less than for the WT ICCR (approximately 43 % inhibition). On the other hand, I296V showed a much lower inhibition (12 %). This result suggests that reduction of the

RESULTS

side chain, by mutation to valine, alter the regulation while, the lack of β branching had no effect. Nevertheless, the different responses obtained with leucine and isoleucine where is a different branching of a methyl group along the side-chain; γ and β position, respectively, suggest that the γ methyl branched into the side chain could stabilize the open state. This suggests that the length of the side-chain and the position of the branch within the side-chain are the critical molecular parameters for the proper regulation of the gate.

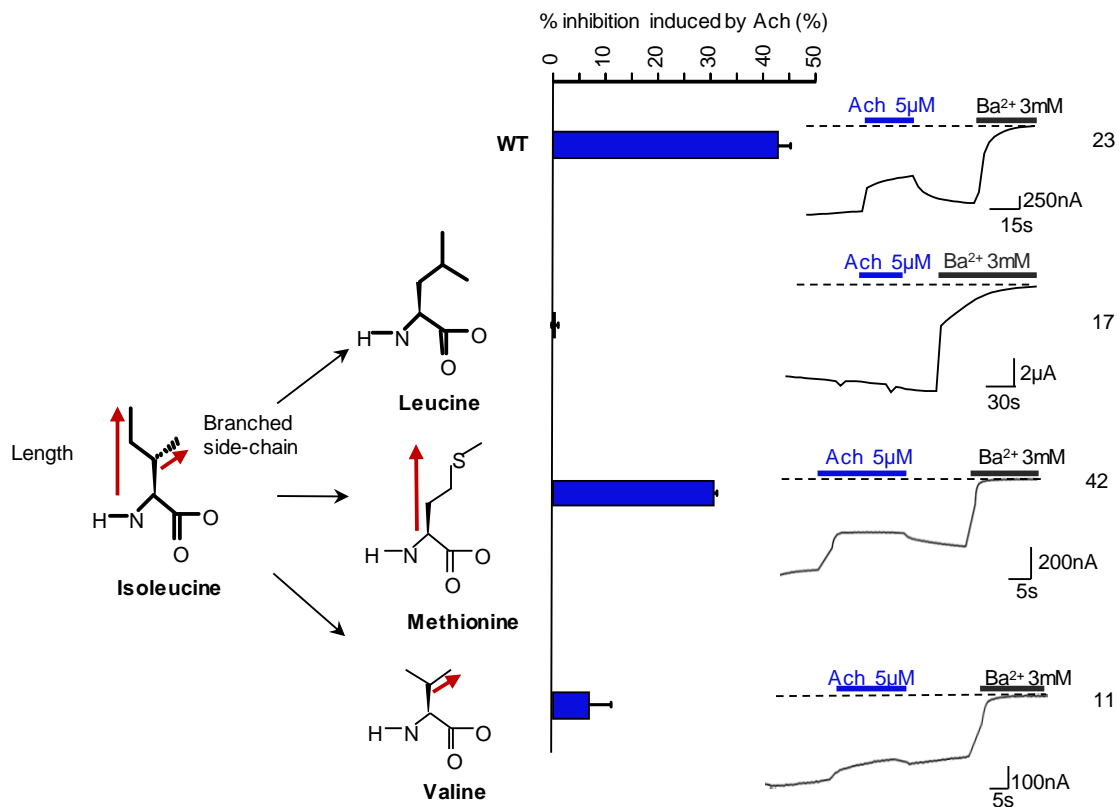


Figure 47. The functionality of the WT and I296 mutant ICCR were measured by Two-Electrode Voltage Clamp (TEVC) using a Hi-clamp robot. TEVC bath has a potassium concentration similar to the intracellular K^+ concentration. Current amplitude was recorded at -50 mV. To the right, representative TEVC traces. Dashed line indicates the Ba^{2+} -sensitive current baseline. Blue bars represent the change in basal current evoked by ACh.

1.e. Do mutations at position M314 in Kir3.4 and I296 in Kir6.2 have the same effect?

Kir6.2 and Kir3 channels are members of the inward rectifiers family. The Kir channels share 2 TM helices plus a P-loop per subunit, and they contain substantial N- and C-terminal domains that are implicated in biological regulation of channel gating (Sansom et al., 2002). They contain the K^+ channel signature sequence amino acids that form the

RESULTS

selectivity filter (Doyle et al., 1998; Nishida and MacKinnon, 2002). Another prominent feature of Kir channels is their regulation by the signaling lipid phosphatidylinositol 4,5-bisphosphate (PIP₂) (Pegan et al., 2005; Lopes et al., 2002). Kir3 channels, there is a complex interplay between the effects on gating of beta–gamma G-protein subunits and PIP₂: both appear to be important for channel opening through direct interactions with the ion channel (Huang et al., 1998), while, when PIP₂ interact with Kir6.2 channel results in an increased open probability (P_o) of K_{ATP} channels (Hilgemann and Ball, 1996; Fan and Makielski, 1997; Shyng and Nichols, 1998).

We extrapolated the study to Kir3 channels. The Kir6.2 I296 equivalent in Kir3.4 is M314, as it is shown in Figure 48A. In order to compare the phenotype of the G loop gate mutants of Kir6.2 with the equivalent in the Kir3.4 channel, the Kir3.4 M314 residue was mutated to an isoleucine (Kir6.2 WT) and a leucine (constitutively opened Kir6.2 channel).

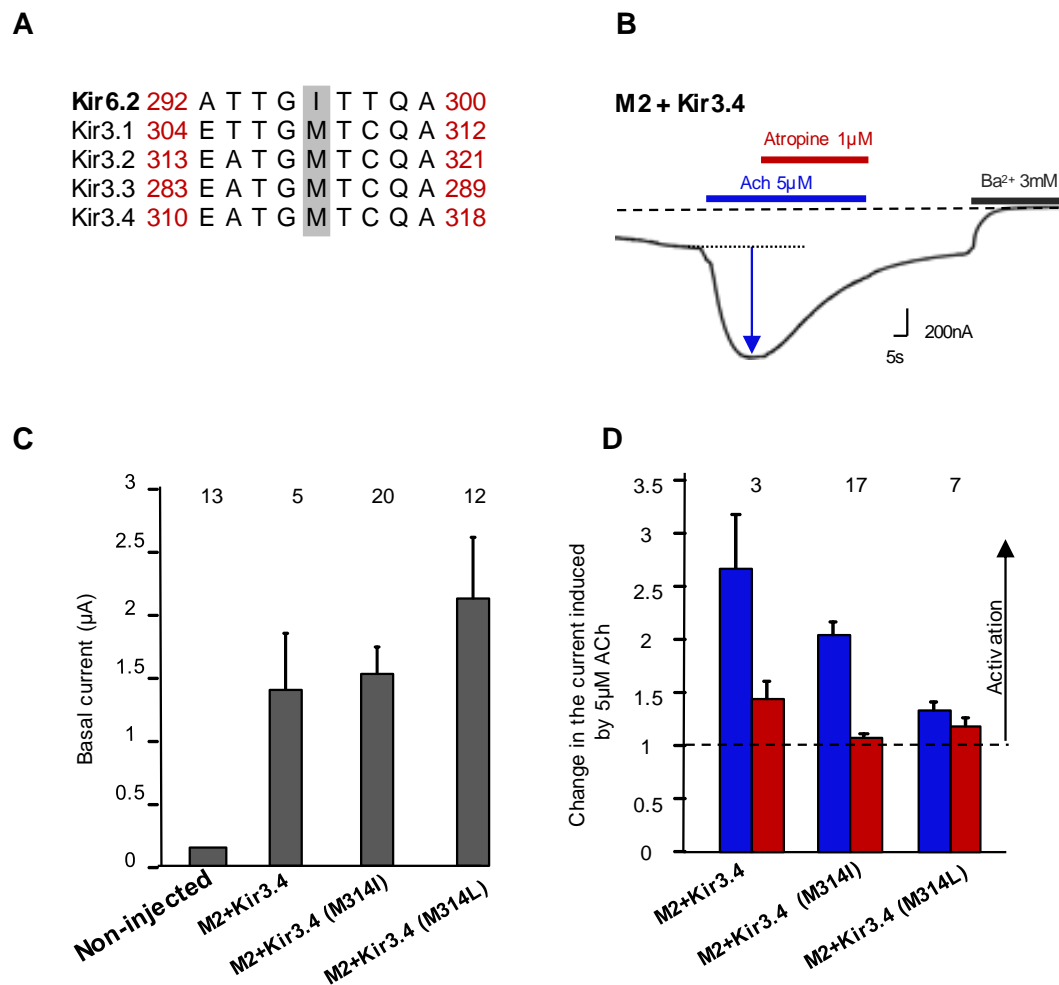
It must be recalled that the Kir3.x channel is physiologically activated via the heterotrimeric Gi/o proteins by the M2 muscarinic receptor. Binding of the endogenous M2 ligand, the agonist acetylcholine (ACh), triggers the activation of Gi/o proteins, the release of Gβγ subunits, and subsequently the opening of Kir3 channels. Additionally, the specific region or amino acids involved in Gβγ binding was further mapped to residues in the N-terminus of the channel (He et al., 2002). On the other hand, the atropine ligand (antagonist) can disturb the binding of ACh causing a loss of the activation.

Here we used a Kir3.4 S143T mutant channel termed as our WT. The Serine¹⁴³ was identified as a residue essential for the physiological heterotrimeric association with Kir3.1 channel. The mutant Kir3.4 S143T allows the surface expression of homomeric Kir3.4 channels which simplifies micro-injection in *Xenopus oocytes*. Additionally, it has been shown that a mutation to a threonine enhances the activity of the channel (Vivaudou et al., 1997). In order to study the Kir3.4 channel, we co-injected with the M2 muscarinic receptor the RNA coding for Kir3.4 (S143T) (WT) and both M314I and M314L mutants. Subsequently, oocytes expressing the M2 + WT and mutant Kir3.4 were tested by TEVC at -50 mV. M314L and M314I mutants showed a slightly larger and similar basal current compared to WT Kir3.4, respectively (Figure 48C). The activation by ACh is conserved when Kir3.4 M314 is mutated to Isoleucine like in WT Kir6.2, indicating that the function of the physiological gate is preserved. However, when Kir3.4 M314 is mutated to leucine, the percentage of activation dropped to 35 % respect to the basal

RESULTS

current compared to the WT (167 %), indicating a significant distortion of the physiological function of the Kir3.4 gate (Figure 48D).

Figure 48. The functionality of the WT Kir3.4 and M314 mutants were measured by TEVC with a



HiClamp robot. **A.** Alignment of human Kir6.2 with human Kir3.x at the G loop level. Highlighted in gray is the position of Kir6.2 L296. **B.** TEVC representative trace from *Xenopus* oocytes expressing M2 + WT Kir3.4. $V_m = -50$ mV. Dashed line indicates the Ba^{2+} -sensitive current baseline. Blue line indicates the application of ACh and red line the application of Atropine **C.** Average basal current for M2 + Kir3.4 WT and M314 mutants. Error bars represent s.e.m. **D.** Average changes in current induced by 5 μ M ACh. Currents were normalized to the basal current level. (A value of 1 represents the current at the basal current level). Blue bars represent the application of ACh and red represent the application of ACh + Atropine, for M2 + Kir3.4 WT and M314 mutants. Error bars represent s.e.m.

1.f. Do GPCR and SUR act on the same gate residues?

Previous studies have demonstrated that Kir6.2 L164A, F168A and I296 mutations can cause a significant loss of the ATP sensitivity by increasing the open probability of the

RESULTS

K_{ATP} channel, and thus disturbing the gate regulation (Proks et al., 2005; Rojas et al., 2007; Koster et al., 1999a). In the ICCR, the Kir6.2 channel is directly fused by its N-terminus to the C-terminus of GPCR. Moreover, it has been shown as well for the wild-type K_{ATP} channel that the N-terminus of Kir6.2 interacts with the C-terminus of SUR creating a binding site for the sulfonylureas (Reimann et al., 1999; Kühner et al., 2012). Additionally, deletion of the Kir6.2 N-terminus causes an increase in the stability of the open state of the K_{ATP} channel, suggesting that the N-terminus is involved in gating regulation (Koster et al., 1999b). Based on this observation we tested the ability of the sulfonylurea drug glibenclamide to close the different G loop gate mutants in the natural K_{ATP} channels. We performed patch-clamp recordings in the inside-out configuration using oocytes expressing the Kir6.2 mutants and the SUR2A receptor subunit. The results (Figure 49) demonstrate the Kir6.2 L164A and I296L mutations can completely abolish the blocking effect of glibenclamide suggesting a common mechanism between the two N-terminally interacting molecules, glibenclamide and the fused M2 receptor. The characterization of the Kir6.2 F168A mutant was impeded by the lack of ATP sensitivity as no baseline can be determined. These results suggest that perhaps the Kir6.2 L164 and I296 residues are gate residues in the K_{ATP} channel, which are regulated by actuation of the N-terminus of the Kir6.2 channel.

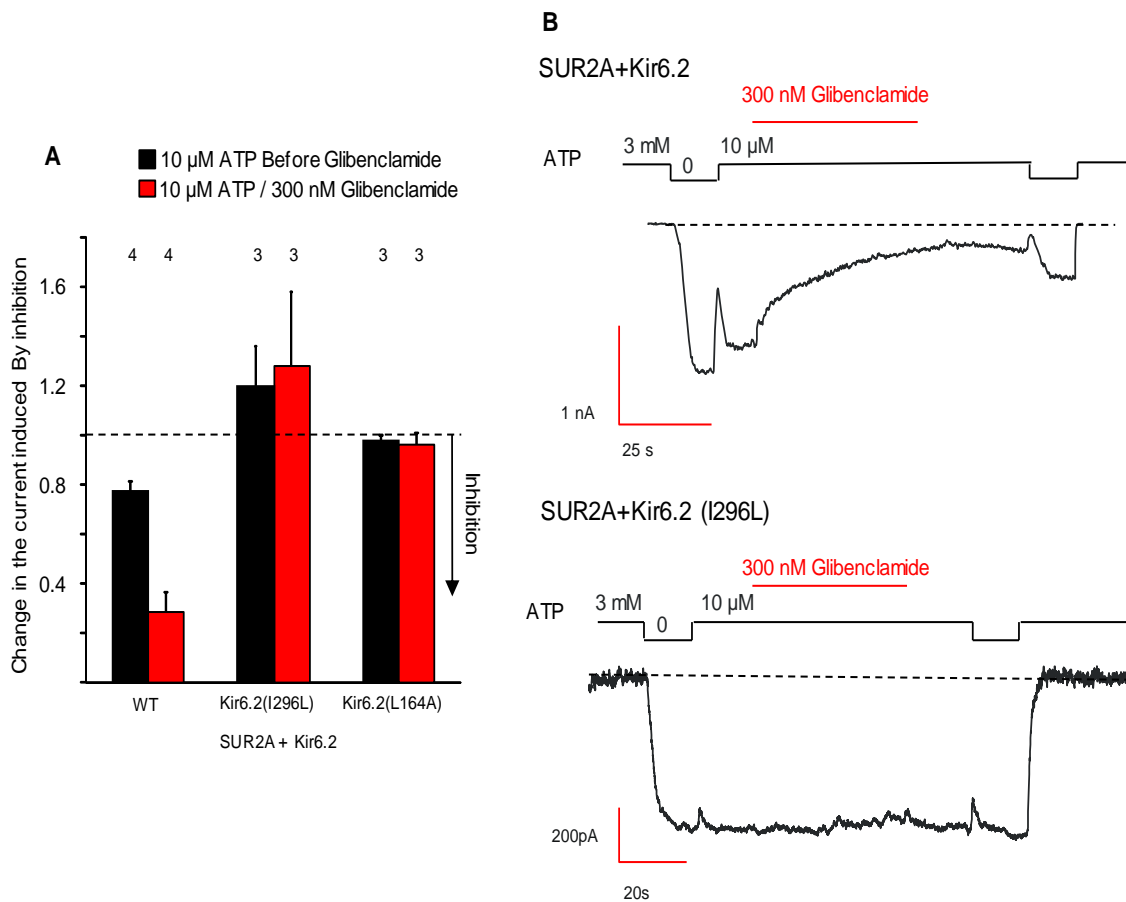


Figure 49. A. Glibenclamide responses of wild-type and mutated K_{ATP} channels. Responses were measured in inside-out patches excised from oocytes co-expressing SUR2A and Kir6.2 wild type or mutant. Glibenclamide (300 nM) was applied in the presence of 10 μ M ATP, and currents were normalized to the current measured in 10 μ M ATP before blocker application. Application of 10 μ M ATP alone (black bars) was used as a control. Numbers indicate the number of patches included in each average. Error bars represent s.e.m. **B.** Representative patch clamp recordings obtained in the excised inside-out configuration. Voltage was clamped at -50 mV and the potassium concentration is symmetrical.

1.g. Discussions and perspectives

It has been proposed that K^+ ion conduction might be regulated by three gates localized in: the selectivity filter (Proks et al., 2003; Cordero-Morales et al., 2006; Cheng et al., 2011); the bundle-crossing region of the transmembrane domain (TMD) (Doyle et al., 1998; Jiang et al., 2002); and the apex of the cytoplasmic domain (CTD) (Pegan et al., 2005; Nishida et al., 2007). We investigated these three regions in order to identify the residues implicated in the regulation of Kir6.2 channel modulated gate(s) by proteins interacting with the channel N-terminus.

RESULTS

The selectivity filter region

The selectivity filter has been proposed as a gate by Proks et al. claiming that the intracellular ligand-regulated gate of Kir6.2 is localized in and above the selectivity filter, however, they did not propose any specific residue (Proks et al. 2003). In other studies, with the KcsA channel, a bacterial homolog of mammalian potassium channels, it was demonstrated that, despite the high rigidity of the selectivity filter, it undergoes a larger conformational excursion than previously estimated. In addition, in the KcsA channel, the E71 residue equivalent to the Kir6.2 channel E126 residue, that constitutes part of an intricate hydrogen bonding network, it was demonstrated by a mutation to an alanine (E71A) to affected the selectivity filter toward a constitutively open state (Cordero-Morales et al., 2006) (Cordero-Morales et al., 2006; Cheng et al., 2011). In our trials we did not observe any macroscopic current generated by the mutant ICCR (E126A), making it impossible to determine if E126 residue constitutes a gate in the Kir6.2 channel. However, we assumed that this mutation could trigger strong structural rearrangements which, in contrast to KcsA, resulted in a non-conductive channel (or incorrectly folded ICCR trapped in the endoplasmic reticulum) (Niescierowicz, 2013).

The helix bundle-crossing region

Crystallographic studies of eukaryotic homologous channels, Kir3.2 (GIRK2) and Kir2.2, revealed that significant motion occurs in this region upon binding of specific ligands. It has also been suggested as an important region for the Kir channel closure, nevertheless the presence of a gate in the Kir channel bundle-crossing has been frequently questioned (Proks et al., 2003; Whorton and MacKinnon, 2011; Hansen et al., 2011; Clarke et al., 2010). It has been found that two constrictions in the ion permeation pathway caused by the two Kir6.2 residues F168 and L164, form two hydrophobic seals that close off the pore at the cytoplasm interface as is shown in Figure 50 (Loussouarn et al., 2001; HAIDER et al., 2005).

RESULTS

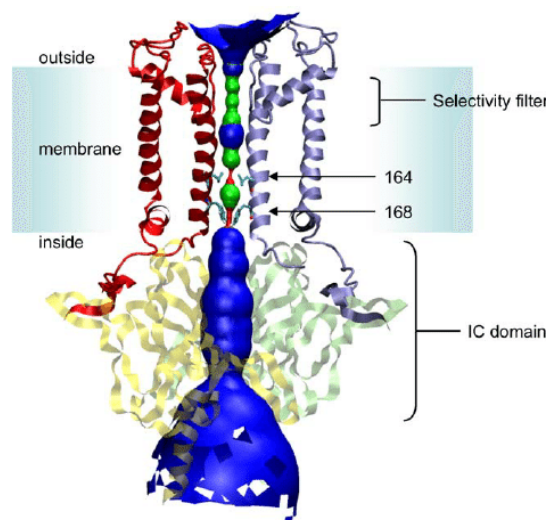


Figure 50. HOLE plot of the permeation pathway of Kir6.2. For precision, the TMs of two subunits and the IC domains of two separate subunits are illustrated (using distinct colors). The color code for the permeation pathway corresponds to the ability of water molecules to pass through a particular protein domain. Red indicates a domain with a radius of $<1.15 \text{ \AA}$, which means that no water can pass (e.g. at residues F168 and L164). Green indicates a radius of $1.5\text{--}2.3 \text{ \AA}$ so single file water molecules can pass, and blue refers to a radius of $>2.3 \text{ \AA}$ which means that multiple water molecules can pass simultaneously. Residues of interest, leucine 164 and phenylalanine 168, create a ring that lies in the plane of the membrane at the level of helix-bundle crossing (HAIDER et al., 2005).

Previous studies of Kir6.2 L164 residue demonstrated the importance of this residue for the proper function of the channel (Tammaro et al., 2008). Nevertheless, it has been suggested that this residue plays a minor or no contribution into the channel gating (Khurana et al., 2011). Our data demonstrated a significant increase in whole-cell currents for the ICCR mutant (L164A), it was approximately 3-fold larger than ones generated by WT proteins. However, despite the higher basal currents, fused GPCR was still capable to partially modulate channel activity. Surprisingly, modulation was significantly lower (10% inhibition of basal currents), than in the case of WT ICCR (43% inhibition), as is shown in Figure 46. The change in generated basal whole-cell currents and a 80% loss of channel modulation suggest implication of L164 in gating control of Kir6.2 channel by the GPCR (Niescierowicz, 2013). On the other hand, previous studies on the Kir6.2 F168 residue demonstrated that a bulky, aromatic phenylalanine residue not only may occlude the ion conduction pathway in the closed state, but can also act as the facilitator (which lowers the energy barrier necessary for the gating transition) in Kir6.2 channel gating (Rojas et al., 2007). In addition it has been proposed that possible conformational changes in the region of F168 can promote channel opening, and are

RESULTS

functionally coupled to the intrinsic ATP-binding site (Khurana et al., 2011). In our results, the F168A mutant did not vary significantly from those generated by WT protein. Theoretically, we should expect much higher basal current due to 'loss-of' a gate; however, one possible explanation could be a higher open probability of the mutant, but a lower surface expression. Nevertheless, whole cell recordings do not allow to distinguish a change in the number of channels and a change in the open probability. Results for both ICCR mutants [M2-K (F168A)-9-25 and M2-K (L164A)-9-25], demonstrated that alanine mutation did not abolish completely the gate regulation of the Kir6.2 channel. This suggests that both residues are implicated in the regulation of the gate but that they do not stand a gate for themselves. This means the existence of a gate which is modulated by a system of different residues (doors), so suppression of one door is not enough to completely alter the gate regulation of the channel. Moreover, these two residues behave as a set of door to form a single gate controlled by the fused GPCR, due to their close spatial proximity in predicted secondary structures (Niescierowicz, 2013).

The G loop region

Previous crystallographic and functional studies of other members of the potassium inward rectifiers family suggest that this region of the channel appears as a gate (Pegan et al., 2005; Whorton and MacKinnon, 2011; Hansen et al., 2011). We decided to test the Kir6.2 I296 residue since it is known that it creates the narrowest section of the cytoplasmic ion permeation pathway (Proks et al., 2005). In our results, the I296A mutation in the ICCR (M2-K (I296A)-9-25) did not produce detectable currents, perhaps due to a non-functional channel. However, earlier studies have demonstrated that another Kir6.2 mutation of I296, I296L, is associated with permanent neonatal diabetes mellitus. Additionally, the Kir6.2 I296L mutation results in developmental delay, muscle weakness and epilepsy (Proks et al. 2005). A previous characterization of the Kir6.2 I296L channel showed a marked increase in resting whole-cell K_{ATP} currents by indirectly reducing the ATP sensitivity through stabilization of the open state of the K_{ATP} channel (Proks et al. 2005). Applying the ICCR approach to the physiopathological Kir6.2 I296L mutation in ICCR (M2-K (I296L)-9-25) produced significantly high whole-cell basal currents and was totally insensitive to M2 regulation. Thus, the I296L mutation completely abolished the regulation of Kir6.2 by the M2 receptor. This is consistent with data concerning natural K_{ATP} channels and strongly suggests that I296 serves as the functional gate under control of the fused receptor. While the Kir6.2 T297 residue (located just below the I296 residue in the predicted secondary structure) has a hydroxyl group that lies in the cytosolic pore and exposes oxygen atoms to K^+ ions as it takes

RESULTS

place in the selectivity filter. The ICCR T297A mutation (M2-K (T297A)-9-25) did not induce any significant change, neither in basal current, nor in regulation induced by applied ligand. This finding clearly verified that residues in close proximity to the G loop gate I296 does not generate the same phenotype, enhancing the role of I296 in the regulation of the Kir6.2 gating.

Kir gate(s) mechanism by regulatory proteins

Today, the presence of three doors that control the opening and closing (gating) of the K_{ATP} channels has been proposed: (1) the selectivity filter, which modulate the fast apertures and closures (*bursts*) (Proks et al., 2003; Cordero-Morales et al., 2006; Cheng et al., 2011), (2) the bundle-crossing region of the transmembrane domain (TMD) (Jiang et al., 2002; Doyle et al., 1998) and (3) the apex of the cytoplasmic domain (CTD) (Pegan et al., 2005; Nishida et al., 2007). Two later doors control the duration of the “*bursts*” and the long closures.

The close spatial proximity in predicted secondary structure of L164A and F168A, and the ICCR approach results (M2-K (L164A)-9-25 and M2-K (F168A)-9-25) suggest that these two residues are involved in the gate mechanism, but that they do not stand as a gate controlled by the fused GPCR alone. This means the presence of a single gate which contains different residues, where the modification of one residue, in our case alanine mutation, is not enough to completely abolish the whole gate modulation by the fused GPCR, as shown in Figure 46. In addition, our test with the ICCR (I296L) mutation (M2-K (I296L)-9-25) as it is shown in Figure 46, strongly suggests that I296 is a crucial gate under control of the fused receptor.

Moreover, it has been found by crystallographic studies of the GIRK2 channel that the gating mechanism by the presence of PIP_2 , causes conformational changes which are associated with a displacement and rotation of the G loop, and a change in the positions of three amino acids that form the gate's constriction, among those is the equivalent residue of Kir6.2 (I296), the M319 residue. Clearly, however, both the G loop gate and the inner helix gate linger closed in the presence of PIP_2 . Nevertheless, the PIP_2 alone is not enough to open GIRK channels in electrophysiological experiments (Whorton and MacKinnon, 2011). Furthermore, a recent study suggests that several K^+ channels seem to possess a highly hydrophobic inner pore that can function as an effective barrier to ion permeation (Aryal et al., 2015). Based on this, we hypothesize that the gate residues in the bundle crossing region (L164 and F168) and the G loop (I296) of the Kir6.2 channel could stand as single gate controlled by the channel N-terminal domain. On the other hand, it could be possible that there are several hydrophobic gates, as shown in Figure

RESULTS

50, but the scanning approach suggests that all three gating residues create a hydrophobic seal (Gate 2) that prevent ion conduction through the pore. Thus we propose the presence of two gates in the Kir6.2 channels, as is shown in Figure 51: one in the selectivity filter (Gate 1) which modulates the fast opening and closing (*bursts*) and the other that forms the slow gate, composed by the three residues in the bundle crossing region and the G loop (Gate 2).

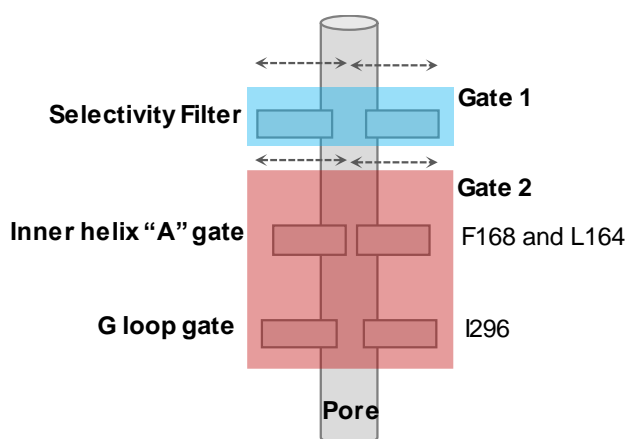


Figure 51. Representation of Kir6.2 channel gating mechanism. The Gate 1 (blue) located in the selective filter would modulate the fast opening and closing (*bursts*) and the gate 2 (red) that controls the duration of the “bursts” and the long closures, which is composed by the bundle crossing region and the G loop residues.

As shown in Figure 47, the results suggest that the Kir6.2 I296 residue mutated to a leucine completely abolished the modulation of the G loop gate by the M2 receptor. This result is puzzling as the leucine and isoleucine side chains are highly similar (same length, same atomic composition and same hydrophobicity). The only difference is the different branching of a methyl group along the side-chain either in γ position (Leu) or in β position (Ile). To investigate whether this difference in branching is involved in the regulation of the G loop gate, we mutated I296 into a valine and a methionine, to either reduce the side chain length or to remove the branching, respectively. As shown in Figure 47, reducing the length of the side chain altered the regulation while, the lack of β branching had no effect suggesting that a relatively long side-chain at position I296 is crucial for the gating regulation while the β branching is not. While keeping a long side chain, the mutant in leucine shows that branching a methyl group in γ position has a dramatic effect on the gating by completely abolishing the regulation. Consequently, a side chain longer than the valine one and an absence of γ -branching is required for the regulation of the gating.

RESULTS

To determine whether this mechanism occurs also in other members of the Kir family, we mutated the G loop gate residue (M314) of Kir3.4 channels into isoleucine and leucine. The same phenotypes were obtained with the Kir3.4 mutants as for the Kir6.2 mutants suggesting that the molecular mechanism of the G loop gate regulation is conserved between Kir6.2 and Kir3.4 channels. As Kir3.4 is physiologically activated by the G $\beta\gamma$ subunits, these results indicate that the G loop gate is involved in this regulation and that the G loop gate residue (M314) must not have γ branching on its side chain. These results strengthen the hypothesis of similar molecular mechanisms of the allosteric regulation of Kir6.2 and Kir3.4 channels by a fused GPCR or the G $\beta\gamma$ subunits, both interacting with the respective ion channel N-terminus.

Based on these results and the partially opened and partially closed crystal structures of Kir3.2 (GIRK2) (Whorton and MacKinnon, 2011; Nishida et al., 2007; Tao et al., 2009; Whorton and MacKinnon, 2013), we hypothesize that a similar molecular mechanism of regulation through the N-terminal domain could occur in other Kir channels. As is shown in Figure 52, the molecular mechanism of the opening and closing of the gate can be imagined as a slight motion of the G loop gate (M319 in Kir3.2 equivalent to I296 in Kir6.2) away from the bundle crossing gate (residues F192 in Kir3.2 equivalent to F168 in Kir6.2). In this configuration, the gate residues interact with their equivalent in adjacent subunits creating a constriction closing the ion conduction pathway. Subsequently, opening is caused by a conformational change characterized by a displacement and rotation of the G loop towards the transmembrane domain bringing the residues F192 and M319 close enough to interact. It results in a break of the inter-subunit interactions and the opening of the gates. On the other hand, our findings demonstrate that a mutation in the G loop gate residue to leucine could cause a stabilization of the open state of the Kir channel. This is due to the γ branching of the side chain. We hypothesize that the double methyl group in γ position of the leucine increase the energy of interaction between F192 and M319L and stabilize the open conformation.

RESULTS

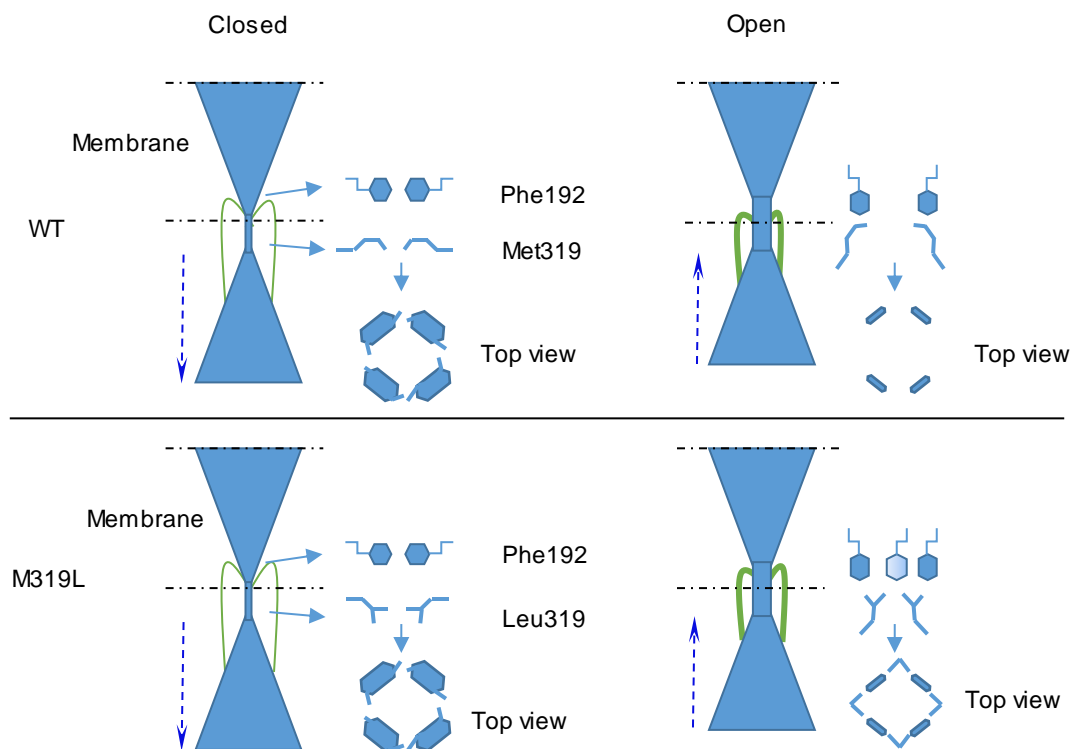


Figure 52. Representation of Kir3.2 channel gating mechanism. The Kir3.2 channel fluctuates between open and close conformations. In the open state it can conduct K⁺ ions. The Closed and open state of the Kir3.2 channel WT and leucine mutant. The flexible linker (Thin green) binds at an interface between the TMD and the CTD and induces a large conformational change (closed state). The flexible linker (Thin green) contracts (thick green), then the CTD moves towards and becomes tethered to the TMD. The G loop inserts into the TMD and the inner helix activation gate opens (open state). Then Phe192 interacts with the M319 residue in order to stabilize the open state. Due to its methyl branched side chain leucine at position 319 in Kir3.2 strongly stabilizes the open state of the channel.

Are the Kir6.2 channel “gates” residues regulated by the fused GPCR the same to those controlled by the native SUR subunit in the K_{ATP} channel?

Kir6.2 constitutes a unique case of the K⁺ inward rectifier channels. Indeed, physiologically it co-assembles at the N-terminus with the SUR regulatory subunit that contributes to the regulation of the channel gating through a long-range propagation of conformational changes from SUR-ligand binding sites to Kir6.2 gate(s). Binding of sulfonylureas such as Glibenclamide or K⁺ channel openers to SUR subunit results in Kir6.2 channel closure or opening, respectively, but the molecular mechanisms underlying the control of the gating process by regulatory proteins is still unknown. By using an Ion Channel-Coupled Receptors approach we were able to identify residues

RESULTS

implicated in the molecular mechanism of the Kir6.2 channel gating regulation by N-terminal-interacting proteins such as SUR and fused GPCRs.

Previous studies on K_{ATP} channels with its natural receptor (SUR) have demonstrated that Kir6.2 L164A, F168A and I296 channel mutations cause a significant loss of the ATP-sensitivity by increasing the open probability of the K_{ATP} channel and thus disturbing the gating regulation of the Kir6.2 channel (Proks et al., 2005; Rojas et al., 2007; Koster et al., 1999a). However, the change in ATP sensitivity alone is not a direct indicator of intrinsic gate stability since the physical interaction between SUR and Kir6.2 can alter ATP sensitivity. To remove this possibility, we used the ICCR approach to functional map these residues demonstrating their functional implication in the gating process involving interacting proteins with the Kir6.2 N-terminal domain. Subsequently, we confirmed that these residues are also regulated gates in the native K_{ATP} channel by using the pharmacological inhibitor Glibenclamide that is known to bind at the interface between SUR and the Kir6.2 N-terminus. The Kir6.2 L164A mutation completely abolishes the inhibitory effect of the blocker, Glibenclamide (Figure 49), and characterization of the Kir6.2 channel mutant I296L in the presence of its receptor SUR also showed a complete loss of the inhibitory effect of the blocker, strongly suggesting that the L164 and I296 residues serves as functional gates under control of the fused SUR protein. Unfortunately, characterization of the F168 mutant was impeded by the lack of ATP sensitivity, making it difficult to determine the effect of the blocker. To overcome this problem experiments using barium as a blocker could be performed.

In conclusion, we propose a new model of Kir channel gating involved in the channel regulation by N-terminus-interacting proteins. This model is based on the regulation of a concerted gate at the interface of the membrane and the cytoplasm and composed of the bundle crossing gate (inner gate A: Kir6.2 L164 and F168, Kir3.4 V183 and F192) and the G loop gate (Kir6.2 I296, Kir3.4 M314). In this model, the K^+ -conducting state is based on the intra-subunit interactions of the gate side chains and the closing state on the inter-subunit interactions. To date no structural data of K_{ATP} channels are available, and the precise map of the SUR/Kir6.2 interacting domains remains unknown, however these results obtained with an artificial ICCR could assist with the comprehension of mechanisms underlying the allosteric regulation of the gating process in K_{ATP} channels.

2. Design of a light-gated ATP-sensitive K⁺ channel

2.a. Objectives

Optogenetics, designated Method of the Year by Nature in 2011, consists of using light sensitive elements expressed in cells to provide ways to control function in a non-invasive manner with high spatial and temporal resolutions. It combines genetic and optical methods to perform either a gain or loss of function of well-defined events in specific cells of living tissue (Deisseroth, 2011). The first optogenetic application used microbial opsin proteins to achieve light control of specific neurons. These light-sensitive proteins require a chemical cofactor called all-*trans* retinal to absorb photons; and once this cofactor is bound, they are termed rhodopsins. When these are expressed in neuronal cells, they can be activated with light to turn ion flux on and off with millisecond speed (Yizhar et al., 2011). Microbial opsins are exogenous elements that only affect indirectly the function of native proteins. An alternative is to use light to control native proteins modified to be photo-sensitive. Such approach opens up the possibility to carry out precise biophysical and functional studies with a target protein (Sandoz and Levitz, 2013).

K_{ATP} channels are found in many excitable tissues (heart, brain, pancreatic islets, smooth muscle, etc.) (Noma, 1983; Ashford et al., 1988; Cook and Hales, 1984; Standen et al., 1989; Winquist et al., 1989). They have been implicated in diverse physiological processes such as memory and the regulation of male reproductive behavior (Betourne et al., 2009; McDevitt et al., 2009). K_{ATP} channels have been extensively studied in glucose homeostasis and ischemic protection (Rorsman et al., 2008; Flagg et al., 2005; Koster et al., 2005). Due to their large distribution and physiological functions, the remote control by light of K_{ATP} channels could be used to regulate action potentials with light, to tune diverse aspects of cellular electrophysiology, and potentially, to develop photo-pharmacology treatments. The availability of light-gated K_{ATP} channels would also be a good tool to test the role of these channels in organs, such as heart and skeletal muscle, where this role remains unclear.

The primary objective of this research is the design of a light-gated K_{ATP} channel that will allow us to understand the consequences of forcing its closure or its opening *in vivo*. To accomplish this, we aim to modulate channel activity in both directions, downregulation and upregulation. Our aim is to engineer a K_{ATP} channel that can be controlled by light while retaining the properties of native channels.

2.b. Light-inhibited K_{ATP} channel

2.b.1. Design of a light-inhibited K_{ATP} channel

With the aim to optically control a protein retaining its native properties, the method termed Photoswitched Tethered Ligands (PTLs) was developed. In order to implement this method, it is necessary to use a photoswitchable compound which is comprised of three essential parts: a moiety which is able to covalently bind to the protein to be studied, an azobenzene bond which isomerizes between *cis* and *trans* conformational states upon irradiation with different wavelengths, and a part containing a ligand adapted to the protein under study. Such a PTL, the MAQ used here, is shown in Figure 53A. The implementation of this technique consists of introducing a cysteine mutation (which may, or may not, perturb the functional behavior of the protein) that will be used to covalently bind the photoswitchable compound to the protein. It is essential that the position of the cysteine residues be near the targeted ligand binding site of the protein, in such a way that the ligand can bind in one isomerization state and not in the other (Sandoz et al., 2012; Chambers et al., 2006; Fortin et al., 2011).

To date, optical control with PTLs has been applied to a few ion channels and receptors, such as the kainate, metabotropic glutamate and nicotinic acetylcholine receptors (Volgraf et al., 2006; Tochitsky et al., 2012; Levitz et al., 2013). Here, we use the synthetic photoswitchable molecule called MAQ. As shown in Figure 53A, MAQ contains a maleimide group (M), a photoisomerizable azobenzene linker (A), and a pore-blocking quaternary ammonium group (Q) (Banghart et al., 2004). The transition between the 500 nm (*trans*) and 380 nm (*cis*) isomers of the azobenzene linker shortens the molecule, changing its ability to block the pore, as shown in Figure 53B. If the PTL is properly positioned, this isomerization can produce a rapid and reversible blockade of the channel. This molecule has already been used successfully to optically control several potassium channels, but none belonging to the Kir family (Chambers et al., 2006; Fortin et al., 2011; Sandoz and Levitz, 2013; Banghart et al., 2004).

In order to optically block the K_{ATP} channel using PTL (Figure 53B), the first task is the selection of suitable locations for engineering cysteine residues into Kir6.2, the pore forming subunit of the K_{ATP} channel. We used a molecular model of Kir6.2 based on the structure of the mouse Kir3.2 channel in a closed state, co-crystallized with K⁺, Na⁺ and a PIP₂ analogue. This model was built initially by our collaborator Nicolas Sapay. To choose the most appropriate positions for the insertion of a cysteine for the attachment of the MAQ, we considered the length of the MAQ (17 Å in *trans*, 10 Å in *cis*) and compared it to the predicted distances between various extracellular amino acids and

RESULTS

the pore entrance. Using this criteria, we identified six suitable positions for mutation to cysteine.

As shown in Figure 53B, the distances between positions G103, G105, and V108 and the selectivity filter are within range of the MAQ isomers to hopefully block the channel. However, since the homology model is based on the crystal structure of a closed state channel, the given distances (18 Å to 20 Å) between positions E104, T106, and N107 and the selectivity filters are too large for the MAQ isomers to block the channel. Therefore, considering the flexibility of this loop, we chose these positions to allow for the possibility of these distances decreasing upon opening of the channel. These residues could then be within range of the MAQ isomers and possibly still be able to block the channel.

RESULTS

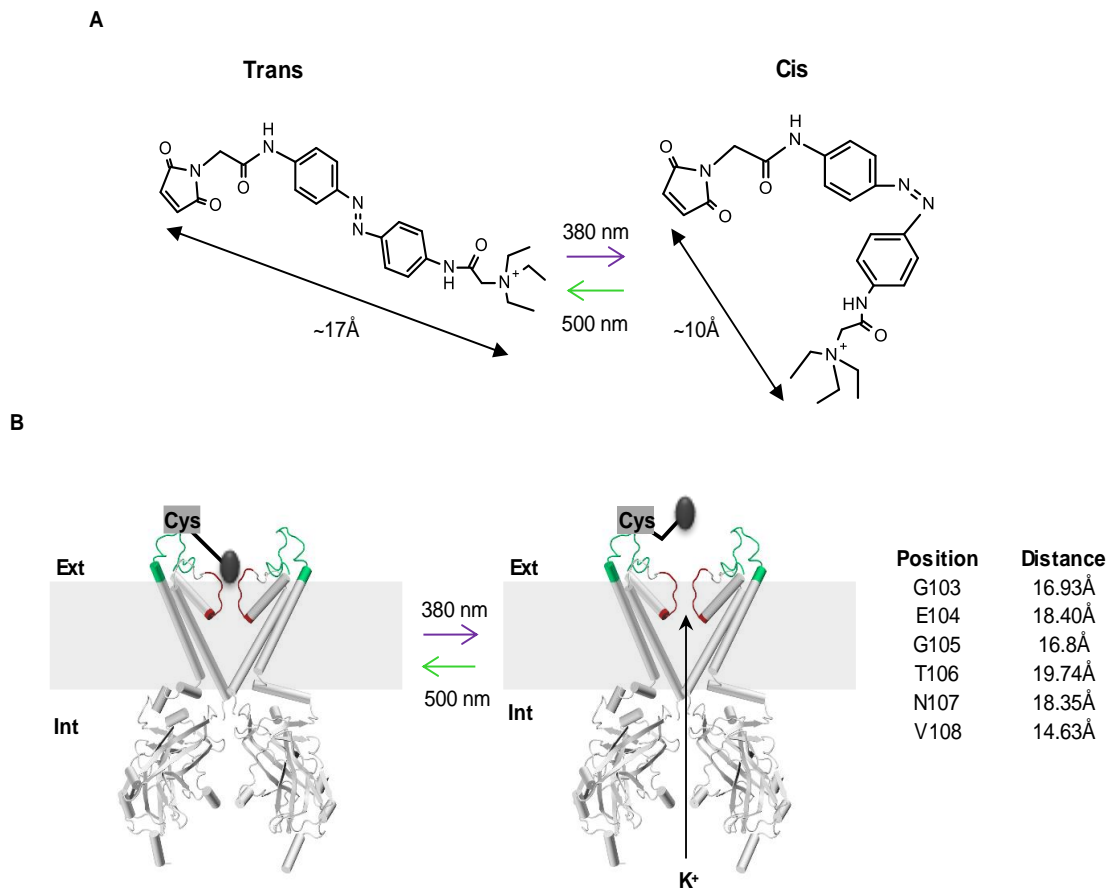


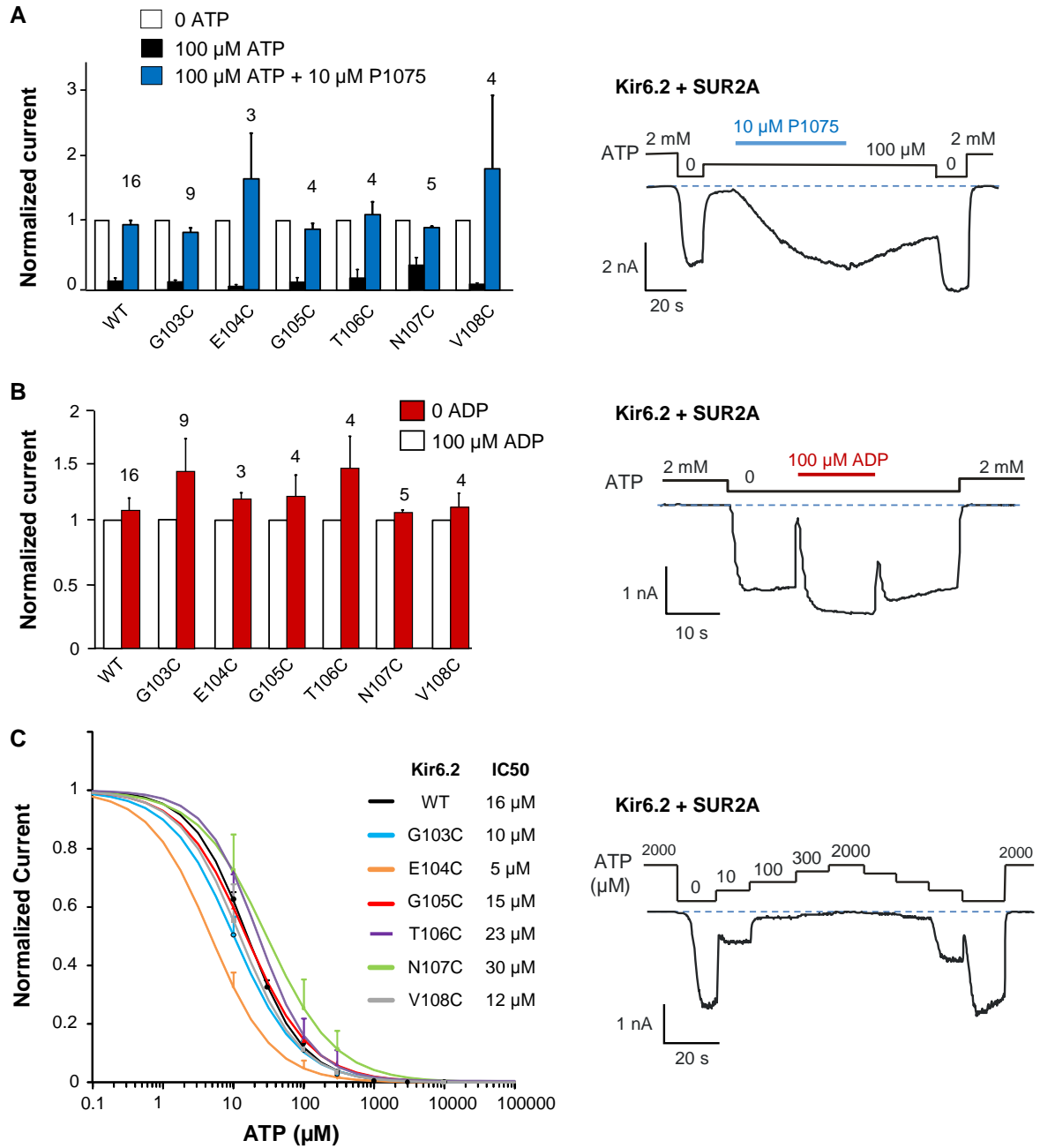
Figure 53. Application of the photoswitchable tethered ligand (PTL) technique to Kir6.2. **A.** MAQ consists of a maleimide (M), which tethers the photoswitch to an engineered cysteine, a photoisomerable azobenzene (A) linker and a quaternary ammonium (Q) potassium channel blocker. MAQ photoisomerizes from trans to cis states upon exposure to 380 nm and 500 nm wavelengths. **B.** Identification of the best positions for anchoring MAQ to Kir6.2. Molecular model of Kir6.2 based on the structure of the mouse Kir3.2 channel in closed state co-crystallized with K^+ , Na^+ and a PIP_2 analogue (Nicolas Sapay, 2014). The extracellular loop linking outer transmembrane helix M1 and pore helix is in green. The selectivity filter is in red. The table at right indicates the measured distances between carbon Ca of residues 103 to 108 and carbon Ca of pore entrance residue G135. Among the measured residues 94-116, these residues 103 to 108 were the best candidates for cysteine replacement as their positions were most compatible with the length of MAQ (17 Å trans 10 Å cis).

2.b.2. Functional impact of the cysteine mutations

To test the functionality of the constructed cysteine variants, inside-out patch-clamp recordings were performed on *Xenopus laevis* oocytes expressing the variants and SUR2A, and compared to oocytes expressing the wild-type SUR2A/Kir6.2. As shown in Figure 54, the normalized currents upon inhibition by ATP, activation by ADP and the

RESULTS

opener P1075 are all similar to the wild-type SUR2A/Kir6.2 suggesting that the introduction of a cysteine residue does not significantly affect the function and therefore the structure of the K_{ATP} channel.



RESULTS

Figure 54. Functional impact of the 6 cysteine mutations. The functionality of the constructed cysteine variants was measured by inside-out patch-clamp recordings that were performed on *Xenopus laevis* oocytes expressing the variants + SUR2A and compared to oocytes expressing WT Kir6.2 + SUR2A. Patches were bathed in solutions containing 150 mM K⁺ on both sides, and they were held at -50 mV. **A.** To the left: histogram with the responses of WT and mutant K_{ATP} channels to the pharmacological opener P1075 (10 μM). P1075 was applied in the presence of 100 μM ATP, and currents were normalized to the current measured in the absence of nucleotides immediately before 100 μM ATP application. Numbers above the bars indicate the number of patches included in each average. To the right: representative patch clamp recording obtained in the excised inside-out configuration. Voltage was clamped at -50 mV. **B.** To the left: Responses of WT and mutant K_{ATP} channels to the physiological activator ADP. Currents were normalized to the current measured in the absence of nucleotides immediately before ADP application. Numbers above the bars indicate the number of patches included in each average. To the right: representative patch clamp recording obtained in the excised inside-out configuration. Voltage was clamped at -50 mV. **C.** To the left: Dose-response relationships for the physiological inhibitor ATP. Currents were normalized to the current measured without ATP. Hill equation fitting yielded $K_{1/2} = 16 \mu\text{M}$ ($h = 1.09$) for WT, $K_{1/2} = 10 \mu\text{M}$ ($h = 0.95$) for G103C mutant, $K_{1/2} = 5 \mu\text{M}$ ($h = 0.98$) for E104C mutant, $K_{1/2} = 15 \mu\text{M}$ ($h = 0.94$) for G105C mutant, $K_{1/2} = 23 \mu\text{M}$ ($h = 1.14$) for T106C mutant, $K_{1/2} = 30 \mu\text{M}$ ($h = 0.89$) for N107C mutant and $K_{1/2} = 12 \mu\text{M}$ ($h = 1.01$) for V108C ($n=3-20$). To the right: representative patch clamp recording obtained in the excised inside-out configuration. Voltage was clamped at -50 mV. Error bars represent s.e.m.

2.b.3. Light-dependent block in HEK-293 mammalian cells

Since MAQ isomerization is induced by two different wavelengths, 380 nm (*cis*) and 500 nm (*trans*), HEK-293 cells co-transfected with the Kir6.2 constructs and SUR2A were continuously irradiated with each wavelength, switching from one to the other every 5 seconds. As shown in Figure 55, the perfusion protocol begins with the application of a control bath solution, followed by the opener P1075 to activate K_{ATP} channels, finishing with Barium (Ba^{2+}) to block the channels. Patch pipettes contained: 154 mmol/L K^+ , 40 mmol/L Cl^- , 1 mmol/L EGTA, 1 mmol/L Mg^{2+} , 10 mmol/L PIPES-KOH (pH 7.1). And the bath solution contained: 154mmol/L K^+ , 146 mmol/L Cl^- , 5 mmol/L Mg^{2+} , and 10 mmol/L PIPES-KOH (pH 7.1).

Kir6.2 possesses on its extracellular face two native cysteines, C110 and C142, which are thought to form a disulfide bridge. These cysteines could possibly react with MAQ during the labeling phase when cells are preincubated with MAQ. Labeling these cysteines could possibly induce photoblock of the wild-type channel. To test this possibility, cells were always pre-treated with DTT to break any disulfide bridge involving C110 and C142, or any of the introduced cysteines, prior to MAQ incubation.

In those conditions, post-labeling whole-cell recordings demonstrate that wild-type currents are not photosensitive (Figure 55A). Each of the 6 cysteine mutants were inhibited to different extents by 500 nm irradiation, meaning that the *trans* MAQ configuration blocks the channel. The block was reversed when a wavelength of 380 nm was applied to induce the *cis* MAQ configuration, returning the current to approximately the initial value before the photoblock. These results clearly show a reversible light-dependent block of the K_{ATP} channel, which can be repeatedly opened and closed (Figure 55B).

We compared the change in current caused by the photoblock of the MAQ attached to the cysteine variants. As shown in Table 9, the G103C mutant showed the highest amplitude of photoblock, making it the best candidate for MAQ attachment. As shown Figure 55, the photoblock was absent in wild-type channels, confirming that the photoblock is due to the attachment of MAQ to the engineered cysteine.

RESULTS

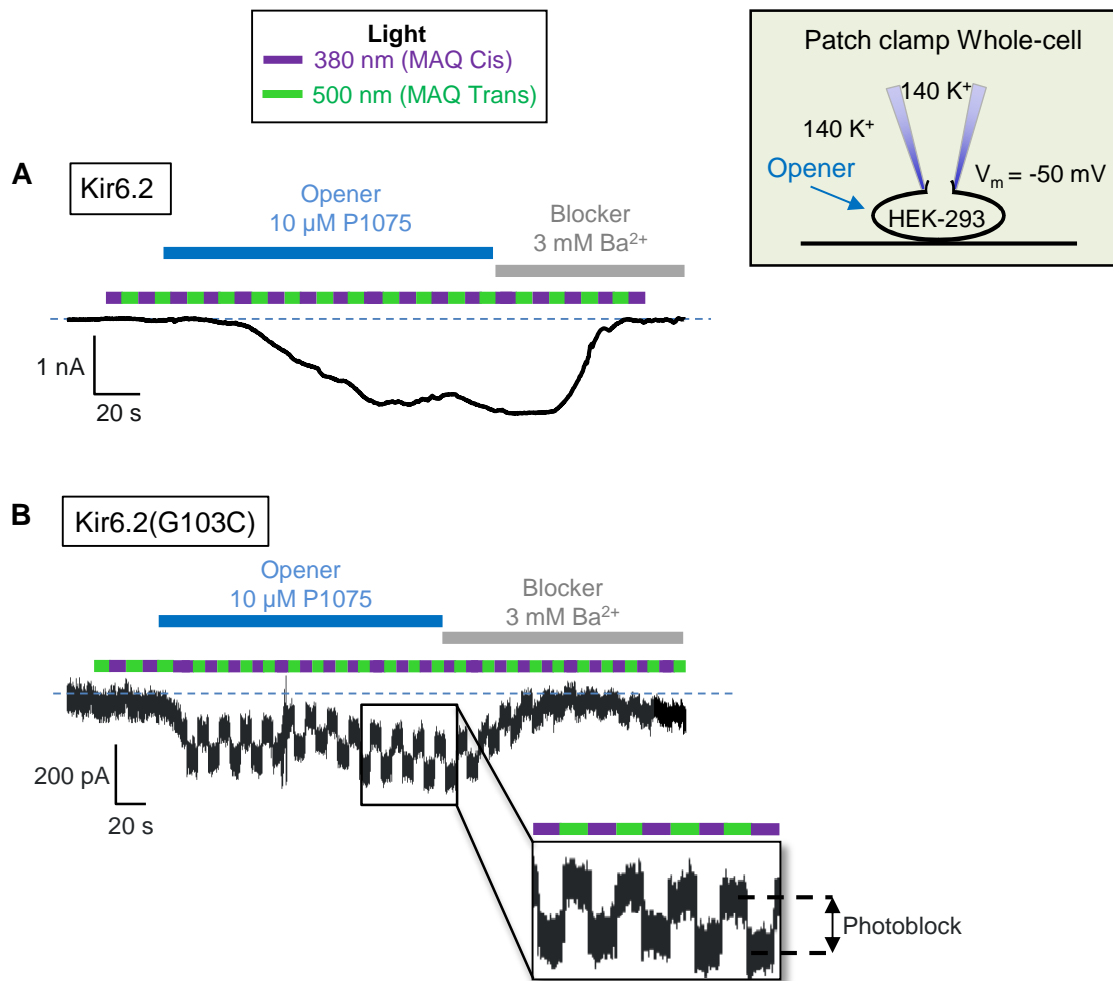


Figure 55. Light-dependent block using the photosensitive ligand (MAQ). Patch-clamp recordings at -50mV in the whole-cell configuration were performed in HEK-293 mammalian cells pre-incubated for 1 hour in 10 μ M MAQ. Light was continuously applied, alternating every 5 s between the 2 wavelengths, using a Polychrome V monochromator (TILL Photonics) **A.** Wild-type SUR2A/Kir6.2 recording showing absence of photoblock. **B.** SUR2A/Kir6.2(G103C) recording showing reversible photoblock (block by 500 nm, unblock by 380 nm).

Position	Distance (Å)	Maximal amplitude of photoblock (pA)
G103	16.9	175
E104	18.4	82.0
G105	16.8	31.0
T106	19.7	26.5
N107	18.3	70.0
V108	14.6	72.0

Table 9. Maximal amplitude of photoblock for each variant.

RESULTS

These experiments were done in collaboration with Guillaume Sandoz and Ryan John Arant (postdoctoral fellow) in the “Biology of ion channels” team at the Institut de Biologie Valrose (iBV) located in Nice, France.

2.b.4. Light-dependent block in inside-out patches from oocytes

Light-dependent block of inward currents

Based on the results shown in Table 9, we examined the cysteine mutation yielding the highest amplitude of photoblock, G103C (16.9 Å from the pore), as well as the mutations with the closest and longest distances from the pore, V108C (14.6 Å from the pore) and T106C (19.7 Å from the pore). Tests were done in excised patches from oocytes coexpressing each Kir6.2 construct and SUR2A. As shown in Figure 56, G103C has the highest amplitude of photoblock by the *trans* isomer, with 88.2 % inhibition. The T106C and V108C variants were less strongly inhibited, at 79.1 % and 62.5 %, respectively. This demonstrates that the distance between cysteine and the pore is an important parameter that affects the efficiency of the MAQ to block the pore of channel.

RESULTS

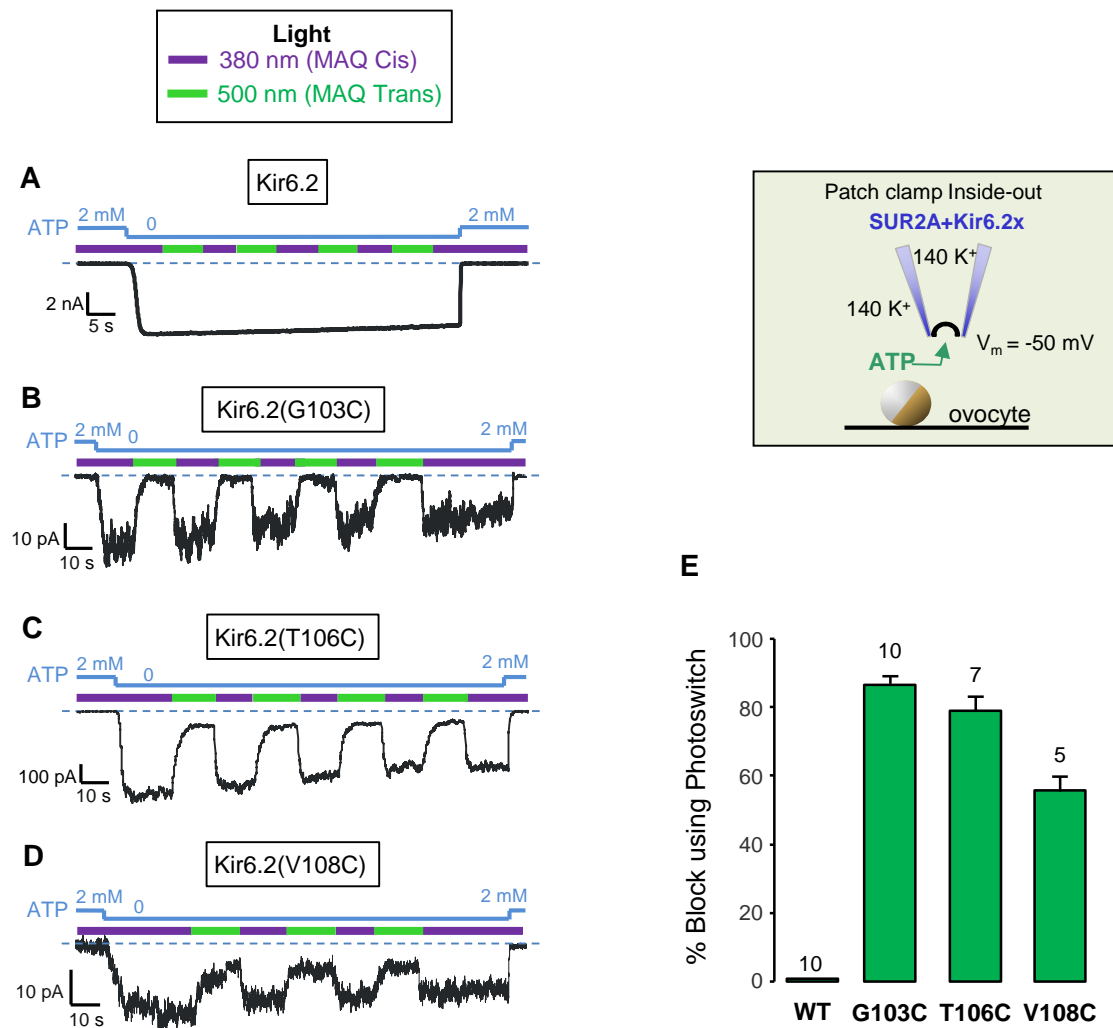


Figure 56. Light-dependent block with the photosensitive ligand (MAQ) in *Xenopus laevis* oocytes using patch clamp in the excised inside-out configuration. The patches were held at -50 mV in symmetrical high K⁺. Oocytes were pre-incubated in 10 μM of MAQ for ~40 min. Alternating illumination between 500 nm (green) and 380 nm (Violet) reversibly blocks and unblocks the K_{ATP} currents. **A.** Representative trace of Kir6.2 + SUR2A **B.** Representative trace of Kir6.2(G103C) + SUR2A **C.** Representative trace of Kir6.2(T106C) + SUR2A **D.** Representative trace of Kir6.2(V108C) + SUR2A **E.** Bar graph representing the average photoblock in percent. Numbers above the bars indicate the number of patches included in the averages.

Light-dependent block of outward currents

To test if the direction of the K⁺ ions current does not disturb the efficiency of the photoblock, we tested the light-dependent block using the three cysteine variants (G103C, T106C and V108C) in conditions where currents are outward. The results demonstrate that, although MAQ probably acts as a cationic open-channel blocker, its block is not noticeably affected by the outward flux of K⁺ ions currents and by the unfavorable electric field, as shown in Figure 57.

RESULTS

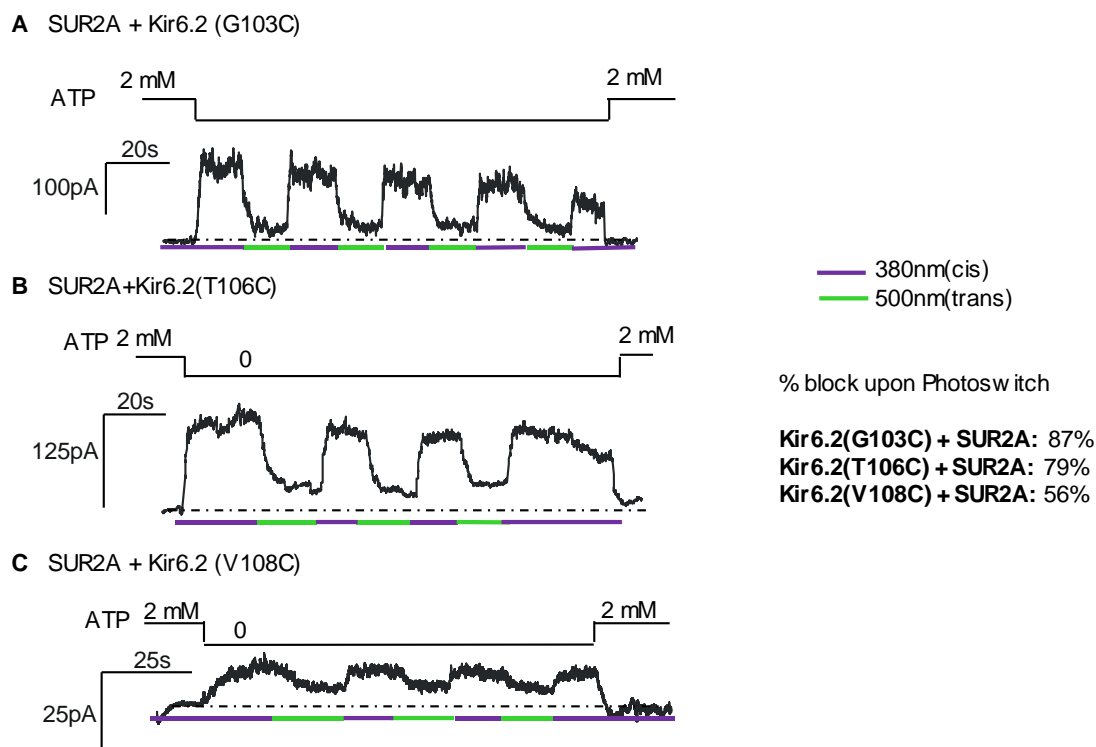


Figure 57. Light-dependent block of outward currents with the photosensitive ligand (MAQ) in *Xenopus laevis* oocytes using patch clamp in the inside-out configuration. The patches were held at +30 mV in symmetrical high K^+ . Oocytes were incubated in 10 μ M of MAQ for about 40 mins. Alternating illumination between 500 nm (green) and 380 nm (Violet) reversibly blocks and unblocks the outward K_{ATP} currents. **A.** Representative trace of Kir6.2(G103C) +SUR2A **B.** Representative trace of Kir6.2(T106C) +SUR2A **C.** Representative trace of Kir6.2(V108C) +SUR2A. ($n=1-3$).

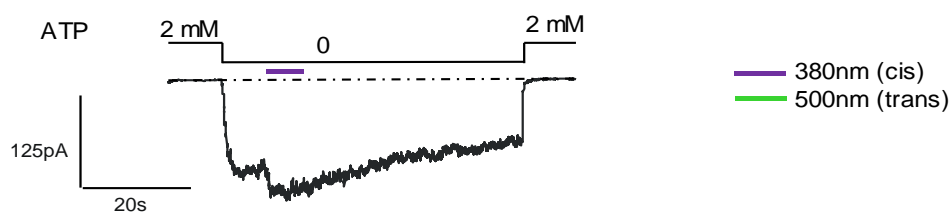
2.b.5. Thermal stability of the photosensitive ligand MAQ

The *trans* configuration of MAQ is the low energy state of the azobenzene, meaning that, in the dark, the MAQ will spontaneously relax to the *trans* configuration (Chambers and Kramer, 2008). However, when the MAQ is attached to the K_{ATP} channel, it will be in a partial block state in normal visible light due to a mixture of the *cis* and *trans* conformations. In order to test the stability of the conformational states of the MAQ when it is attached to the K_{ATP} channel, two experiments were performed. Firstly, a brief flash (5 s) of UV light at 380 nm was applied to induce the *cis* MAQ conformational state and relieve any block of the K_{ATP} channels. After a period of approximately 2 mins in visible light a decrease in current back to the initial partial blocked state was observed in oocytes. Secondly, the opposite experiment was performed. A brief flash (5 s) of UV light at 500 nm was applied to induce the *trans* MAQ configuration state and achieve maximum photoblock. After a period of approximately 40 mins in visible light, no change

RESULTS

in current was observed, as shown in Figure 58. These results suggest that the thermal relaxation from *cis* to *trans* of azobenzene, as well as the stability of the MAQ in the *trans* state, are preserved when MAQ is attached to the K_{ATP} channel.

A SUR2A + Kir6.2 (G103C)



B SUR2A + Kir6.2 (G103C)

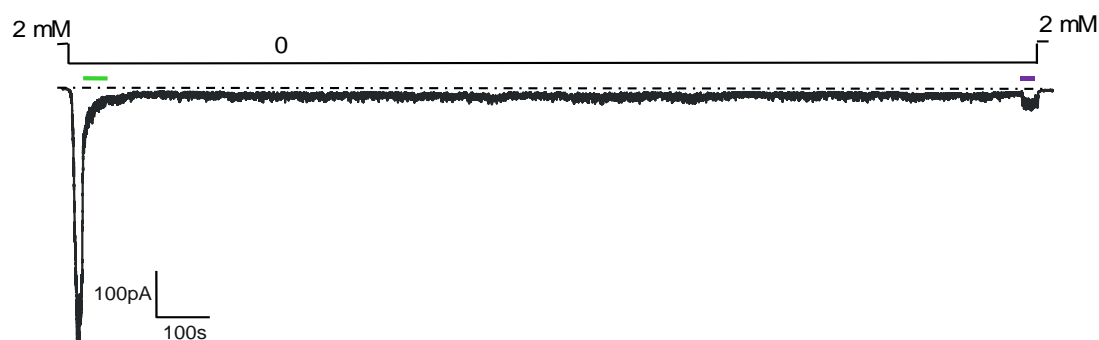


Figure 58. Thermal stability of the photosensitive ligand (MAQ), in excised inside-out patches from *Xenopus laevis* oocytes. A. Opening by 380 nm light and thermal relaxation at room light in ~2 mins ($n=3$). B. Persistent light-induced block by 500 nm light for more than 40 mins ($n=2$).

2.b.6. Light-dependent block in INS-1E glucose-sensitive cells

The function of K_{ATP} channels is best understood in the pancreatic β -cells, where they are implicated in linking insulin secretion to glucose metabolism (Ashcroft et al., 1984). In order to prove the efficacy in a native physiological environment, we tested the light-dependent block in INS-1E glucose-sensitive cells because these cells express K_{ATP} channels and are able to secrete insulin in response to glucose concentrations similar to pancreatic β -cells (Merglen et al., 2004). Electrophysiological trials were conducted to verify proper expression, and integration with endogenous channels, of exogenous light-sensitive Kir6.2 in INS-1E cells. Kir6.2(G103C) DNA was transfected and tested by patch clamp in the inside-out configuration.

Initially, ATP-sensitive currents were barely detectable, suggesting low expression levels of the K_{ATP} channel. Since both the Kir6.2 and SUR1 subunits are required for trafficking of the functional octamer channel to the cell surface, this could be due to restrictive levels of native SUR1 receptors available in INS-1E cells. In order to bypass this limitation, we

RESULTS

co-transfected the SUR2A/Kir6.2(G103C) DNAs. This resulted in an increase in ATP-sensitive inward current and to the observation of a light-dependent block, as shown in Figure 59 indicating that the Kir6.2(G103C) was well expressed in INS-1E cells.

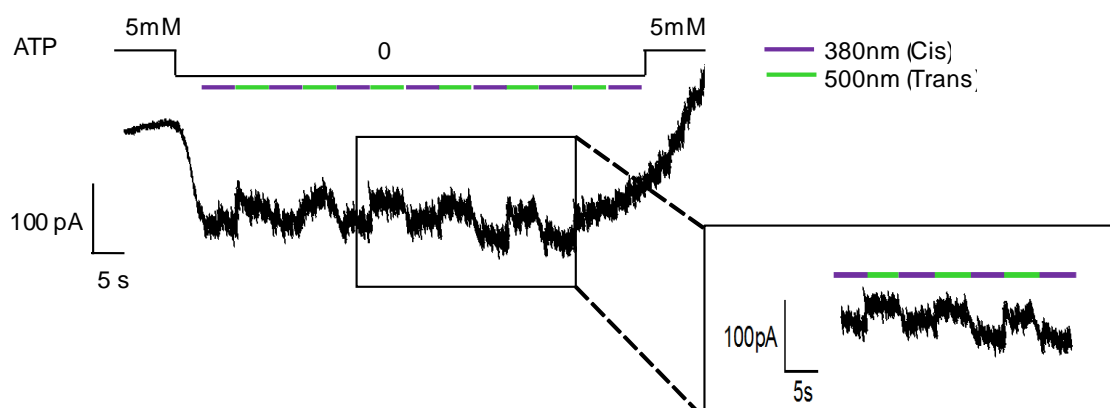


Figure 59. Light-dependent block using the photosensitive ligand (MAQ). Patch-clamp recordings at -50 mV in the inside-out configuration were performed in INS-1E cells transfected with SUR2A and Kir6.2(G103C) and pre-incubated in 10 μ M of MAQ for 1 hour. Light was applied as indicated using a Polychrome V monochromator (TILL Photonics). Trace shows a reversible photoblock (block 500 nm, unblock 380 nm).

These experiments were done in collaboration with Guillaume Sandoz and Brigitte Wdziekonski (technical engineer) in the “Biology of ion channels” team at the Institut de Biologie Valrose (iBV) located in Nice, France.

2.c. Light-activated K_{ATP} channel

2.c.1. Design of a light-activated K_{ATP} channel

With the aim to optically activate the channel we performed a screening of positions for the incorporation of cysteine residues using the Kir6.2 model as a reference (Nicolas Sapay and Serge Crouzy, iRTSV, Grenoble, France). We have identified several positions within four key regions of the K^+ channel as the most suitable for the insertion of a cysteine. Firstly, mutation of the extracellular residue S143 in the Kir3.4 channel (equivalent to Kir6.2 S124 position) can enhance the activity of that channel (Vivaudou et al., 1997), suggesting that a specific change in this region could trigger channel activation. Secondly, previous structural and functional studies of two prokaryotic K^+ channels, KcsA and MthK from the archaea *Methanobacterium thermoautotrophicum*, suggested that activation of those channels occurs via bending and rotation of the second transmembrane helix (M2) through a highly conserved glycine, suggesting that the M2 region plays a key role in channel gating (Jiang et al., 2002b; a; Sadjja et al.,

RESULTS

2001). Thirdly, amino acids located in the pore helix that are pointing to the neighboring helix. Once the photoswitchable molecule is attached, the transition between cis and trans states could trigger a twist of the pore helices causing an opening of the gate. Finally, in the selectivity filter, KcsA E71 (equivalent to Kir6.2 E126) constitutes part of an intricate hydrogen bond network, and can function as a gate (Cordero-Morales et al., 2006). It is possible that mutating amino acids located near the selectivity filter; where a transition between cis and trans of the photoswitchable molecule occurs; could cause a deformation of the filter and therefore disturb the gating of the channel. Focusing on these four regions, we selected fifteen different positions to attach the photoswitchable molecule, as shown in Figure 60.

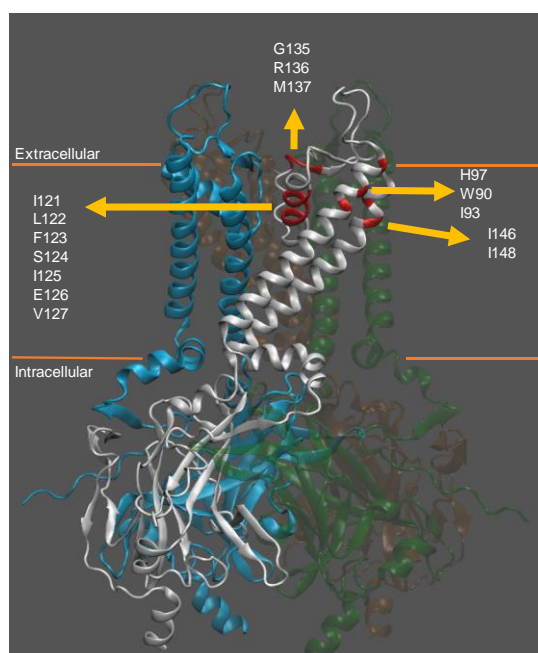


Figure 60. Proposed positions to attach the MAQ to Kir6.2 in order to elicit channel activation. The molecular model of Kir6.2 used is based on the mouse Kir3.2 channel as previously described. Each Kir6.2 subunit are in different colors (blue, green, orange, white). Highlighted in red are the residue positions proposed for MAQ attachment. These include the Kir6.2 S124 residue which is equivalent to Kir3.4 S143, the residues I121, L122, F123, I125, E125, E126, and V127 which surround S124 in the pore-forming region, the residues H97, W90, I93, I146, and I148 located in M1 and M2, and the residues G135, R136, M137 located in the extracellular vestibule.

2.c.2. Testing light-dependent activation in excised patches

The fifteen different cysteine mutations were introduced in Kir6.2 and all variants were expressed in *Xenopus laevis* oocytes. All variants had reasonable expression levels as verified in excised inside-out patch-clamp recordings. Preliminary tests show that MAQ labeling did not result in any detectable photosensitive currents as shown in Table 10. Further tests need to be conducted.

Residue	Oocyte batches	Light sensitive
F121	2	no
L122	1	no
F123	2	no
S124	1	no
I125	3	no
E126	1	no
E126	1	no
V127	1	no
W90	3	no
I93	1	no
H97	1	no
G135	1	no
R136	1	no
M137	3	no
I146	2	no
I148	2	no

Table 10. Summary of the preliminary tests to attach the MAQ to the specified Kir6.2 residues in order to elicit channel activation.

2.d. Discussions and Perspectives

Light-dependent block of K_{ATP} channels

Over the last decade, photopharmacology has grown significantly with the development of new photoswitchable compounds (Velema et al., 2014; Gorostiza and Isacoff, 2008; Fehrentz et al., 2011; Broichhagen et al., 2014b), enzyme inhibitors (Broichhagen et al., 2014a; Velema et al., 2013) and the design of light-sensitive receptors and ion channels (Lemoine et al., 2013; Tochitsky et al., 2012; Stein et al., 2012; Fortin et al., 2011; Mourot et al., 2012). Most of these were developed to perform an optogenetic mimicry of neuronal signaling, it is worth highlighting that only one of these targets was a K_{ATP} channel. In that case, a sulfonylurea incorporating an azobenzene moiety (JB253) was able to produce a reversible photoblock of the K_{ATP} channels through the SUR1 subunit

RESULTS

(Broichhagen et al., 2014b). The transient *cis* conformation of JB253 is the active conformation while the resting *trans* conformation does not block the channel, ensuring a minimal effect in control conditions. This approach is interesting but remains limited to SUR1-based K_{ATP} channels. There is also a need to demonstrate that JB253 does not interact with other targets.

As an alternative approach, we designed a light-gated Kir6.2 channel that permits the study of all Kir6.2-based channels. Unlike JB253 which requires constant illumination to maintain channel block, our construct requires constant illumination to remain open. The two approaches are therefore complementary.

We demonstrated that the amino acid G103 of Kir6.2 is the best position to attach the photoswitchable compound MAQ. At this position, MAQ in the *trans* conformation produces a solid inhibition of approximately 90% while the *cis* conformation is ineffective. This light-dependent block of the K_{ATP} channel is fully repeatable and reversible. A brief flash of UV (500 nm) is enough to provoke the change to the stable *trans* MAQ conformational state, producing a persistent block over a long period of time (more than 40 min) in visible light. The modified photosensitive Kir6.2 appears equivalent to the wild-type Kir6.2, in terms of assembly with SUR2A and in terms of physiological and pharmacological regulations. It constitutes therefore a new tool for *in vitro* and *in vivo* study of K_{ATP} channel physiology.

However, the use of this tool in native tissues must still be validated. Since it is well known that in pancreatic β -cells, the secretion of insulin is linked to the closure of the K_{ATP} channel (Ashcroft et al., 1984), this opens two questions: (1) Can light-induced block of K_{ATP} channels mimic the effect of antidiabetic sulfonylurea blockers on insulin secretion? (2) Can light-induced block of K_{ATP} channels modulate the glucose-insulin coupling in varying concentrations of plasma glucose? Tests are still in progress to answer these questions in model β -cell lines. Looking ahead, the final test will be to express this light-gated K_{ATP} channel *in vivo*, possibly in zebrafish due to their transparency and amenability to genetic manipulation (Del Bene and Wyart, 2012). These results could allow to consider this optically modulated K_{ATP} channel both as a research tool, and possible as an optopharmacological agent.

As said before, other non-Kir potassium channels have been optically controlled using the PTL approach. Members of the mammalian family of voltage-gated K⁺ channels (Kv) are highly homologous to the *Drosophila* Shaker K⁺ channels. Therefore a cysteine was introduced into the extracellular loop at the position equivalent to that in Shaker-based SPARK to achieve light-dependent block of mammalian Kv channels (Fortin et al., 2011).

RESULTS

Kir channels share with Kv channels, and among themselves, a conserved pore topology of 2 TM helices plus a P-loop per subunit. They also contain substantial N- and C-terminal intracellular domains that are implicated in biological regulation of channel gating (Sansom et al., 2002). Because of this homology among Kir family members, it is conceivable that our findings with Kir6.2 could easily serve to confer light inhibition to others Kir channels (Figure 61).

	% Identity		103	
Kir6.2	100%	89	V W W L I A F A H G D L A P G	127
Kir3.1	40%	101	M W W V I A Y T R G D L N K A	140
Kir3.2	41%	110	I W W L I A Y I R G D M D H I	149
Kir3.3	43%	78	I W W L I A Y G R G D L E H L	117
Kir3.4	42%	107	I W W L I A Y I R G D L D H V	146

Figure 61. Alignment of the rat Kir6.2 sequence with human Kir3.x sequences. The G103 and matching residues are boxed. In spite of divergence around G103, the presence of surrounding identical regions suggests a conserved structure of the extracellular region.

Light-activated K_{ATP} channels

None of the engineered cysteines selected Table 10 displayed light-induced modulation of the K_{ATP} channel. This could be due to poor accessibility of the engineered cysteines to the extracellularly applied MAQ. To produce activation, we indeed selected positions located near or in the transmembrane area of the channel. These positions, which are more buried in the protein than the positions used to block the channel, might not be accessible to a soluble ligand. It could also be that the cysteines are correctly labeled by the MAQ but the change of conformation (*cis* and *trans*) of MAQ is insufficient to disturb the K_{ATP} channel gate.

Our preliminary data should certainly be repeated. We also plan to test other kinds of photoswitchable molecules, similar to MAQ but with different properties, such as length and charge of the ligand moiety. In particular, an uncharged molecule might be better able to reach a cysteine buried within the protein. Another possibility would be to focus on the SUR2 subunit. This subunit is the target of K Channel openers and the key residues of the binding site of openers have been identified. The residues close to these key residues could be targeted as candidates for attachment of photosensitive molecules.

3. Mechanism of action of Cantù syndrome mutations

3.a. Relevance of the study

K_{ATP} channels results from the interaction of two proteins, the Sulfonylurea Receptor (SUR) subunit, an ABC protein with three transmembrane domains (TMD0, TMD1, and TMD2) as shown in Figure 62 and the inward rectifier K^+ channel Kir6.2, pore-forming subunit. The SUR subunit modulates channel gating in response to the binding of intracellular nucleotides or drugs. By itself, the association of SUR with Kir6.x causes an increased sensitivity to inhibition by ATP (Fürst et al., 2014).

Cantù syndrome (CS) (MIM 239850) is a rare genetic disorder, first recognized in 1982 by Jose Maria Cantù Garza (Cantù et al., 1982), characterized by multiple cardiovascular abnormalities, congenital hypertrichosis (excess hair growth), neonatal macrosomia (coarse facial features), and distinct osteochondrodysplasia (alteration in the size, shape or strength of bone) (Grange et al., 2014). In the last few years, it has been found that point mutations in the ABCC9 gene encoding SUR2 (Harakalova et al., 2012; van Bon et al., 2012; Hiraki et al., 2014; Park et al., 2014) and in the KCNJ8 gene encoding Kir6.1 are implicated in CS (Brownstein et al., 2013; Cooper et al., 2014).

To date, the only pathology associated primarily with SUR2 mutations is CS. The CS mutations in the SUR2 subunit are believed to cause hyperactivity of K_{ATP} channels although not all mutations have been functionally characterized (Figure 62). We examined the functional consequences of two uncharacterized Cantù mutations, H60Y and D207E, the only such mutations located in the TMD0 domain (Figure 62). The objective is to correlate molecular observations and pathological consequences, as well as to gain insight on the function of the TMD0 in the control of Kir6.2 gating.

RESULTS

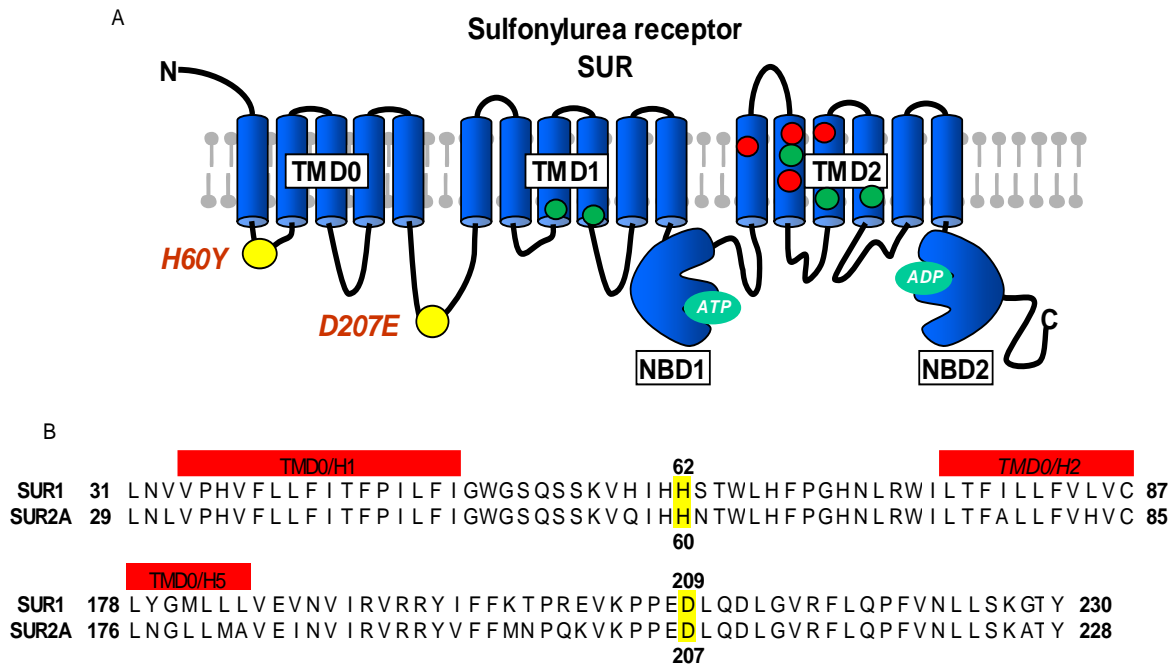


Figure 62. The K_{ATP} channel and Cantù syndrome associated mutations (yellow circles in panel A). **A.** Cantù syndrome associated mutations in SUR2: Green circles indicate Cantù mutations already characterized (P432L, A478V, C1043Y, R1116H, R1154W) showing a gain of function of the K_{ATP} channel. Red circles indicate mutations that have not been characterized (S1020P, F1039S, S1054Y, R1116C). Highlighted in yellow are mutations in TMD0 not yet characterized and studied in this work (H60Y, D207E). **B.** Alignment of human SUR2 with human SUR1 at the TMD0 level. Highlighted in yellow are the equivalent positions of the Cantù syndrome mutations in TMD0.

3.b. Project background and experimental approaches

A few dozen cases of CS have been reported in the literature, and twenty-five of those carry a mutation in the SUR2 gene (van Bon et al., 2012; Harakalova et al., 2012). The constant features reported for this condition are: congenital hypertrichosis, macrosomia, macrocephaly, cardiomegaly and multiple dysmorphic features (Grange et al., 2006). Similarly, patients treated with K_{ATP} pharmacological openers like Diazoxide, Minoxidil and other related drugs (Lietman et al., 1977) often report side-effects similar to the features of CS, suggesting that CS results from a K_{ATP} channel overactivity (Grange et al., 2006).

Today, fifteen CS-associated SUR2 mutations have been described (Table 11), of which five (R1154W, R1116H, P432L, A478V and C1043Y) located in the TMD1 and TMD2 have been engineered and characterized (van Bon et al., 2012; Harakalova et al., 2012; Hiraki et al., 2014; Park et al., 2014). Results have shown that CS mutations lead to

RESULTS

overactive K_{ATP} channels (Harakalova et al., 2012; Cooper et al., 2015). Until now, there are two pathways proposed to explain the cause of this Gain Of Function (GOF): a decrease in ATP-sensitivity and an enhanced Mg-ADP activation (Cooper et al., 2015). In addition, two Kir6.1 mutations (V65M and C176S) have been related with CS, of which only C176S has been characterized, showing a decrease of ATP sensitivity leading to a GOF of K_{ATP} channels (Brownstein et al., 2013; Cooper et al., 2014).

Here we show the physiological study of two human SUR2 CS mutants. The point mutations H60Y and D207E are both located in the transmembrane domain 0 (TMD0). TMD0 from SUR is a key domain in the interaction between SUR and Kir6 subunits and it is implicated in the regulation of Kir6 gating and trafficking (Fang et al., 2006; Chan et al., 2003).

DNA Nucleotide	Protein Amino Acid	Reference
c.178C>T	p.H60Y	(Harakalova et al., 2012)
c.621C>A	p.D207E	
c.1138G>T	p.G380C	
c.1295C>T	p.P432L	(Harakalova et al., 2012; Cooper et al.)
c.1433C>T	p.A478V	(van Bon et al., 2012)
c.3058T>C	p.S1020P	(Harakalova et al., 2012)
c.3116T>C	p.F1039S	
c.3128G>A	p.C1043T	(Harakalova et al., 2012; van Bon et al.,
c.3161C>A	p.S1054Y	(Harakalova et al., 2012)
c.3347G>A	p.R1116H	
c.3346C>T	p.R1116C	
c.3460C>T	p.R1154W	(Harakalova et al., 2012; van Bon et al., 2012)
c.3461G>A	p.R1154G	
c.3605C>T	p.T1202M	(Hiraki et al., 2014)
c.4385C>G	p.A1462G	(Park et al., 2014)

Table 11. *Cantù syndrome mutations in the ABCC9 gene (SUR2) (Grange et al., 2014)*

3.c. Functionality of the SUR2A variants H60Y and D207E

K_{ATP} channels are physiologically regulated by molecules that can target SUR or Kir6 or both. The SUR subunit confers to the K_{ATP} channel the capability to be activated by Mg-nucleotides, while this class of molecules naturally inhibits Kir6. Moreover, SUR is the target of drugs that can regulate either opening or blocking of the pore.

3.c.1. Response to the physiological inhibitor ATP

Channel inhibition results from binding of ATP to Kir6.2 in a Mg-independent manner (Gribble et al., 1998b; Tucker et al., 1998). The K_{ATP} channel is spontaneously active in the absence of ATP. Previous characterization of CS mutants has shown a GOF of the K_{ATP} channels which can be due to a decreased sensitivity to ATP inhibition (Cooper et al. 2014; Cooper et al. 2015; Harakalova et al. 2012). Here, wild-type and mutant K_{ATP} channels were tested using the patch clamp technique in the inside-out configuration. Responses to varying concentrations of ATP were measured, as shown in Figure 63. Similar to previous CS mutations already characterized, the SUR2A mutation D207E induced a clear loss of sensitivity to ATP compared to wild-type ($IC_{50}=60.5 \mu\text{M}$ versus $13 \mu\text{M}$ for the wild-type), while the H60Y mutation did not change the sensitivity to ATP compared to wild-type ($IC_{50}=14.5 \mu\text{M}$). This unexpected result suggests that mutation H60Y affects a different regulatory pathway than D207E.

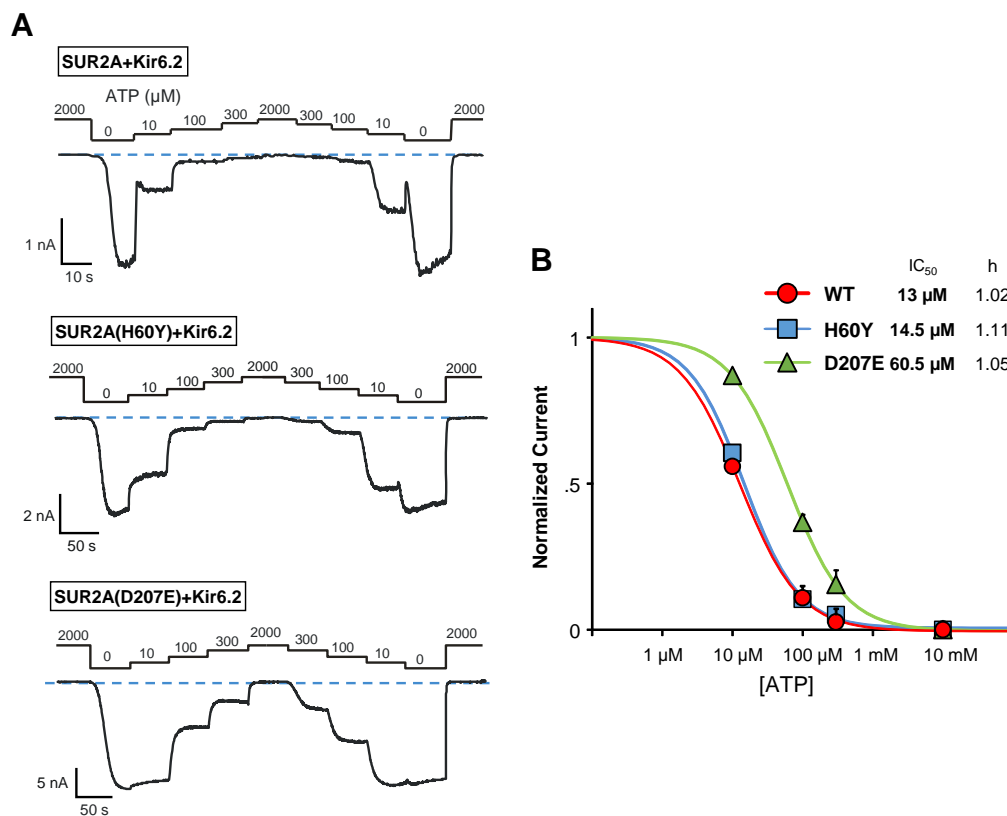


Figure 63 ATP inhibition is reduced by mutation D207E, not by H60Y. Inside-out patch-clamp recordings were performed at -50 mV on *Xenopus* oocytes expressing wild-type and mutated SUR2A with Kir6.2. **A.** Examples of recordings obtained in response to varying concentrations of ATP. **B.** Plots of normalized current vs ATP concentration. Currents were normalized to the current measured in absence of nucleotides ($n=10-21$). Hill equation fitting yielded the indicated $K_{1/2}$ (half-maximal inhibitory concentration) and h (Hill coefficient). Error bars represent s.e.m.

3.c.2. Responses to the physiological opener ADP

Mg-ADP (and to a lesser extent Mg-ATP) has a dual effect on K_{ATP} channels; inhibition when the nucleotide binds to Kir6.2, and activation when the nucleotide binds to SUR. Activation requires Mg^{2+} , while inhibition does not (Proks et al., 2010; Dupuis et al., 2008; Hosy and Vivaudou, 2014). In the presence of Mg^{2+} , the two effects add up to produce, either an increase in channel activity at lower ADP concentrations, or a decrease at higher concentrations (Hosy and Vivaudou, 2014). We tested increasing concentrations of ADP on the mutants (Figure 64). In spite of the inherent variability of K_{ATP} channels toward ADP activation, it is seen that channels containing wild-type and mutant SUR2A had a similar pattern of responses to the different concentrations of Mg-ADP.

In a quantitatively similar way, all channels were activated by 100 μM Mg-ADP and inhibited by 300 μM ADP. Differences are seen for 10 μM ADP but these differences will need a larger sample size to be confirmed as statistically significant.

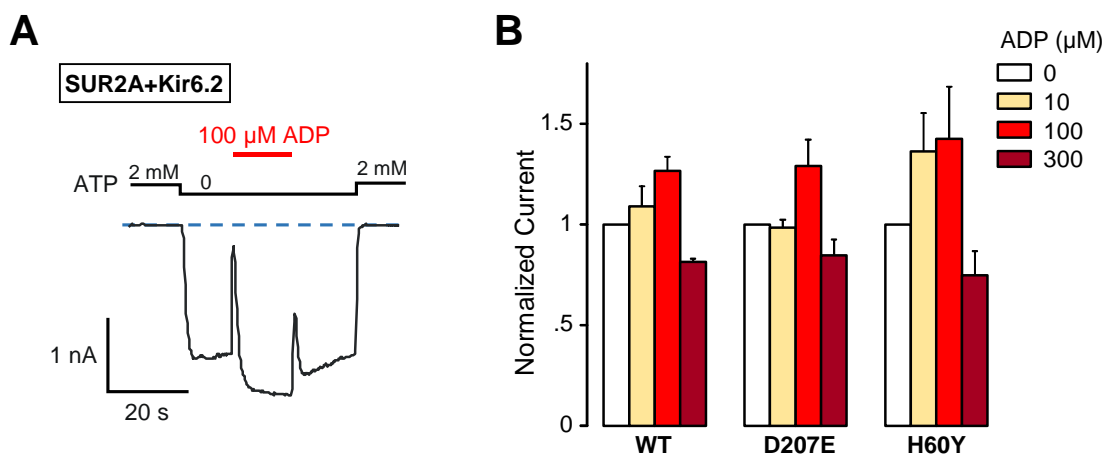


Figure 64. Activation by ADP of CS mutants. Inside-out patch-clamp recordings were performed at -50 mV on *Xenopus laevis* oocytes expressing wild-type and mutated SUR2A with Kir6.2. **A.** Examples of a recording of wild-type channels showing activation by 100 μM ADP in absence of ATP. **B.** Histogram of normalized current vs ADP concentration. Currents were normalized to the current measured in the absence of nucleotides ($n=2-10$). Error bars represent s.e.m.

These tests were conducted in absence of ATP. We also performed ADP experiments in the presence of ATP, a more physiological setting. Results are presented in Figure 65. The interpretation of the data is difficult because the mutations change the degree of inhibition by ATP, in turn affecting the amplitude of activation by ADP. This is clear with mutation D207E. Nonetheless, it can be said that ADP activation is not augmented by the CS mutations. It has been reported that some CS mutants enhanced the Mg-ADP

RESULTS

activation (Cooper et al., 2015) but this appears not to be the case for mutations D207E and H60Y.

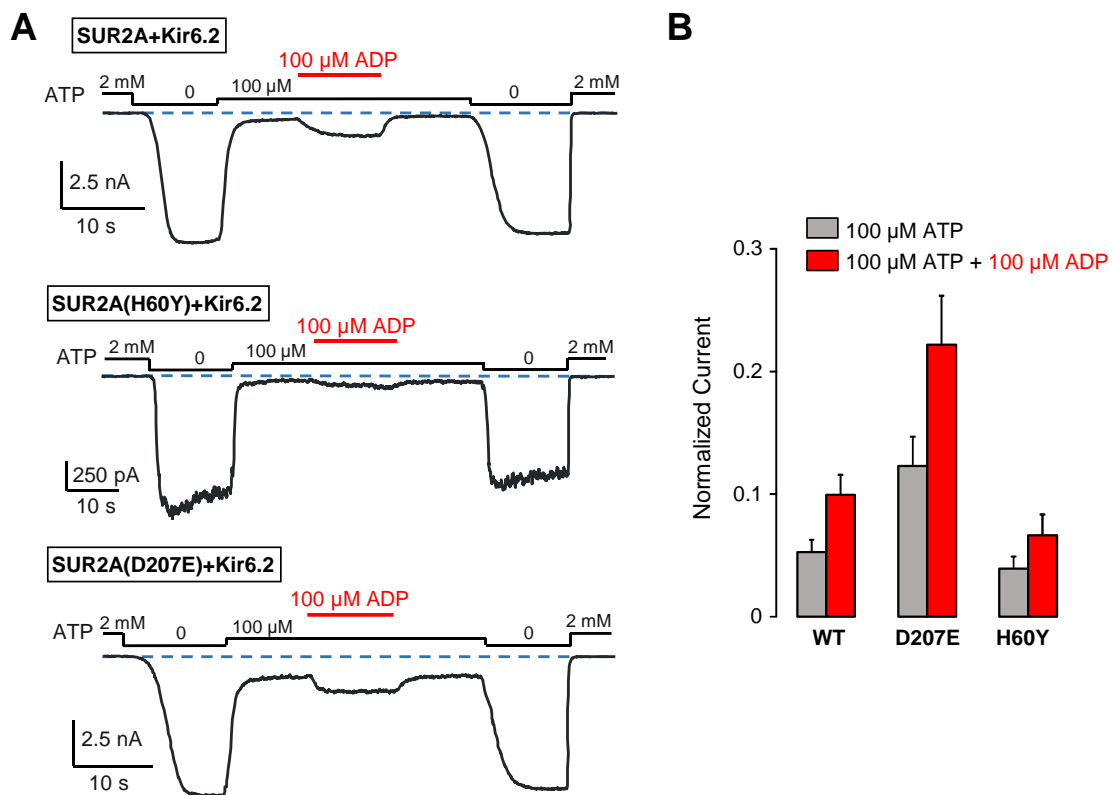


Figure 65. ADP activation is not augmented by mutations D207E and H60Y. **A.** Examples of excised inside-out patch-clamp recordings obtained in response to application of 100 μM ADP in the presence of 100 μM ATP. **B.** Summary of data obtained in 6 patches as in panel A. In each patch, currents were normalized to the current measured in the absence of nucleotides, and averaged over all patches. Error bars represent s.e.m.

3.c.3. Response to PIP₂

Like many ion channels, Kir6 activity has been shown to be dependent on phosphatidylinositol-(4,5)-bisphosphate (PIP₂). In particular, PIP₂ stabilizes the open state of the channel in the absence of ATP and reduces the inhibitory effect of ATP by decreasing the channel apparent affinity for the molecule (Hilgemann and Ball, 1996; Fan and Makielski, 1997; Shyng and Nichols, 1998).

Ci-VSP is a protein that consists of a voltage sensor domain (VSD) and a cytoplasmic phosphatase region. Upon membrane depolarization, a conformational change of the VSD triggers the enzyme phosphatase activity causing dephosphorylation of PIP₂ (Sakata et al., 2011).

RESULTS

We used Ci-VSP to examine the PIP₂ sensitivity of whole-cell K_{ATP} currents recorded from oocytes by TEVC. The principle of our approach is illustrated in Figure 66. Basically, Ci-VSP is activated by a sustained strong depolarization and reduces PIP₂ levels drastically. Upon repolarization, PIP₂ is regenerated by endogenous enzymes within minutes and reactivates PIP₂-sensitive currents. Assuming regeneration speed is similar in all oocytes, the speed of reactivation can be correlated with the sensitivity of currents to activation by PIP₂, with a higher sensitivity yielding faster reactivation.

TEVC recordings were performed on *Xenopus laevis* oocytes expressing SUR2A and Kir6.2 co-expressed with Ci-VSP. In basal conditions, cytoplasmic ATP is too high to allow opening of K_{ATP} channels. Thus, the metabolic inhibitor azide is used to lower internal ATP. For SUR2A-based channels, azide is not sufficient, and it is necessary to apply an activator (here, P1075) to see K_{ATP} currents. Subsequently, a depolarization to +70mV is applied for 60 s in order to activate Ci-VSP. Upon repolarization, currents are usually very low, reflecting the loss of PIP₂, and recover in minutes to their initial values. This protocol is illustrated in Figure 67, where it is also shown that depolarization alone, without coexpressed Ci-VSP, has no effect on recorded currents.

Analysis of the reactivation time course is rendered difficult because it is superimposed on a moving baseline due to the very slow current activation by the opener P1075. This baseline is therefore extrapolated interactively with a polynomial curve and that curve is subtracted from the reactivation currents to correct for ongoing activation. The corrected time course is then fitted with a single exponential to evaluate its time constant. The results of this analysis with SUR2A wild-type and mutants are given in Figure 67. All constructs displayed a near-complete loss of activity after depolarization (panel E). However, both mutants H60Y and D207E reactivated more rapidly than the wild-type (panel F) suggesting that the mutations cause an increase in PIP₂ sensitivity. Such an increase could explain hyperactivity of these mutants. Thus, these experiments suggest a new possible mechanism by which CS mutations induce a gain-of-function of the K_{ATP} channel.

RESULTS

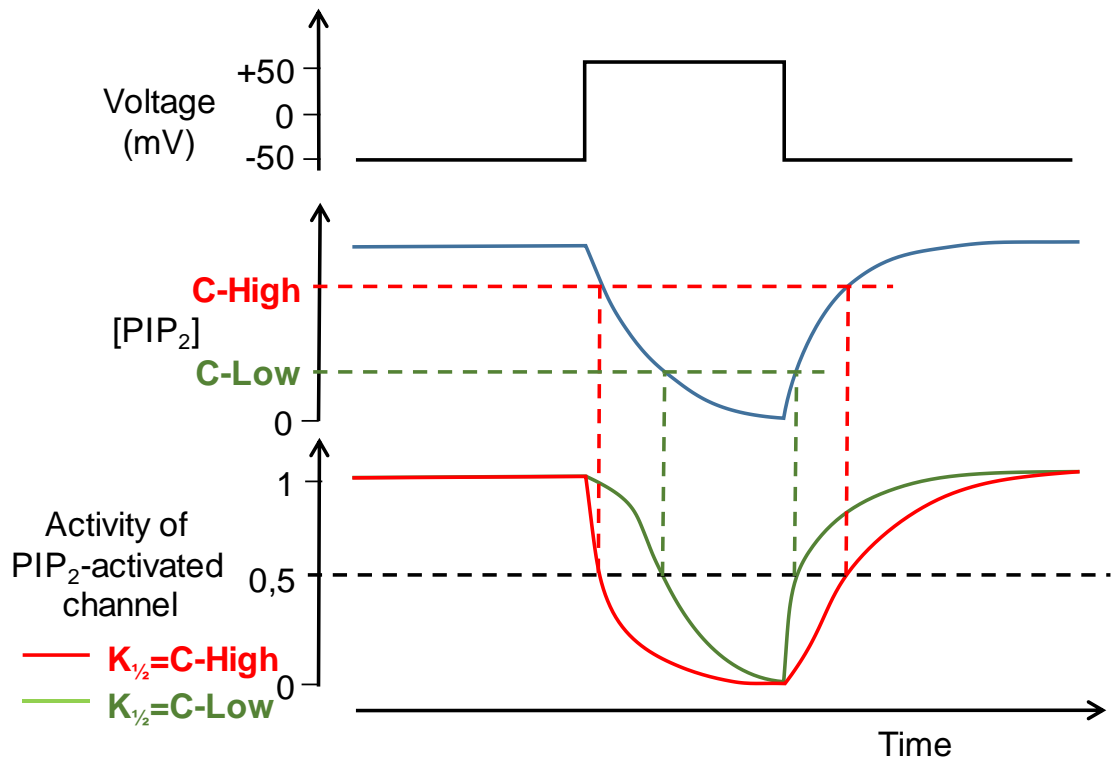


Figure 66. Testing channel PIP_2 sensitivity using the PIP_2 voltage-activated phosphatase Ci-VSP. Ci-VSP can be co-expressed with PIP_2 -sensitive channels, like the K_{ATP} channel, in *Xenopus* oocytes. When the oocyte is depolarized, Ci-VSP is activated and hydrolyzes rapidly PIP_2 . Upon repolarization, PIP_2 rapidly returns to basal levels under the action of endogenous kinases. A channel which requires high-level of PIP_2 to function ($K_{1/2}=C-High$) will be slowly reactivated upon repolarization, compared to a channel which only needs low levels of PIP_2 to function ($K_{1/2}=C-Low$). Thus, the time constant of reactivation is an indicator of channel sensitivity to activation by PIP_2 . A larger time constant means therefore a channel which is less sensitive to PIP_2 .

RESULTS

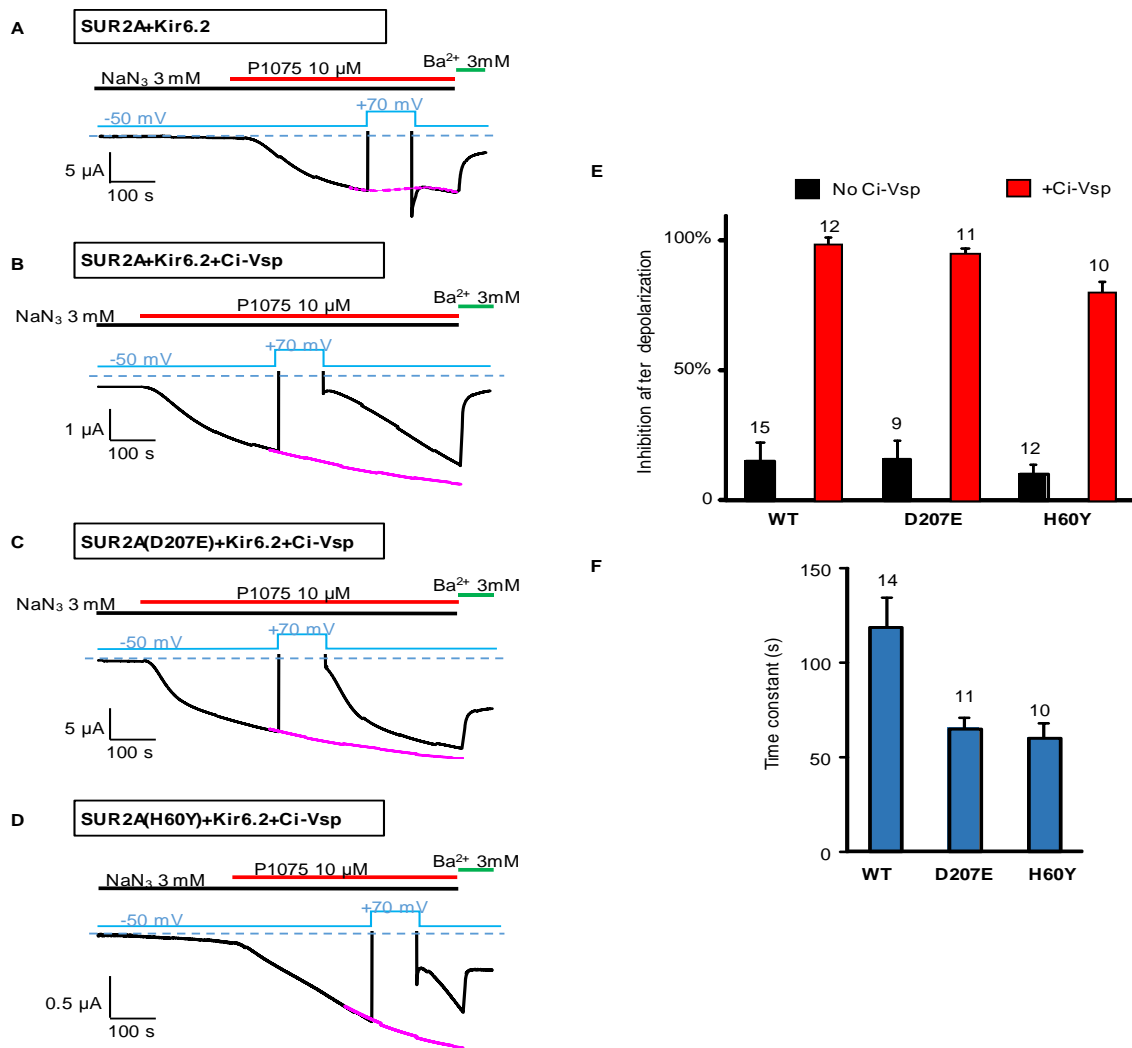


Figure 67. Mutations D207E and H60Y render SUR2A+Kir6.2 K_{ATP} channels more sensitive to activation by PIP₂. To test PIP₂ sensitivity, WT or mutated SUR2A were co-expressed with Kir6.2 and Ci-VSP in *Xenopus* oocytes. Whole-cell K_{ATP} currents were recorded by two-electrode voltage clamp with a HiClamp robot. To elicit currents, application of 3 mM azide to reduce internal ATP levels, and of the K_{ATP} channel activator P1075 (10 μM) was required. PIP₂ levels were decreased by a 60-s depolarization to +70 mV. Upon repolarization, currents were nearly fully inactivated, and returned to basal levels slowly. The reactivation time course was fitted using a single-exponential to yield the level of inhibition after depolarization and the time constant of reactivation. Because P1075 produces a slow activation which does not reach a plateau before many minutes, this activation is extrapolated using a polynomial curve (pink curve) and this curve is used to correct the reactivation time course before fitting. **A-D.** Representative TEVC recordings. **A.** Control experiment, SUR2A+Kir6.2, without Ci-VSP shows no significant inhibition after depolarization. **B.** Same experiment with co-expressed Ci-VSP demonstrates a near-complete loss of activity of WT channels with slow reactivation. **C&D.** Same experiments with mutants demonstrate also a near-complete loss of activity, but with a faster reactivation. **E.** Average level of inhibition of each construct upon repolarization, without and with Ci-VSP. **F.** Average time constants of reactivation are smaller for mutants than for WT.

3.c.4. Response to the pharmacological opener P1075

In order to assess the influence of mutations on the pharmacological properties of K_{ATP} channels, we first examined the response of mutants to the opener P1075 which preferentially targets SUR2A (Moreau et al., 2000). As shown in Figure 68, results demonstrate that both mutants are strongly activated by a saturating concentration of P1075 (10 μ M). The responses of mutants were comparable to that of the wild-type although a more detailed analysis would be required to evaluate any difference.

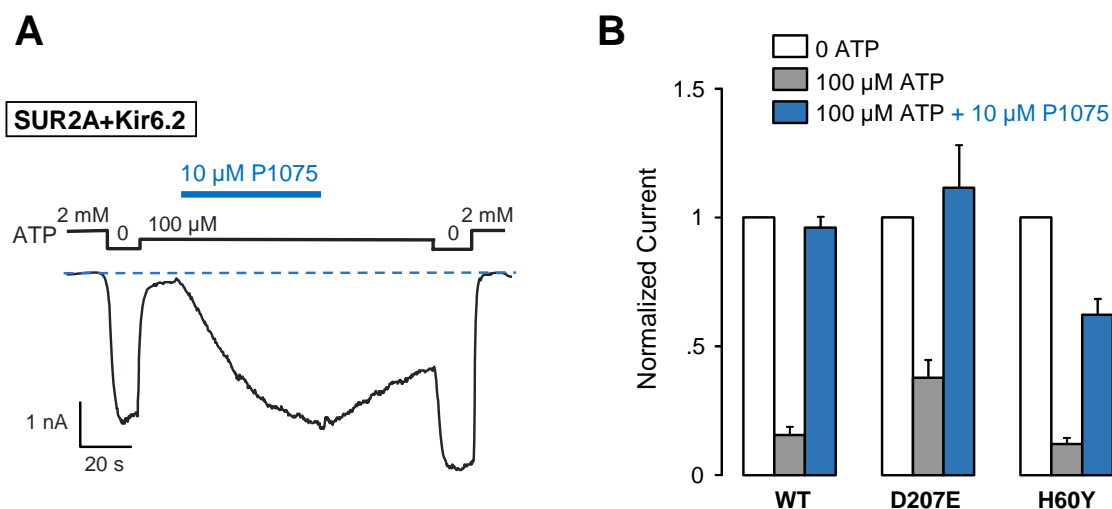


Figure 68. CS mutants are activated by the opener P1075. Responses of the Cantù mutants to the pinacidil analogue P1075 were measured in inside-out patches excised from oocytes co-expressing wild-type or mutated SUR2A, and Kir6.2. **A.** Representative patch clamp recording of wild-type channels illustrating the protocol employed. Voltage was clamped at -50 mV. **B.** Summary of data from experiments as described in panel A. P1075 (10 μ M) was applied in the presence of 100 μ M ATP, and currents were normalized to the average of the currents measured in the absence of nucleotides before opener application.

3.c.5. Response to the pharmacological blocker glibenclamide.

Some neonatal diabetes mellitus (NDM) patients with GOF mutations in Kir6.2 or SUR1 have successfully been switched from insulin therapy to K_{ATP} inhibitors such as glibenclamide (Zung et al., 2004). Nevertheless, a correlation between increased channel activity and diminished effectiveness of such drugs has been noted (Koster et al., 2005). Therefore, we examined the effectiveness of the archetypal K_{ATP} channel blocker, glibenclamide, on overactive D207E and H60Y channels, using patch-clamp recordings. Results are shown in Figure 69. A single concentration of glibenclamide of 300 nM was tested. This concentration is nearly saturating for SUR2A-based channels.

RESULTS

Because the effect of glibenclamide is more consistent in the presence of ATP, it was tested in the presence of 10 μM ATP, a concentration which causes only weak inhibition of K_{ATP} channels. Our results indicate that inhibition by glibenclamide appears unaffected by the D207E mutation, but is reduced by mutation H60Y. However, these preliminary results need to be confirmed to reach a definite conclusion.

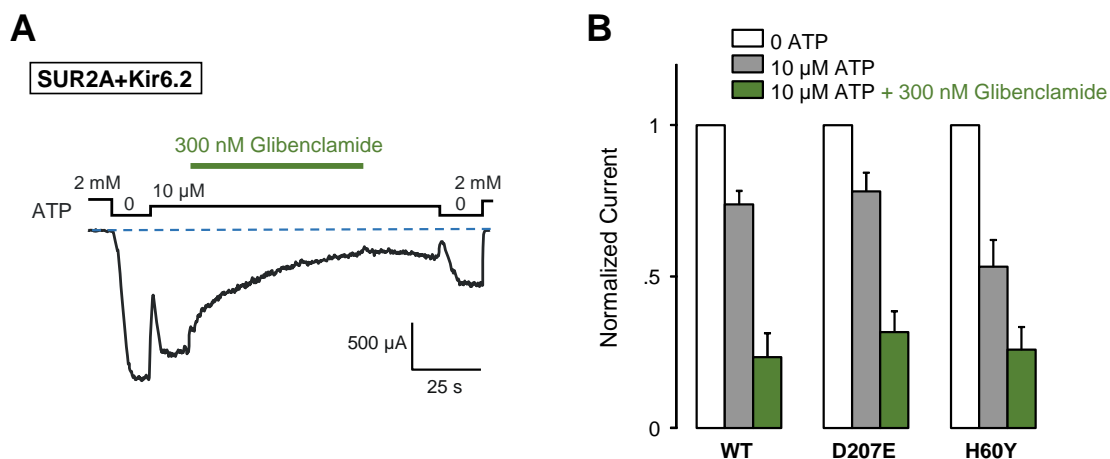


Figure 69. CS mutants are inhibited by the sulfonylurea glibenclamide. Glibenclamide responses of wild-type and mutated K_{ATP} channels were measured in inside-out patches excised from oocytes co-expressing wild-type or mutated SUR2A, and Kir6.2. **A.** Representative patch clamp recording. Voltage was clamped at -50 mV . **B.** Summary of experiments as described in panel A ($n=5-9$). Glibenclamide (300 nM) was applied in the presence of 10 μM ATP, and currents were normalized to the current measured in the absence of nucleotides before glibenclamide application.

3.d. Discussion and perspectives

Today, CS is the only pathology associated with SUR2A mutations which, when functionally characterized, cause a GOF of the K_{ATP} channel. Here, we characterized two CS SUR2 mutants: H60Y located in the TMD0 region of SUR protein and D207E located in the cytosolic linker (L0) which connects TMD0 to the core domain of SUR. TMD0 is a key domain which is involved in a tight physical interaction between SUR and the Kir6 subunits of the K_{ATP} channel. In addition, TMD0 has a crucial role in the regulation of Kir6 gating and trafficking (Chan et al., 2003; Fang et al., 2006). Previous characterization of CS mutations located in TMD1 and TMD2 have shown an increase in the activity of K_{ATP} channels (Cooper et al., 2014, 2015; Harakalova et al., 2012). Two different pathways have been found to explain how these pathological mutations affect the functionality of K_{ATP} channels: reduction of the ATP binding affinity and enhancement of the Mg-ADP activation. It has also been shown that a SUR CS mutation increases the intrinsic open

RESULTS

probability, thus causing a decrease in the apparent ATP sensitivity (Cooper et al., 2015; Harakalova et al., 2012).

Our experiments show that the two SUR2 mutations (H60Y and E207E) cause K_{ATP} channel hyperactivity through two divergent mechanisms. The D207E mutation decreases sensitivity to ATP inhibition, in a similar manner to CS-associated mutations already tested (Cooper et al., 2014, 2015; Harakalova et al., 2012). We also observed that this mutation increased sensitivity to PIP_2 . It may be noted that, the equivalent SUR1 mutation (E209D) is associated to permanent neonatal diabetes by increasing the activity of ATP channels (Ellard et al., 2007; Edghill et al., 2010). These results identify E207 as an important SUR2 residue for K_{ATP} gating. In contrast, the H60Y mutation did not affect ATP sensitivity and Mg-ADP activation. However it rendered the channel more sensitive to PIP_2 (Figure 66). This suggests that the H60Y stabilizes the open state of the Kir6.2 (Hilgemann and Ball, 1996; Fan and Makielski, 1997) causing a hyperactivity of the K_{ATP} channel. This result is unexpected, since the increase in the open probability of the channel intrinsically affect the ATP sensitivity of the channel. A similar observation was made for another SUR2 CS mutation, C1039Y. However this mutation decreased ATP sensitivity while H60Y does not (Cooper et al., 2015). These findings underscore the critical role of TMD0 in the gating modulation of Kir6.2. They demonstrate in particular that domain TMD0 can control the response of the channel to intracellular effectors (ATP and PIP_2) that bind to Kir6.2, implying tight physical interactions between Kir6.2 and the TMD0 region of SUR.

In conclusion, today seven CS-associated mutations have been characterized and all of them lead to an over-activity of K_{ATP} channels (Cooper et al., 2014, 2015; Harakalova et al., 2012). However, some CS patients had no identifiable ABCC9 or KCNJ8 gene mutation, suggesting that additional gene defects may be involved (Nichols et al., 2013).

The ABCC9 gene encodes two splice variants: SUR2A and SUR2B, which differ only in their last 40 amino acids. All CS SUR2 mutations identified thus far are found within the core of the SUR2 protein, such that these mutations will be present in both SUR2A and SUR2B (Cooper et al., 2015). SUR2A is predominant in skeletal muscle and heart, while SUR2B is expressed in the vasculature. Today the vascular phenotypes have been the most common anomalies present in CS patients in addition to the cardiac phenotypes of heart enlargement, concentric hypertrophy of the ventricles, pulmonary hypertension and pericardial effusion (Nichols et al., 2013). However, the severity of symptoms varies between CS patients such that not all reported features are exhibited by all patients

RESULTS

(Cooper et al., 2015). Information about the specific medical features caused by H60Y and D207E SUR2 CS mutations is not yet available in the literature.

Today, all CS mutants are linked to a K_{ATP} channel GOF. This opens the possibility of treatment with sulfonylureas, a K_{ATP} channel inhibitor (Nelson et al., 2015). However, GOF mutations in Kir6.2 (Koster et al., 2005) and SUR1 (Takagi et al., 2013), also normally decrease sensitivity to sulfonylureas, which may result in a lack of sulfonylurea therapeutic efficacy. Nevertheless, we demonstrated here that the H60Y and D207E SUR2 mutations do not significantly affect glibenclamide block, thus opening the door to sulfonylureas to treat CS patients which have these mutations.

BIBLIOGRAPHY

- Aguilar-Bryan, L., and J. Bryan. 1999. Molecular biology of adenosine triphosphate-sensitive potassium channels. *Endocr. Rev.* 20:101–35. doi:10.1210/edrv.20.2.0361.
- Aguilar-Bryan, L., C.G. Nichols, S.W. Wechsler, J.P. Clement, A.E. Boyd, G. González, H. Herrera-Sosa, K. Nguy, J. Bryan, and D.A. Nelson. 1995. Cloning of the beta cell high-affinity sulfonylurea receptor: a regulator of insulin secretion. *Science*. 268:423–6.
- Akrouh, A., S.E. Halcomb, C.G. Nichols, and M. Sala-Rabanal. 2009. Molecular biology of K(ATP) channels and implications for health and disease. *IUBMB Life*. 61:971–8. doi:10.1002/iub.246.
- Aller, S.G., J. Yu, A. Ward, Y. Weng, S. Chittaboina, R. Zhuo, P.M. Harrell, Y.T. Trinh, Q. Zhang, I.L. Urbatsch, and G. Chang. 2009. Structure of P-glycoprotein reveals a molecular basis for poly-specific drug binding. *Science*. 323:1718–1722. doi:10.1126/science.1168750.
- Antcliff, J.F., S. Haider, P. Proks, M.S.P. Sansom, and F.M. Ashcroft. 2005. Functional analysis of a structural model of the ATP-binding site of the KATP channel Kir6.2 subunit. *EMBO J.* 24:229–39. doi:10.1038/sj.emboj.7600487.
- Aryal, P., M.S.P. Sansom, and S.J. Tucker. 2015. Hydrophobic Gating in Ion Channels. *J. Mol. Biol.* 427:121–130. doi:10.1016/j.jmb.2014.07.030.
- Ashcroft, F.M. 2005. ATP-sensitive potassium channelopathies: focus on insulin secretion. *J. Clin. Invest.* 115:2047–2058. doi:10.1172/JCI25495.
- Ashcroft, F.M., and F.M. Gribble. 1999. ATP-sensitive K⁺ channels and insulin secretion: their role in health and disease. *Diabetologia*. 42:903–919. doi:10.1007/s001250051247.
- Ashcroft, F.M., D.E. Harrison, and S.J. Ashcroft. 1984. Glucose induces closure of single potassium channels in isolated rat pancreatic beta-cells. *Nature*. 312:446–8.
- Ashfield, R., F.M. Gribble, S.J. Ashcroft, and F.M. Ashcroft. 1999. Identification of the high-affinity tolbutamide site on the SUR1 subunit of the K(ATP) channel. *Diabetes*. 48:1341–1347.
- Ashford, M.L., N.C. Sturgess, N.J. Trout, N.J. Gardner, and C.N. Hales. 1988. Adenosine-5'-triphosphate-sensitive ion channels in neonatal rat cultured central neurones. *Pflügers Arch. Eur. J. Physiol.* 412:297–304.
- Babenko, A.P., and J. Bryan. 2003. Sur domains that associate with and gate KATP pores define a novel gatekeeper. *J. Biol. Chem.* 278:41577–80. doi:10.1074/jbc.C300363200.
- Babenko, A.P., G. Gonzalez, and J. Bryan. 2000. Pharmaco-topology of sulfonylurea receptors. Separate domains of the regulatory subunits of K(ATP) channel isoforms are required for selective interaction with K(+) channel openers. *J. Biol. Chem.* 275:717–720.
- Bancila, V., T. Cens, D. Monnier, F. Chanson, C. Faure, Y. Dunant, and A. Bloc. 2005. Two SUR1-specific histidine residues mandatory for zinc-induced activation of the rat KATP channel. *J. Biol. Chem.* 280:8793–8799. doi:10.1074/jbc.M413426200.
- Banghart, M., K. Borges, E. Isacoff, D. Trauner, and R.H. Kramer. 2004. Light-activated ion channels for remote control of neuronal firing. *Nat. Neurosci.* 7:1381–6. doi:10.1038/nn1356.
- Baukrowitz, T., U. Schulte, D. Oliver, S. Herlitze, T. Krauter, S.J. Tucker, J.P. Ruppersberg, and B. Fakler. 1998. PIP2 and PIP as determinants for ATP inhibition of KATP channels. *Science*. 282:1141–4.
- Baumgartner, W., L. Islas, and F.J. Sigworth. 1999. Two-microelectrode voltage clamp of *Xenopus* oocytes: voltage errors and compensation for local current flow. *Biophys. J.* 77:1980–91. doi:10.1016/S0006-3495(99)77039-6.
- Beek, J. ter, A. Guskov, and D.J. Slotboom. 2014. Structural diversity of ABC transporters. *J. Gen. Physiol.* 143:419–35. doi:10.1085/jgp.201411164.
- Del Bene, F., and C. Wyart. 2012. Optogenetics: a new enlightenment age for zebrafish neurobiology. *Dev. Neurobiol.* 72:404–14. doi:10.1002/dneu.20914.

- Berndt, A., S.Y. Lee, C. Ramakrishnan, and K. Deisseroth. 2014. Structure-guided transformation of channelrhodopsin into a light-activated chloride channel. *Science*. 344:420–4. doi:10.1126/science.1252367.
- Betourne, A., A.M. Bertholet, E. Labroue, H. Halley, H.S. Sun, A. Lorisignol, Z.-P. Feng, R.J. French, L. Penicaud, J.-M. Lassalle, and B. Frances. 2009. Involvement of hippocampal CA3 K(ATP) channels in contextual memory. *Neuropharmacology*. 56:615–25. doi:10.1016/j.neuropharm.2008.11.001.
- Bichet, D., F.A. Haass, and L.Y. Jan. 2003. Merging functional studies with structures of inward-rectifier K(+) channels. 4. doi:10.1038/nrn1244.
- Bienengraeber, M., A.E. Alekseev, M.R. Abraham, A.J. Carrasco, C. Moreau, M. Vivaudou, P.P. Dzeja, and A. Terzic. 2000. ATPase activity of the sulfonylurea receptor: a catalytic function for the KATP channel complex. *FASEB J.* 14:1943–52. doi:10.1096/fj.00-0027com.
- Blaustein, R.O., P.A. Cole, C. Williams, and C. Miller. 2000. Tethered blockers as molecular “tape measures” for a voltage-gated K⁺ channel. *Nat. Struct. Biol.* 7:309–11. doi:10.1038/74076.
- van Bon, B.W.M., C. Gilissen, D.K. Grange, R.C.M. Hennekam, H. Kayserili, H. Engels, H. Reutter, J.R. Ostergaard, E. Morava, K. Tsiakas, B. Isidor, M. Le Merrer, M. Eser, N. Wieskamp, P. de Vries, M. Steehouwer, J.A. Veltman, S.P. Robertson, H.G. Brunner, B.B.A. de Vries, and A. Hoischen. 2012. Cantú Syndrome Is Caused by Mutations in ABCC9. *Am. J. Hum. Genet.* 90:1094–1101. doi:10.1016/j.ajhg.2012.04.014.
- Boyden, E.S., F. Zhang, E. Bamberg, G. Nagel, and K. Deisseroth. 2005. Millisecond-timescale, genetically targeted optical control of neural activity. *Nat. Neurosci.* 8:1263–8. doi:10.1038/nn1525.
- Broichhagen, J., I. Jurastow, K. Iwan, W. Kummer, and D. Trauner. 2014a. Optical control of acetylcholinesterase with a tacrine switch. *Angew. Chem. Int. Ed. Engl.* 53:7657–60. doi:10.1002/anie.201403666.
- Broichhagen, J., M. Schönberger, S.C. Cork, J.A. Frank, P. Marchetti, M. Bugliani, A.M.J. Shapiro, S. Trapp, G.A. Rutter, D.J. Hodson, and D. Trauner. 2014b. Optical control of insulin release using a photoswitchable sulfonylurea. *Nat. Commun.* 5:5116. doi:10.1038/ncomms6116.
- Brownstein, C.A., M.C. Towne, L.J. Luquette, D.J. Harris, N.S. Marinakis, P. Meinecke, K. Kutsche, P.M. Campeau, T.W. Yu, D.M. Margulies, P.B. Agrawal, and A.H. Beggs. 2013. Mutation of KCNJ8 in a patient with Cantú syndrome with unique vascular abnormalities - support for the role of K(ATP) channels in this condition. *Eur. J. Med. Genet.* 56:678–82. doi:10.1016/j.ejmg.2013.09.009.
- Cantú, J.M., D. García-Cruz, J. Sánchez-Corona, A. Hernández, and Z. Nazará. 1982. A distinct osteochondrodysplasia with hypertrichosis - Individualization of a probable autosomal recessive entity. *Hum. Genet.* 60:36–41.
- Caro, L.N., C.J. Moreau, A. Estrada-Mondragón, O.P. Ernst, and M. Vivaudou. 2012. Engineering of an Artificial Light-Modulated Potassium Channel. *PLoS One*. 7:e43766. doi:10.1371/journal.pone.0043766.
- Caro, L.N., C.J. Moreau, J. Revilloud, and M. Vivaudou. 2011. β 2-Adrenergic Ion-Channel Coupled Receptors as Conformational Motion Detectors. *PLoS One*. 6:e18226. doi:10.1371/journal.pone.0018226.
- Chambers, J.J., M.R. Banghart, D. Trauner, and R.H. Kramer. 2006. Light-induced depolarization of neurons using a modified Shaker K(+) channel and a molecular photoswitch. *J. Neurophysiol.* 96:2792–6. doi:10.1152/jn.00318.2006.
- Chambers, J.J., and R.H. Kramer. 2008. Light-activated ion channels for remote control of neural activity. *Methods Cell Biol.* 90:217–32. doi:10.1016/S0091-679X(08)00811-X.
- Chan, K.W., H. Zhang, and D.E. Logothetis. 2003. N-terminal transmembrane domain of the SUR controls trafficking and gating of Kir6 channel subunits. *EMBO J.* 22:3833–43. doi:10.1093/emboj/cdg376.

- Cheng, W.W.L., J.G. McCoy, A.N. Thompson, C.G. Nichols, and C.M. Nimigean. 2011. Mechanism for selectivity-inactivation coupling in KcsA potassium channels. *Proc. Natl. Acad. Sci. U. S. A.* 108:5272–7. doi:10.1073/pnas.1014186108.
- Choudhury, H.G., Z. Tong, I. Mathavan, Y. Li, S. Iwata, S. Zirah, S. Rebuffat, H.W. van Veen, and K. Beis. 2014. Structure of an antibacterial peptide ATP-binding cassette transporter in a novel outward occluded state. *Proc. Natl. Acad. Sci. U. S. A.* 111:9145–9150. doi:10.1073/pnas.1320506111.
- Clarke, O.B., A.T. Caputo, A.P. Hill, J.I. Vandenberg, B.J. Smith, and J.M. Gulbis. 2010. Domain reorientation and rotation of an intracellular assembly regulate conduction in Kir potassium channels. *Cell.* 141:1018–29.
- Clement, J.P., K. Kunjilwar, G. Gonzalez, M. Schwanstecher, U. Panten, L. Aguilar-Bryan, and J. Bryan. 1997. Association and Stoichiometry of KATP Channel Subunits. *Neuron.* 18:827–838. doi:10.1016/S0896-6273(00)80321-9.
- Cole, S.P.C. 2014. Multidrug resistance protein 1 (MRP1, ABCC1), a “multitasking” ATP-binding cassette (ABC) transporter. *J. Biol. Chem.* 289:30880–8. doi:10.1074/jbc.R114.609248.
- Cook, D.L., and C.N. Hales. 1984. Intracellular ATP directly blocks K⁺ channels in pancreatic B-cells. *Nature.* 311:271–3.
- Cooper, P.E., H. Reutter, J. Woelfle, H. Engels, D.K. Grange, G. van Haften, B.W. van Bon, A. Hoischen, and C.G. Nichols. 2014. Cantú syndrome resulting from activating mutation in the KCNJ8 gene. *Hum. Mutat.* 35:809–13. doi:10.1002/humu.22555.
- Cooper, P.E., M. Sala-Rabanal, S.J. Lee, and C.G. Nichols. 2015. Differential mechanisms of Cantú syndrome-associated gain of function mutations in the ABCC9 (SUR2) subunit of the KATP channel. *J. Gen. Physiol.* 146:527–40. doi:10.1085/jgp.201511495.
- Cordero-Morales, J.F., L.G. Cuello, Y. Zhao, V. Jogini, D.M. Cortes, B. Roux, and E. Perozo. 2006. Molecular determinants of gating at the potassium-channel selectivity filter. *Nat. Struct. Mol. Biol.* 13:311–8. doi:10.1038/nsmb1069.
- Craig, T.J., K. Shimomura, R.W. Holl, S.E. Flanagan, S. Ellard, and F.M. Ashcroft. 2009. An In-Frame Deletion in Kir6.2 (KCNJ11) Causing Neonatal Diabetes Reveals a Site of Interaction between Kir6.2 and SUR1. *J Clin Endocrinol Metab.* 94:2551–2557. doi:10.1210/jc.2009-0159.
- Cukras, C.A., I. Jeliaskova, and C.G. Nichols. 2002. Structural and Functional Determinants of Conserved Lipid Interaction Domains of Inward Rectifying Kir6.2 Channels. *J. Gen. Physiol.* 119:581–591. doi:10.1085/jgp.20028562.
- D’ahan, N., C. Moreau, A.L. Prost, H. Jacquet, A.E. Alekseev, A. Terzic, and M. Vivaudou. 1999. Pharmacological plasticity of cardiac ATP-sensitive potassium channels toward diazoxide revealed by ADP. *Proc. Natl. Acad. Sci. U. S. A.* 96:12162–12167.
- Dabrowski, M., A. Tarasov, and F.M. Ashcroft. 2004. Mapping the architecture of the ATP-binding site of the KATP channel subunit Kir6.2. *J. Physiol.* 557:347–54. doi:10.1113/jphysiol.2003.059105.
- Dawson, R.J.P., and K.P. Locher. 2006. Structure of a bacterial multidrug ABC transporter. *Nature.* 443:180–185. doi:10.1038/nature05155.
- Deisseroth, K. 2011. Optogenetics. *Nat. Methods.* 8:26–9. doi:10.1038/nmeth.f.324.
- Dorsam, R.T., and J.S. Gutkind. 2007. G-protein-coupled receptors and cancer. *Nat. Rev. Cancer.* 7:79–94. doi:10.1038/nrc2069.
- Doupnik, C.A., N. Davidson, and H.A. Lester. 1995. The inward rectifier potassium channel family. *Curr. Opin. Neurobiol.* 5:268–77.
- Doyle, D.A., J. Morais Cabral, R.A. Pfuetzner, A. Kuo, J.M. Gulbis, S.L. Cohen, B.T. Chait, and R. MacKinnon. 1998. The structure of the potassium channel: molecular basis of K⁺ conduction and selectivity. *Science.* 280:69–77.
- Drain, P., L. Li, and J. Wang. 1998. KATP channel inhibition by ATP requires distinct functional domains of the cytoplasmic C terminus of the pore-forming subunit. *Proc.*

- Natl. Acad. Sci. U. S. A.* 95:13953–8.
- Dupuis, J.P., J. Revilloud, C.J. Moreau, and M. Vivaudou. 2008. Three C-terminal residues from the sulphonylurea receptor contribute to the functional coupling between the K(ATP) channel subunits SUR2A and Kir6.2. *J. Physiol.* 586:3075–85. doi:10.1113/jphysiol.2008.152744.
- Edghill, E.L., S.E. Flanagan, and S. Ellard. 2010. Permanent neonatal diabetes due to activating mutations in ABCC8 and KCNJ11. *Rev. Endocr. Metab. Disord.* 11:193–8. doi:10.1007/s11154-010-9149-x.
- Ellard, S., S.E. Flanagan, C.A. Girard, A.-M. Patch, L.W. Harries, A. Parrish, E.L. Edghill, D.J.G. Mackay, P. Proks, K. Shimomura, H. Haberland, D.J. Carson, J.P.H. Shield, A.T. Hattersley, and F.M. Ashcroft. 2007. Permanent neonatal diabetes caused by dominant, recessive, or compound heterozygous SUR1 mutations with opposite functional effects. *Am. J. Hum. Genet.* 81:375–82. doi:10.1086/519174.
- Fan, Z., and J.C.C. Makielski. 1997. Anionic Phospholipids Activate ATP-sensitive Potassium Channels. *J. Biol. Chem.* 272:5388–5395. doi:10.1074/jbc.272.9.5388.
- Fang, K., L. Csanády, and K.W. Chan. 2006. The N-terminal transmembrane domain (TMD0) and a cytosolic linker (L0) of sulphonylurea receptor define the unique intrinsic gating of KATP channels. *J. Physiol.* 576:379–89. doi:10.1113/jphysiol.2006.112748.
- Fehrentz, T., M. Schönberger, and D. Trauner. 2011. Optochemical genetics. *Angew. Chem. Int. Ed. Engl.* 50:12156–82. doi:10.1002/anie.201103236.
- Flagg, T.P., M.S. Remedi, R. Masia, J. Gomes, M. McLerie, A.N. Lopatin, and C.G. Nichols. 2005. Transgenic overexpression of SUR1 in the heart suppresses sarcolemmal K(ATP). *J. Mol. Cell. Cardiol.* 39:647–56. doi:10.1016/j.yjmcc.2005.06.003.
- Fortin, D.L., T.W. Dunn, A. Fedorchak, D. Allen, R. Montpetit, M.R. Banghart, D. Trauner, J.P. Adelman, and R.H. Kramer. 2011. Optogenetic photochemical control of designer K⁺ channels in mammalian neurons. *J. Neurophysiol.* 106:488–496. doi:10.1152/jn.00251.2011.
- Fredriksson, R., M.C. Lagerström, L.-G. Lundin, and H.B. Schiöth. 2003. The G-Protein-Coupled Receptors in the Human Genome Form Five Main Families. Phylogenetic Analysis, Paralogon Groups, and Fingerprints. *Mol. Pharmacol.* 63:1256–1272. doi:10.1124/mol.63.6.1256.
- Fürst, O., B. Mondou, and N. D'Avanzo. 2014. Phosphoinositide regulation of inward rectifier potassium (Kir) channels. *Front. Physiol.* 4:404. doi:10.3389/fphys.2013.00404.
- Gloyn, A.L., J. Siddiqui, and S. Ellard. 2006. Mutations in the genes encoding the pancreatic beta-cell KATP channel subunits Kir6.2 (KCNJ11) and SUR1 (ABCC8) in diabetes mellitus and hyperinsulinism. *Hum. Mutat.* 27:220–231. doi:10.1002/humu.20292.
- Gorostiza, P., and E. Isacoff. 2007. Optical switches and triggers for the manipulation of ion channels and pores. *Mol. Biosyst.* 3:686–704. doi:10.1039/b710287a.
- Gorostiza, P., and E.Y. Isacoff. 2008. Optical switches for remote and noninvasive control of cell signaling. *Science.* 322:395–9. doi:10.1126/science.1166022.
- Govorunova, E.G., O.A. Sineshchekov, R. Janz, X. Liu, and J.L. Spudich. 2015. NEUROSCIENCE. Natural light-gated anion channels: A family of microbial rhodopsins for advanced optogenetics. *Science.* 349:647–50. doi:10.1126/science.aaa7484.
- Grange, D.K., S.M. Lorch, P.L. Cole, and G.K. Singh. 2006. Cantu syndrome in a woman and her two daughters: Further confirmation of autosomal dominant inheritance and review of the cardiac manifestations. *Am. J. Med. Genet. A.* 140:1673–80. doi:10.1002/ajmg.a.31348.
- Grange, D.K., C.G. Nichols, and G.K. Singh. 2014. Cantú Syndrome and Related Disorders.
- Gribble, F.M., R. Ashfield, C. Ammälä, and F.M. Ashcroft. 1997a. Properties of cloned

- ATP-sensitive K⁺ currents expressed in *Xenopus* oocytes. *J. Physiol.* 498 (Pt 1:87–98.
- Gribble, F.M., P. Proks, B.E. Corkey, and F.M. Ashcroft. 1998a. Mechanism of Cloned ATP-sensitive Potassium Channel Activation by Oleoyl-CoA. *J. Biol. Chem.* 273:26383–26387. doi:10.1074/jbc.273.41.26383.
- Gribble, F.M., S.J. Tucker, and F.M. Ashcroft. 1997b. The Interaction of nucleotides with the tolbutamide block of cloned atp-sensitive k⁺ channel currents expressed in xenopus oocytes: a reinterpretation. *J. Physiol.* 504:35–45. doi:10.1111/j.1469-7793.1997.00035.x.
- Gribble, F.M., S.J. Tucker, T. Haug, and F.M. Ashcroft. 1998b. MgATP activates the beta cell KATP channel by interaction with its SUR1 subunit. *Proc. Natl. Acad. Sci. U. S. A.* 95:7185–90.
- Gumina, R.J., D.F. O’Cochlain, C.E. Kurtz, P. Bast, D. Pucar, P. Mishra, T. Miki, S. Seino, S. Macura, and A. Terzic. 2006. KATP channel knockout worsens myocardial calcium stress load in vivo and impairs recovery in stunned heart. *AJP Hear. Circ. Physiol.* 292:H1706–H1713. doi:10.1152/ajpheart.01305.2006.
- Habermacher, C., A. Martz, N. Calimet, D. Lemoine, L. Peverini, A. Specht, M. Cecchini, and T. Grutter. 2016. Photo-switchable tweezers illuminate pore-opening motions of an ATP-gated P2X ion channel. *Elife.* 5:e11050. doi:10.7554/eLife.11050.
- Haga, K., A.C. Kruse, H. Asada, T. Yurugi-Kobayashi, M. Shiroishi, C. Zhang, W.I. Weis, T. Okada, B.K. Kobilka, T. Haga, and T. Kobayashi. 2012. Structure of the human M2 muscarinic acetylcholine receptor bound to an antagonist. *Nature.* 482:547–551. doi:10.1038/nature10753.
- HAIDER, S., J. ANTCLIFF, P. PROKS, M. SANSOM, and F. ASHCROFT. 2005. Focus on Kir6.2: a key component of the ATP-sensitive potassium channel. *J. Mol. Cell. Cardiol.* 38:927–936. doi:10.1016/j.yjmcc.2005.01.007.
- Hansen, S.B., X. Tao, and R. MacKinnon. 2011. Structural basis of PIP2 activation of the classical inward rectifier K⁺ channel Kir2.2. *Nature.* 477:495–8. doi:10.1038/nature10370.
- Harakalova, M., J.J.T. van Harsse, P.A. Terhal, S. van Lieshout, K. Duran, I. Renkens, D.J. Amor, L.C. Wilson, E.P. Kirk, C.L.S. Turner, D. Shears, S. Garcia-Minaur, M.M. Lees, A. Ross, H. Venselaar, G. Vriend, H. Takanari, M.B. Rook, M.A.G. van der Heyden, F.W. Asselbergs, H.M. Breur, M.E. Swinkels, I.J. Scurr, S.F. Smithson, N. V Knoers, J.J. van der Smagt, I.J. Nijman, W.P. Kloosterman, M.M. van Haelst, G. van Haften, and E. Cuppen. 2012. Dominant missense mutations in ABCC9 cause Cantú syndrome. *Nat. Genet.* 44:793–796. doi:10.1038/ng.2324.
- He, C., X. Yan, H. Zhang, T. Mirshahi, T. Jin, A. Huang, and D.E. Logothetis. 2002. Identification of Critical Residues Controlling G Protein-gated Inwardly Rectifying K⁺ Channel Activity through Interactions with the Subunits of G Proteins. *J. Biol. Chem.* 277:6088–6096. doi:10.1074/jbc.M104851200.
- Hernández-Sánchez, C., A.S. Basile, I. Fedorova, H. Arima, B. Stannard, A.M. Fernandez, Y. Ito, and D. LeRoith. 2001. Mice transgenically overexpressing sulfonylurea receptor 1 in forebrain resist seizure induction and excitotoxic neuron death. *Proc. Natl. Acad. Sci. U. S. A.* 98:3549–3554. doi:10.1073/pnas.051012898.
- Heusser, K., H. Yuan, I. Neagoe, A.I. Tarasov, F.M. Ashcroft, and B. Schwappach. 2006. Scavenging of 14-3-3 proteins reveals their involvement in the cell-surface transport of ATP-sensitive K⁺ channels. *J. Cell Sci.* 119:4353–63. doi:10.1242/jcs.03196.
- Hibino, H., A. Inanobe, K. Furutani, S. Murakami, I. Findlay, and Y. Kurachi. 2010. Inwardly rectifying potassium channels: their structure, function, and physiological roles. *Physiol. Rev.* 90:291–366. doi:10.1152/physrev.00021.2009.
- Hilgemann, D.W., and R. Ball. 1996. Regulation of Cardiac Na⁺,Ca²⁺ Exchange and KATP Potassium Channels by PIP2. *Science (80-).* 273:956–959. doi:10.1126/science.273.5277.956.
- Hiraki, Y., S. Miyatake, M. Hayashidani, Y. Nishimura, H. Matsuura, M. Kamada, T. Kawagoe, K. Yunoki, N. Okamoto, H. Yofune, M. Nakashima, Y. Tsurusaki, H.

- Satisu, A. Murakami, N. Miyake, G. Nishimura, and N. Matsumoto. 2014. Aortic aneurysm and craniosynostosis in a family with Cantu syndrome. *Am. J. Med. Genet. A.* 164A:231–6. doi:10.1002/ajmg.a.36228.
- Hohl, M., C. Briand, M.G. Grütter, and M.A. Seeger. 2012. Crystal structure of a heterodimeric ABC transporter in its inward-facing conformation. *Nat. Struct. Mol. Biol.* 19:395–402. doi:10.1038/nsmb.2267.
- Hollenstein, K., D.C. Frei, and K.P. Locher. 2007. Structure of an ABC transporter in complex with its binding protein. *Nature.* 446:213–216. doi:10.1038/nature05626.
- Hosey, M.M., J.L. Benovic, S.K. DebBurman, and R.M. Richardson. 1995. Multiple mechanisms involving protein phosphorylation are linked to desensitization of muscarinic receptors. *Life Sci.* 56:951–955.
- Hosy, E., and M. Vivaudou. 2014. The unusual stoichiometry of ADP activation of the KATP channel. *Front. Physiol.* 5:11. doi:10.3389/fphys.2014.00011.
- Huang, C.L., S. Feng, and D.W. Hilgemann. 1998. Direct activation of inward rectifier potassium channels by PIP2 and its stabilization by Gbetagamma. *Nature.* 391:803–6. doi:10.1038/35882.
- Inagaki, N., T. Gono, J.P. Clement, N. Namba, J. Inazawa, G. Gonzalez, L. Aguilar-Bryan, S. Seino, and J. Bryan. 1995. Reconstitution of IKATP: an inward rectifier subunit plus the sulfonylurea receptor. *Science.* 270:1166–70.
- Inagaki, N., T. Gono, and S. Seino. 1997. Subunit stoichiometry of the pancreatic beta-cell ATP-sensitive K⁺ channel. *FEBS Lett.* 409:232–6.
- Isomoto, S., C. Kondo, M. Yamada, S. Matsumoto, O. Higashiguchi, Y. Horio, Y. Matsuzawa, and Y. Kurachi. 1996. A novel sulfonylurea receptor forms with BIR (Kir6.2) a smooth muscle type ATP-sensitive K⁺ channel. *J. Biol. Chem.* 271:24321–4.
- Jiang, Y., A. Lee, J. Chen, M. Cadene, B.T. Chait, and R. MacKinnon. 2002. Crystal structure and mechanism of a calcium-gated potassium channel. *Nature.* 417:515–22. doi:10.1038/417515a.
- Kadaba, N.S., J.T. Kaiser, E. Johnson, A. Lee, and D.C. Rees. 2008. The high-affinity E. coli methionine ABC transporter: structure and allosteric regulation. *Science.* 321:250–253. doi:10.1126/science.1157987.
- Karger, A.B., S. Park, S. Reyes, M. Bienengraeber, R.B. Dyer, A. Terzic, and A.E. Alekseev. 2008. Role for SUR2A ED domain in allosteric coupling within the K(ATP) channel complex. *J. Gen. Physiol.* 131:185–96. doi:10.1085/jgp.200709852.
- Karschin, C., C. Ecke, F.M. Ashcroft, and A. Karschin. 1997. Overlapping distribution of K(ATP) channel-forming Kir6.2 subunit and the sulfonylurea receptor SUR1 in rodent brain. *FEBS Lett.* 401:59–64.
- Kato, H.E., F. Zhang, O. Yizhar, C. Ramakrishnan, T. Nishizawa, K. Hirata, J. Ito, Y. Aita, T. Tsukazaki, S. Hayashi, P. Hegemann, A.D. Maturana, R. Ishitani, K. Deisseroth, and O. Nureki. 2012. Crystal structure of the channelrhodopsin light-gated cation channel. *Nature.* 482:369–374. doi:10.1038/nature10870.
- Katritch, V., V. Cherezov, and R.C. Stevens. 2012. Diversity and modularity of G protein-coupled receptor structures. *Trends Pharmacol. Sci.* 33:17–27. doi:10.1016/j.tips.2011.09.003.
- Khurana, A., E.S. Shao, R.Y. Kim, Y.Y. Vilin, X. Huang, R. Yang, and H.T. Kurata. 2011. Forced gating motions by a substituted titratable side chain at the bundle crossing of a potassium channel. *J. Biol. Chem.* 286:36686–93. doi:10.1074/jbc.M111.249110.
- Kofuji, P., N. Davidson, and H.A. Lester. 1995. Evidence that neuronal G-protein-gated inwardly rectifying K⁺ channels are activated by G β 3 subunits and function as heteromultimers. *Neurobiology.* 92:6542–6546.
- Kolakowski, L.F. 1994. GCRDb: a G-protein-coupled receptor database. *Receptors Channels.* 2:1–7.
- Koster, J.C., M.A. Permutt, and C.G. Nichols. 2005a. Diabetes and Insulin Secretion: The ATP-Sensitive K⁺ Channel (KATP) Connection. *Diabetes.* 54:3065–3072.

- doi:10.2337/diabetes.54.11.3065.
- Koster, J.C., M.A. Permutt, and C.G. Nichols. 2005b. Diabetes and insulin secretion: the ATP-sensitive K⁺ channel (K_{ATP}) connection. *Diabetes*. 54:3065–72.
- Koster, J.C., Q. Sha, and C.G. Nichols. 1999a. Sulfonylurea and K⁽⁺⁾-channel opener sensitivity of K_{ATP} channels. Functional coupling of Kir6.2 and SUR1 subunits. *J. Gen. Physiol.* 114:203–13.
- Koster, J.C., Q. Sha, S.-L. Shyng, and C.G. Nichols. 1999b. ATP inhibition of K_{ATP} channels: control of nucleotide sensitivity by the N-terminal domain of the Kir6.2 subunit. *J. Physiol.* 515:19–30. doi:10.1111/j.1469-7793.1999.019ad.x.
- Kramer, R.H., A. Mourrot, and H. Adesnik. 2013. Optogenetic pharmacology for control of native neuronal signaling proteins. *Nat. Neurosci.* 16:816–823. doi:10.1038/nn.3424.
- Krapivinsky, G., E.A. Gordon, K. Wickman, B. Velimirović, L. Krapivinsky, and D.E. Clapham. 1995. The G-protein-gated atrial K⁺ channel IK_{ACh} is a heteromultimer of two inwardly rectifying K⁽⁺⁾-channel proteins. *Nature*. 374:135–41. doi:10.1038/374135a0.
- Krasnoperov, V., Y. Lu, L. Buryanovsky, T.A. Neubert, K. Ichtchenko, and A.G. Petrenko. 2002. Post-translational proteolytic processing of the calcium-independent receptor of alpha-latrotoxin (CIRL), a natural chimera of the cell adhesion protein and the G protein-coupled receptor. Role of the G protein-coupled receptor proteolysis site (GPS) moti. *J. Biol. Chem.* 277:46518–46526. doi:10.1074/jbc.M206415200.
- Kruse, A.C., A.M. Ring, A. Manglik, J. Hu, K. Hu, K. Eitel, H. Hübner, E. Pardon, C. Valant, P.M. Sexton, A. Christopoulos, C.C. Felder, P. Gmeiner, J. Steyaert, W.I. Weis, K.C. Garcia, J. Wess, and B.K. Kobilka. 2013. Activation and allosteric modulation of a muscarinic acetylcholine receptor. *Nature*. 504:101–106. doi:10.1038/nature12735.
- Kühner, P., R. Prager, D. Stephan, U. Russ, M. Winkler, D. Ortiz, J. Bryan, and U. Quast. 2012. Importance of the Kir6.2 N-terminus for the interaction of glibenclamide and repaglinide with the pancreatic K_{ATP} channel. *Naunyn. Schmiedeberg's. Arch. Pharmacol.* 385:299–311. doi:10.1007/s00210-011-0709-8.
- Kuo, A., J.M. Gulbis, J.F. Antcliff, T. Rahman, E.D. Lowe, J. Zimmer, J. Cuthbertson, F.M. Ashcroft, T. Ezaki, and D.A. Doyle. 2003. Crystal structure of the potassium channel KirBac1.1 in the closed state. *Science*. 300:1922–6. doi:10.1126/science.1085028.
- Lagerström, M.C., and H.B. Schiöth. 2008. Structural diversity of G protein-coupled receptors and significance for drug discovery. *Nat. Rev. Drug Discov.* 7:339–357. doi:10.1038/nrd2518.
- Lee, J.Y., J.G. Yang, D. Zhitnitsky, O. Lewinson, and D.C. Rees. 2014. Structural basis for heavy metal detoxification by an Atm1-type ABC exporter. *Science*. 343:1133–1136. doi:10.1126/science.1246489.
- Lemoine, D., C. Habermacher, A. Martz, P.-F. Méry, N. Bouquier, F. Diverchy, A. Taly, F. Rassendren, A. Specht, and T. Grutter. 2013. Optical control of an ion channel gate. *Proc. Natl. Acad. Sci. U. S. A.* 110:20813–8. doi:10.1073/pnas.1318715110.
- Lester, H.A., M.E. Krouse, M.M. Nass, N.H. Wassermann, and B.F. Erlanger. 1980. A covalently bound photoisomerizable agonist: comparison with reversibly bound agonists at Electrophorus electroplaques. *J. Gen. Physiol.* 75:207–32.
- Levitz, J., C. Pantoja, B. Gaub, H. Janovjak, A. Reiner, A. Hoagland, D. Schoppik, B. Kane, P. Stawski, A.F. Schier, D. Trauner, and E.Y. Isacoff. 2013. Optical control of metabotropic glutamate receptors. *Nat. Neurosci.* 16:507–16. doi:10.1038/nn.3346.
- Lietman, P.S., A.J. Pennisi, M. Takahashi, B.H. Bernstein, B.H. Singen, C. Uittenbogaart, R.B. Ettenger, M.H. Malekzadeh, V. Hanson, and R.N. Fine. 1977. Minoxidil therapy in children with severe hypertension. *J. Pediatr.* 90:813–819. doi:10.1016/S0022-3476(77)81260-2.
- Lim, J.H., E.H. Oh, J. Park, S. Hong, and T.H. Park. 2015. Ion-channel-coupled receptor-based platform for a real-time measurement of G-protein-coupled receptor

- activities. *ACS Nano*. 9:1699–1706. doi:10.1021/nn506494e.
- Lin, W.-C., C.M. Davenport, A. Mouro, D. Vytla, C.M. Smith, K.A. Medeiros, J.J. Chambers, and R.H. Kramer. 2014. Engineering a light-regulated GABAA receptor for optical control of neural inhibition. *ACS Chem. Biol.* 9:1414–9. doi:10.1021/cb500167u.
- Linton, K.J. 2007. Structure and function of ABC transporters. *Physiology (Bethesda)*. 22:122–30. doi:10.1152/physiol.00046.2006.
- Liss, B., R. Bruns, and J. Roeper. 1999. Alternative sulfonyleurea receptor expression defines metabolic sensitivity of K-ATP channels in dopaminergic midbrain neurons. *EMBO J.* 18:833–846. doi:10.1093/emboj/18.4.833.
- Locher, K.P., A.T. Lee, and D.C. Rees. 2002. The E. coli BtuCD Structure: A Framework for ABC Transporter Architecture and Mechanism. *Science (80-)*. 296:1091–1098. doi:10.1126/science.1071142.
- Lodwick, D., R.D. Rainbow, H.N. Rubaiy, J.M. Al, G.W. Vuister, and R.I. Norman. 2014. Sulphonylurea receptors regulate the channel pore in ATP-sensitive potassium channels via an inter-subunit salt bridge. *Biochem. J.* 354:343–354. doi:10.1042/BJ20140273.
- Lopes, C.M.B., H. Zhang, T. Rohacs, T. Jin, J. Yang, and D.E. Logothetis. 2002. Alterations in conserved Kir channel-PIP2 interactions underlie channelopathies. *Neuron*. 34:933–944. doi:10.1016/S0896-6273(02)00725-0.
- Lorenz, E., and A. Terzic. 1999. Physical association between recombinant cardiac ATP-sensitive K⁺ channel subunits Kir6.2 and SUR2A. *J. Mol. Cell. Cardiol.* 31:425–34. doi:10.1006/jmcc.1998.0876.
- Loussouarn, G., L.R. Phillips, R. Masia, T. Rose, and C.G. Nichols. 2001. Flexibility of the Kir6.2 inward rectifier K(+) channel pore. *Proc. Natl. Acad. Sci. U. S. A.* 98:4227–32. doi:10.1073/pnas.061452698.
- Lu, Z., and R. MacKinnon. 1994. Electrostatic tuning of Mg²⁺ affinity in an inward-rectifier K⁺ channel. *Nature*. 371:243–6. doi:10.1038/371243a0.
- MacKinnon, R. 2004. Potassium channels and the atomic basis of selective ion conduction (Nobel Lecture). *Angew. Chem. Int. Ed. Engl.* 43:4265–77. doi:10.1002/anie.200400662.
- Maeda, A., K. Okano, P.S.-H. Park, J. Lem, R.K. Crouch, T. Maeda, and K. Palczewski. 2010. Palmitoylation stabilizes unliganded rod opsin. *Proc. Natl. Acad. Sci. U. S. A.* 107:8428–8433. doi:10.1073/pnas.1000640107.
- Markworth, E., C. Schwanstecher, and M. Schwanstecher. 2000. ATP₄⁻ mediates closure of pancreatic beta-cell ATP-sensitive potassium channels by interaction with 1 of 4 identical sites. *Diabetes*. 49:1413–1418.
- Matsuoka, T., K. Matsushita, Y. Katayama, A. Fujita, K. Inageda, M. Tanemoto, A. Inanobe, S. Yamashita, Y. Matsuzawa, and Y. Kurachi. 2000. C-Terminal Tails of Sulfonyleurea Receptors Control ADP-Induced Activation and Diazoxide Modulation of ATP-Sensitive K⁺ Channels. *Circ. Res.* 87:873–880. doi:10.1161/01.RES.87.10.873.
- Matthews, K.A., L.H. Kuller, K. Sutton-Tyrrell, and Y.F. Chang. 2001. Changes in cardiovascular risk factors during the perimenopause and postmenopause and carotid artery atherosclerosis in healthy women. *Stroke*. 32:1104–11.
- McDevitt, M.A., R.J. Thorsness, and J.E. Levine. 2009. A role for ATP-sensitive potassium channels in male sexual behavior. *Horm. Behav.* 55:366–74. doi:10.1016/j.yhbeh.2008.08.014.
- Merglen, A., S. Theander, B. Rubi, G. Chaffard, C.B. Wollheim, and P. Maechler. 2004. Glucose sensitivity and metabolism-secretion coupling studied during two-year continuous culture in INS-1E insulinoma cells. *Endocrinology*. 145:667–78. doi:10.1210/en.2003-1099.
- Mikhailov, M. V., E.A. Mikhailova, and S.J. Ashcroft. 2001. Molecular structure of the glibenclamide binding site of the beta-cell K(ATP) channel. *FEBS Lett.* 499:154–160.

- Mikhailov, M. V, J.D. Campbell, H. de Wet, K. Shimomura, B. Zadek, R.F. Collins, M.S.P. Sansom, R.C. Ford, and F.M. Ashcroft. 2005. 3-D structural and functional characterization of the purified KATP channel complex Kir6.2-SUR1. *EMBO J.* 24:4166–75. doi:10.1038/sj.emboj.7600877.
- Moreau, C., F. Gally, H. Jacquet-Bouix, and M. Vivaudou. 2005a. The size of a single residue of the sulfonylurea receptor dictates the effectiveness of K ATP channel openers. *Mol. Pharmacol.* 67:1026–33. doi:10.1124/mol.104.008698.
- Moreau, C., H. Jacquet, A.L. Prost, N. D'ahan, and M. Vivaudou. 2000. The molecular basis of the specificity of action of K(ATP) channel openers. *EMBO J.* 19:6644–51. doi:10.1093/emboj/19.24.6644.
- Moreau, C., A.-L. Prost, R. Dérand, and M. Vivaudou. 2005b. SUR, ABC proteins targeted by KATP channel openers. *J. Mol. Cell. Cardiol.* 38:951–963. doi:10.1016/j.yjmcc.2004.11.030.
- Moreau, C.J., J.P. Dupuis, J. Revilloud, K. Arumugam, and M. Vivaudou. 2008. Coupling ion channels to receptors for biomolecule sensing. *Nat. Nanotechnol.* 3:620–5. doi:10.1038/nnano.2008.242.
- Mourot, A., T. Fehrentz, Y. Le Feuvre, C.M. Smith, C. Herold, D. Dalkara, F. Nagy, D. Trauner, and R.H. Kramer. 2012. Rapid optical control of nociception with an ion-channel photoswitch. *Nat. Methods.* 9:396–402. doi:10.1038/nmeth.1897.
- Mukai, E., H. Ishida, M. Horie, A. Noma, Y. Seino, and M. Takano. 1998. The antiarrhythmic agent cibenzoline inhibits KATP channels by binding to Kir6.2. *Biochem. Biophys. Res. Commun.* 251:477–481. doi:10.1006/bbrc.1998.9492.
- Nelson, P.T., G.A. Jicha, W.-X. Wang, E. Ighodaro, S. Artiushin, C.G. Nichols, and D.W. Fardo. 2015. ABCC9/SUR2 in the brain: Implications for hippocampal sclerosis of aging and a potential therapeutic target. *Ageing Res. Rev.* 24:111–25. doi:10.1016/j.arr.2015.07.007.
- Nichols, C.G., and A.N. Lopatin. 1997. Inward rectifier potassium channels. *Annu. Rev. Physiol.* 59:171–91. doi:10.1146/annurev.physiol.59.1.171.
- Nichols, C.G., G.K. Singh, and D.K. Grange. 2013. KATP channels and cardiovascular disease: suddenly a syndrome. *Circ. Res.* 112:1059–72. doi:10.1161/CIRCRESAHA.112.300514.
- Niescierowicz, K. 2013. Développement de la technologie des récepteurs couplés à un canal ionique pour des études structure-fonction des récepteurs couplés aux protéines G et du canal Kir6.2. Grenoble.
- Niescierowicz, K., L. Caro, V. Cherezov, M. Vivaudou, and C.J. Moreau. 2014. Functional assay for T4 lysozyme-engineered G protein-coupled receptors with an ion channel reporter. *Struct. (London, Engl. 1993).* 22:149–155. doi:10.1016/j.str.2013.10.002.
- Nishida, M., M. Cadene, B.T. Chait, and R. MacKinnon. 2007. Crystal structure of a Kir3.1-prokaryotic Kir channel chimera. *EMBO J.* 26:4005–15. doi:10.1038/sj.emboj.7601828.
- Nishida, M., and R. MacKinnon. 2002. Structural basis of inward rectification: Cytoplasmic pore of the G protein-gated inward rectifier GIRK1 at 1.8 Å resolution. *Cell.* 111:957–965. doi:10.1016/S0092-8674(02)01227-8.
- Noma, A. 1983. ATP-regulated K⁺ channels in cardiac muscle. *Nature.* 305:147–8.
- Ockenga, W., S. Kühne, S. Bocksberger, A. Banning, and R. Tikkanen. 2013. Non-Neuronal Functions of the M2 Muscarinic Acetylcholine Receptor. *Genes (Basel).* 4:171–197. doi:10.3390/genes4020171.
- Oh, E.H., S.H. Lee, H.J. Ko, J.H. Lim, and T.H. Park. 2015. Coupling of olfactory receptor and ion channel for rapid and sensitive visualization of odorant response. *Acta Biomater.* 22:1–7. doi:10.1016/j.actbio.2015.04.034.
- Oldham, M.L., D. Khare, F.A. Quijcho, A.L. Davidson, and J. Chen. 2007. Crystal structure of a catalytic intermediate of the maltose transporter. *Nature.* 450:515–521. doi:10.1038/nature06264.
- Park, J.Y., S.H. Koo, Y.J. Jung, Y.-J. Lim, and M.L. Chung. 2014. A patient with Cantú

- syndrome associated with fatal bronchopulmonary dysplasia and pulmonary hypertension. *Am. J. Med. Genet. A.* 164A:2118–20. doi:10.1002/ajmg.a.36563.
- Pegan, S., C. Arrabit, W. Zhou, W. Kwiatkowski, A. Collins, P.A. Slesinger, and S. Choe. 2005. Cytoplasmic domain structures of Kir2.1 and Kir3.1 show sites for modulating gating and rectification. *Nat. Neurosci.* 8:279–87. doi:10.1038/nn1411.
- Pinkett, H.W., A.T. Lee, P. Lum, K.P. Locher, and D.C. Rees. 2007. An inward-facing conformation of a putative metal-chelate-type ABC transporter. *Science.* 315:373–377. doi:10.1126/science.1133488.
- Principalli, M.A. 2015. Etude structure-fonction du canal Kir6.2 et de son couplage avec des partenaires naturels et artificiels.
- Principalli, M.A., J.P. Dupuis, C.J. Moreau, M. Vivaudou, and J. Revilloud. 2015. Kir6.2 activation by sulfonylurea receptors: a different mechanism of action for SUR1 and SUR2A subunits via the same residues. *Physiol. Rep.* 3. doi:10.14814/phy2.12533.
- Proks, P., J.F. Antcliff, and F.M. Ashcroft. 2003. The ligand-sensitive gate of a potassium channel lies close to the selectivity filter. *EMBO Rep.* 4:70–5. doi:10.1038/sj.embor.embor708.
- Proks, P., C. Girard, S. Haider, A.L. Gloyn, A.T. Hattersley, M.S.P. Sansom, and F.M. Ashcroft. 2005. A gating mutation at the internal mouth of the Kir6.2 pore is associated with DEND syndrome. *EMBO Rep.* 6:470–5. doi:10.1038/sj.embor.7400393.
- Proks, P., F.M. Gribble, R. Adhikari, S.J. Tucker, and F.M. Ashcroft. 1999. Involvement of the N-terminus of Kir6.2 in the inhibition of the K(ATP) channel by ATP. *J. Physiol.* 514:19–25. doi:10.1111/j.1469-7793.1999.019af.x.
- Proks, P., F. Reimann, N. Green, F. Gribble, and F. Ashcroft. 2002. Sulfonylurea stimulation of insulin secretion. *Diabetes.* 51 Suppl 3:S368-376.
- Proks, P., H. de Wet, and F.M. Ashcroft. 2010. Activation of the K(ATP) channel by Mg-nucleotide interaction with SUR1. *J. Gen. Physiol.* 136:389–405. doi:10.1085/jgp.201010475.
- Prost, A.-L., A. Bloc, N. Hussy, R. Derand, and M. Vivaudou. 2004. Zinc is both an intracellular and extracellular regulator of KATP channel function. *J. Physiol.* 559:157–167. doi:10.1113/jphysiol.2004.065094.
- Rainbow, R.D., D. Lodwick, D. Hudman, N.W. Davies, R.I. Norman, and N.B. Standen. 2004. SUR2A C-terminal fragments reduce KATP currents and ischaemic tolerance of rat cardiac myocytes. *J. Physiol.* 557:785–794. doi:10.1113/jphysiol.2004.061655.
- Reimann, F., and F.M. Ashcroft. 1999. Inwardly rectifying potassium channels. *Curr. Opin. Cell Biol.* 11:503–8. doi:10.1016/S0955-0674(99)80073-8.
- Reimann, F., S.J. Tucker, P. Proks, and F.M. Ashcroft. 1999. Involvement of the N-terminus of Kir6.2 in coupling to the sulphonylurea receptor. *J. Physiol.* 518:325–336. doi:10.1111/j.1469-7793.1999.0325p.x.
- Rojas, A., J. Wu, R. Wang, and C. Jiang. 2007. Gating of the ATP-sensitive K⁺ channel by a pore-lining phenylalanine residue. *Biochim. Biophys. Acta - Biomembr.* 1768:39–51. doi:10.1016/j.bbamem.2006.06.027.
- Rorsman, P., S.A. Salehi, F. Abdulkader, M. Braun, and P.E. MacDonald. 2008. K(ATP)-channels and glucose-regulated glucagon secretion. *Trends Endocrinol. Metab.* 19:277–84. doi:10.1016/j.tem.2008.07.003.
- Russ, U., U. Lange, C. Löffler-Walz, A. Hambrock, and U. Quast. 2001. Interaction of the sulfonylthiourea HMR 1833 with sulfonylurea receptors and recombinant ATP-sensitive K(+) channels: comparison with glibenclamide. *J. Pharmacol. Exp. Ther.* 299:1049–1055.
- Sakata, S., M.I. Hossain, and Y. Okamura. 2011. Coupling of the phosphatase activity of Ci-VSP to its voltage sensor activity over the entire range of voltage sensitivity. *J. Physiol.* 589:2687–705. doi:10.1113/jphysiol.2011.208165.
- Sandoz, G., and J. Levitz. 2013. Optogenetic techniques for the study of native potassium channels. *Front. Mol. Neurosci.* 6:6. doi:10.3389/fnmol.2013.00006.

- Sandoz, G., J. Levitz, R.H. Kramer, and E.Y. Isacoff. 2012. Optical Control of Endogenous Proteins with a Photoswitchable Conditional Subunit Reveals a Role for TREK1 in GABAB Signaling. *Neuron*. 74:1005–1014. doi:10.1016/j.neuron.2012.04.026.
- Sansom, M.S.P., I.H. Shrivastava, J.N. Bright, J. Tate, C.E. Capener, and P.C. Biggin. 2002. Potassium channels: structures, models, simulations. *Biochim. Biophys. Acta*. 1565:294–307.
- Sauer, D.B., W. Zeng, S. Raghunathan, and Y. Jiang. 2011. Protein interactions central to stabilizing the K⁺ channel selectivity filter in a four-sited configuration for selective K⁺ permeation. *Proc. Natl. Acad. Sci. U. S. A.* 108:16634–9. doi:10.1073/pnas.1111688108.
- Schulze, D., T. Krauter, H. Fritzenschaft, M. Soom, and T. Baukowitz. 2003. Phosphatidylinositol 4,5-bisphosphate (PIP₂) modulation of ATP and pH sensitivity in Kir channels. A tale of an active and a silent PIP₂ site in the N terminus. *J. Biol. Chem.* 278:10500–5. doi:10.1074/jbc.M208413200.
- Schwanstecher, M., C. Sieverding, H. Dörschner, I. Gross, L. Aguilar-Bryan, C. Schwanstecher, and J. Bryan. 1998. Potassium channel openers require ATP to bind to and act through sulfonylurea receptors. *EMBO J.* 17:5529–5535. doi:10.1093/emboj/17.19.5529.
- Schwappach, B., N. Zerangue, Y.N. Jan, and L.Y. Jan. 2000. Molecular Basis for KATP Assembly. *Neuron*. 26:155–167. doi:10.1016/S0896-6273(00)81146-0.
- Shieh, C.C., M. Coghlan, J.P. Sullivan, and M. Gopalakrishnan. 2000. Potassium channels: molecular defects, diseases, and therapeutic opportunities. *Pharmacol. Rev.* 52:557–94.
- Shintre, C.A., A.C.W. Pike, Q. Li, J.-I. Kim, A.J. Barr, S. Goubin, L. Shrestha, J. Yang, G. Berridge, J. Ross, P.J. Stansfeld, M.S.P. Sansom, A.M. Edwards, C. Bountra, B.D. Marsden, F. von Delft, A.N. Bullock, O. Gileadi, N.A. Burgess-Brown, and E.P. Carpenter. 2013. Structures of ABCB10, a human ATP-binding cassette transporter in apo- and nucleotide-bound states. *Proc Natl Acad Sci USA*. 110:9710–9715. doi:10.1073/pnas.1217042110.
- Shyng, S.L., C.A. Cukras, J. Harwood, and C.G. Nichols. 2000. Structural determinants of PIP₂ regulation of inward rectifier K(ATP) channels. *J. Gen. Physiol.* 116:599–608. doi:10.1085/jgp.116.5.599.
- Shyng, S.L., and C.G. Nichols. 1998. Membrane phospholipid control of nucleotide sensitivity of KATP channels. *Science*. 282:1138–41.
- Srinivasan, V., A.J. Pierik, and R. Lill. 2014. Crystal structures of nucleotide-free and glutathione-bound mitochondrial ABC transporter Atm1. *Science*. 343:1137–1140. doi:10.1126/science.1246729.
- Standen, N.B., J.M. Quayle, N.W. Davies, J.E. Brayden, Y. Huang, and M.T. Nelson. 1989. Hyperpolarizing vasodilators activate ATP-sensitive K⁺ channels in arterial smooth muscle. *Science*. 245:177–80.
- Stein, M., S.J. Middendorp, V. Carta, E. Pejo, D.E. Raines, S.A. Forman, E. Sigel, and D. Trauner. 2012. Azo-propofols: photochromic potentiators of GABA(A) receptors. *Angew. Chem. Int. Ed. Engl.* 51:10500–4. doi:10.1002/anie.201205475.
- Sturgess, N.C., M.L. Ashford, D.L. Cook, and C.N. Hales. 1985. The sulphonylurea receptor may be an ATP-sensitive potassium channel. *Lancet (London, England)*. 2:474–475.
- Suzuki, M., K. Fujikura, N. Inagaki, S. Seino, and K. Takata. 1997. Localization of the ATP-sensitive K⁺ channel subunit Kir6.2 in mouse pancreas. *Diabetes*. 46:1440–4.
- Suzuki, M., R.A. Li, T. Miki, H. Uemura, N. Sakamoto, Y. Ohmoto-Sekine, M. Tamagawa, T. Ogura, S. Seino, E. Marbán, and H. Nakaya. 2001. Functional roles of cardiac and vascular ATP-sensitive potassium channels clarified by Kir6.2-knockout mice. *Circ. Res.* 88:570–7.
- Takagi, T., H. Furuta, M. Miyawaki, K. Nagashima, T. Shimada, A. Doi, S. Matsuno, D. Tanaka, M. Nishi, H. Sasaki, N. Inagaki, N. Yoshikawa, K. Nanjo, and T. Akamizu.

2013. Clinical and functional characterization of the Pro1198Leu *ABCC8* gene mutation associated with permanent neonatal diabetes mellitus. *J. Diabetes Investig.* 4:269–273. doi:10.1111/jdi.12049.
- Tamargo, J., R. Caballero, R. Gómez, C. Valenzuela, and E. Delpón. 2004. Pharmacology of cardiac potassium channels. *Cardiovasc. Res.* 62:9–33. doi:10.1016/j.cardiores.2003.12.026.
- Tammaro, P., and F.M. Ashcroft. 2007. A mutation in the ATP-binding site of the Kir6.2 subunit of the K_{ATP} channel alters coupling with the SUR2A subunit. *J. Physiol.* 584:743–753. doi:10.1113/jphysiol.2007.143149.
- Tammaro, P., S.E. Flanagan, B. Zadek, S. Srinivasan, H. Woodhead, S. Hameed, I. Klimes, A.T. Hattersley, S. Ellard, and F.M. Ashcroft. 2008. A Kir6.2 mutation causing severe functional effects in vitro produces neonatal diabetes without the expected neurological complications. *Diabetologia.* 51:802–10. doi:10.1007/s00125-008-0923-1.
- Tao, X., J.L. Avalos, J. Chen, and R. MacKinnon. 2009. Crystal structure of the eukaryotic strong inward-rectifier K⁺ channel Kir2.2 at 3.1 Å resolution. *Science.* 326:1668–74. doi:10.1126/science.1180310.
- Tate, C.G. 2012. A crystal clear solution for determining G-protein-coupled receptor structures. *Trends Biochem. Sci.* 37:343–352. doi:10.1016/j.tibs.2012.06.003.
- Teramoto, N. 2006. Pharmacological Profile of U-37883A, a Channel Blocker of Smooth Muscle-Type ATP-Sensitive K Channels. *Cardiovasc. Drug Rev.* 24:25–32. doi:10.1111/j.1527-3466.2006.00025.x.
- Tochitsky, I., M.R. Banghart, A. Mouro, J.Z. Yao, B. Gaub, R.H. Kramer, and D. Trauner. 2012. Optochemical control of genetically engineered neuronal nicotinic acetylcholine receptors. *Nat. Chem.* 4:105–11. doi:10.1038/nchem.1234.
- Trapp, S., S.J. Tucker, and F.M. Ashcroft. 1997. Activation and inhibition of K-ATP currents by guanine nucleotides is mediated by different channel subunits. *Proc. Natl. Acad. Sci. U. S. A.* 94:8872–7.
- Tucker, S.J., F.M. Gribble, P. Proks, S. Trapp, T.J. Ryder, T. Haug, F. Reimann, and F.M. Ashcroft. 1998. Molecular determinants of KATP channel inhibition by ATP. *EMBO J.* 17:3290–3296. doi:10.1093/emboj/17.12.3290.
- Tucker, S.J., F.M. Gribble, C. Zhao, S. Trapp, and F.M. Ashcroft. 1997. Truncation of Kir6.2 produces ATP-sensitive K⁺ channels in the absence of the sulphonylurea receptor. *Nature.* 387:179–83. doi:10.1038/387179a0.
- Tusnády, G.E., B. Sarkadi, I. Simon, and A. Váradi. 2006. Membrane topology of human ABC proteins. *FEBS Lett.* 580:1017–1022. doi:10.1016/j.febslet.2005.11.040.
- Ueda, K., N. Inagaki, and S. Seino. 1997. MgADP antagonism to Mg²⁺-independent ATP binding of the sulfonylurea receptor SUR1. *J. Biol. Chem.* 272:22983–6.
- Uhde, I., A. Toman, I. Gross, C. Schwanstecher, and M. Schwanstecher. 1999. Identification of the potassium channel opener site on sulfonylurea receptors. *J. Biol. Chem.* 274:28079–28082.
- Vasiliou, V., K. Vasiliou, and D.W. Nebert. 2009. Human ATP-binding cassette (ABC) transporter family. *Hum. Genomics.* 3:281–90.
- Velema, W.A., J.P. van der Berg, M.J. Hansen, W. Szymanski, A.J.M. Driessen, and B.L. Feringa. 2013. Optical control of antibacterial activity. *Nat. Chem.* 5:924–8. doi:10.1038/nchem.1750.
- Velema, W.A., W. Szymanski, and B.L. Feringa. 2014. Photopharmacology: beyond proof of principle. *J. Am. Chem. Soc.* 136:2178–91. doi:10.1021/ja413063e.
- Vergani, P., S.W. Lockless, A.C. Nairn, and D.C. Gadsby. 2005. CFTR channel opening by ATP-driven tight dimerization of its nucleotide-binding domains. *Nature.* 433:876–80. doi:10.1038/nature03313.
- Vila-Carriles, W.H., G. Zhao, and J. Bryan. 2007. Defining a binding pocket for sulfonylureas in ATP-sensitive potassium channels. *FASEB J.* 21:18–25. doi:10.1096/fj.06-6730hyp.
- Vivaudou, M., K.W. Chan, J.-L.L. Sui, L.Y. Jan, E. Reuveny, and D.E. Logothetis. 1997.

- Probing the G-protein Regulation of GIRK1 and GIRK4, the Two Subunits of the KACH Channel, Using Functional Homomeric Mutants. *J. Biol. Chem.* 272:31553–31560. doi:10.1074/jbc.272.50.31553.
- Vivaudou, M., C.J. Moreau, and A. Terzic. 2009. Intracellular Ligand-Gated Ion Channels 4.4.3 Atp-Sensitive K + Channels. 454–473.
- Volgraf, M., P. Gorostiza, R. Numano, R.H. Kramer, E.Y. Isacoff, and D. Trauner. 2006. Allosteric control of an ionotropic glutamate receptor with an optical switch. *Nat. Chem. Biol.* 2:47–52. doi:10.1038/nchembio756.
- Ward, A., C.L. Reyes, J. Yu, C.B. Roth, and G. Chang. 2007. Flexibility in the ABC transporter MsbA: Alternating access with a twist. *Proc. Natl. Acad. Sci. U. S. A.* 104:19005–19010. doi:10.1073/pnas.0709388104.
- Whorton, M.R., and R. MacKinnon. 2011. Crystal Structure of the Mammalian GIRK2 K(+) Channel and Gating Regulation by G Proteins, PIP(2), and Sodium. *Cell.* 147:199–208. doi:10.1016/j.cell.2011.07.046.
- Whorton, M.R., and R. MacKinnon. 2013. X-ray structure of the mammalian GIRK2- β g G-protein complex. *Nature.* 498:190–197. doi:10.1038/nature12241.
- Wieboldt, R., K.R. Gee, L. Niu, D. Ramesh, B.K. Carpenter, and G.P. Hess. 1994. Photolabile precursors of glutamate: synthesis, photochemical properties, and activation of glutamate receptors on a microsecond time scale. *Proc. Natl. Acad. Sci. U. S. A.* 91:8752–6.
- Wilkins, S. 2015. Structure and mechanism of ABC transporters. *F1000Prime Rep.* 7:14. doi:10.12703/P7-14.
- Winqvist, R.J., L.A. Heaney, A.A. Wallace, E.P. Baskin, R.B. Stein, M.L. Garcia, and G.J. Kaczorowski. 1989. Glyburide blocks the relaxation response to BRL 34915 (cromakalim), minoxidil sulfate and diazoxide in vascular smooth muscle. *J. Pharmacol. Exp. Ther.* 248:149–56.
- Wise, A., K. Gearing, and S. Rees. 2002. Target validation of G-protein coupled receptors. *Drug Discov. Today.* 7:235–246. doi:10.1016/S1359-6446(01)02131-6.
- Woo, J.-S., A. Zeltina, B.A. Goetz, and K.P. Locher. 2012. X-ray structure of the *Yersinia pestis* heme transporter HmuUV. *Nat. Struct. Mol. Biol.* 19:1310–1315. doi:10.1038/nsmb.2417.
- Yamada, K., J. Ji, H. Yuan, T. Miki, S. Sato, N. Horimoto, T. Shimizu, S. Seino, and N. Inagaki. 2001. Protective role of ATP-sensitive potassium channels in hypoxia-induced generalized seizure. *Science.* 292:1543–1546. doi:10.1126/science.1059829.
- Yamada, M., A. Inanobe, and Y. Kurachi. 1998. G protein regulation of potassium ion channels. *Pharmacol. Rev.* 50:723–60.
- Yang, J., Y.N. Jan, and L.Y. Jan. 1995. Control of rectification and permeation by residues in two distinct domains in an inward rectifier K⁺ channel. *Neuron.* 14:1047–54.
- Yizhar, O., L. Fenno, F. Zhang, P. Hegemann, and K. Diesseroth. 2011. Microbial Opsins: A Family of Single-Component Tools for Optical Control of Neural Activity. *Cold Spring Harb. Protoc.* 2011:top102. doi:10.1101/pdb.top102.
- Zerangue, N., B. Schwappach, Y.N. Jan, and L.Y. Jan. 1999. A new ER trafficking signal regulates the subunit stoichiometry of plasma membrane K(ATP) channels. *Neuron.* 22:537–48.
- Zhang, F., J. Vierock, O. Yizhar, L.E.L.E. Fenno, S.P.S. Tsunoda, A. Kianianmomeni, M. Prigge, A. Berndt, J. Cushman, J. Polle, J. Magnuson, P. Hegemann, K. Diesseroth, R.D. Airan, K.R. Thompson, L.E.L.E. Fenno, H. Bernstein, K. Diesseroth, N.S. Baliga, R. Bonneau, M.T. Facciotti, M. Pan, G. Glusman, E.W. Deutsch, P. Shannon, Y. Chiu, R.S. Weng, R.R. Gan, et al., C. Bamann, T. Kirsch, G. Nagel, E. Bamberg, C. Bamann, R. Gueta, S. Kleinlogel, G. Nagel, E. Bamberg, E. Bamberg, P. Hegemann, D. Oesterhelt, O. Béjà, E.N. Spudich, J.L. Spudich, M. Leclerc, E.F. DeLong, A. Berndt, O. Yizhar, L.A. Gunaydin, P. Hegemann, K. Diesseroth, P. Berthold, S.P.S. Tsunoda, O.P. Ernst, W. Magés, D. Gradmann, P.

- Hegemann, J.A. Bieszke, E.L. Braun, L.E. Bean, S. Kang, D.O. Natvig, K.A. Borkovich, R.A. Bogomolni, J.L. Spudich, E.S. Boyden, F. Zhang, E. Bamberg, G. Nagel, K. Deisseroth, G. Büldt, J. Heberle, N.A. Dencher, H.J. Sass, X. Chen, J.L. Spudich, B.Y. Chow, X. Han, A.S. Dobry, X. Qian, A.S. Chuong, M. Li, M.A. Henninger, G.M. Belfort, Y. Lin, P.E. Monahan, E.S. Boyden, K. Deisseroth, K. Deisseroth, G. Feng, A.K. Majewska, G. Miesenböck, A. Ting, M.J. Schnitzer, R. Dunn, J. McCoy, M. Simsek, A. Majumdar, et al. 2011. The microbial opsin family of optogenetic tools. *Cell*. 147:1446–57. doi:10.1016/j.cell.2011.12.004.
- Zhou, Y., J.H. Morais-Cabral, A. Kaufman, and R. MacKinnon. 2001. Chemistry of ion coordination and hydration revealed by a K⁺ channel-Fab complex at 2.0 Å resolution. *Nature*. 414:43–8. doi:10.1038/35102009.
- Zung, A., B. Glaser, R. Nimri, and Z. Zadik. 2004. Glibenclamide treatment in permanent neonatal diabetes mellitus due to an activating mutation in Kir6.2. *J. Clin. Endocrinol. Metab.* 89:5504–7. doi:10.1210/jc.2004-1241.

Title: Molecular studies of ATP-sensitive potassium channels: Gating, pathology, and optogenetics

Abstract: ATP-sensitive K⁺ (K_{ATP}) channels are ubiquitous channels designed to couple excitability to cellular energy. They perform this function by sensing the relative levels of the intracellular nucleotides ATP and ADP, with ATP blocking the channel and ADP activating it. Additionally, the phospholipid phosphatidylinositol 4,5-bisphosphate (PIP₂) is known to be a strong regulator of K_{ATP} channels. These channels are present in many excitable tissues and involved in many physiological functions. The main aim of this thesis is to design a light-dependent K_{ATP} channel for use as a tool in physiological studies as well as in optogenetics. Light-dependent block was accomplished by attaching a photosensitive blocker to specific residues. This light-inhibited K_{ATP} channel, could be used to regulate action potentials with light to tune diverse aspects of cellular electrophysiology and potentially for photo-pharmacology treatment. We also performed a functional mapping of the Kir6.2 channel gate(s) under the control of membrane proteins interacting with the N-terminal domain. This was performed by using an artificial ligand-gated Kir6.2 channel formed by attaching a GPCR to its N-terminus. Crystallographic structures and functional characterizations of potassium channels suggested the presence of two gates in the transmembrane domains, the selectivity filter and the "A" gate at the cytoplasmic interface, and of a third gate, the G loop gate, in the cytoplasmic domain of Kir channels. Unexpectedly, our results demonstrated that several gates could be involved suggesting a concerted mechanism. Finally, we characterized two single-point mutations in the ABCC9 gene encoding SUR2 that are associated with Cantù syndrome (CS). These mutations are localized in transmembrane domain 0 (TMD0) of SUR2A, an essential domain which mediates the interaction between Kir6.2 and SUR within the K-ATP channel complex. Results suggest that the two mutations cause K_{ATP} channel hyperactivity through two divergent mechanisms: (1) a decreased sensitivity to ATP inhibition and (2) an increased sensitivity to activation by PIP₂. These discoveries underline the essential role of TMD0 in the gating modulation of Kir6.2. They demonstrate in particular that it can control the response of the channel to intracellular effectors that bind to Kir6.2, implying tight interactions between Kir6.2 and the TMD0 region.

Keywords: Physiology, K_{ATP} channels, sulfonylurea receptor, optogenetics

Titre: Etudes moléculaires du canal potassique sensible à l'ATP : « gating », pathologie et optogénétique

Résumé: Les canaux potassiques sensibles à l'ATP (K_{ATP}) sont des canaux omniprésents liant excitabilité et énergie cellulaire. Ils fonctionnent en captant le niveau relatif des nucléotides ATP et ADP à l'intérieur des cellules, l'ATP bloquant le canal et l'ADP l'activant. De plus le phospholipide phosphatidylinositol4,5-bisphosphate (PIP_2) est connu pour être un puissant régulateur des canaux K_{ATP} . Ceux-ci sont présents dans la plupart des tissus excitables et sont impliqués dans un grand nombre de fonctions physiologiques. L'objectif de ma thèse consiste à concevoir un canal K_{ATP} contrôlable par la lumière, qui servira d'outil pour les études physiologiques ainsi que pour l'optogénétique. Une inhibition induite par la lumière a été obtenue par greffage d'un bloqueur photosensible à des résidus spécifiques. Ce canal K_{ATP} inhibé par la lumière pourrait être utilisé pour réguler les potentiels d'action via la lumière afin de piloter les propriétés électrophysiologiques de certaines cellules ainsi que pour des applications de photopharmacologie. J'ai également réalisé la cartographie fonctionnelle des résidus impliqués dans le gating du canal Kir6.2 sous le contrôle de protéines membranaires interagissant avec le domaine N-terminal. Cela a été réalisé en utilisant un canal artificiel Kir6.2 modulable par des ligands, créé en attachant un RCPG au N-terminal du canal. Des structures cristallographiques et des caractérisations fonctionnelles des canaux potassiques ont permis de mettre en évidence la présence de deux portes dans les domaines transmembranaires, le filtre de sélectivité et le « gate A » à l'interface cytoplasmique, et d'une troisième porte, la «G loop gate», dans le domaine cytoplasmique des canaux Kir. Enfin j'ai caractérisé deux mutations du gène ABCC9 codant pour SUR2A associées au syndrome de Cantú (CS). Ces mutations sont localisées dans le domaine transmembranaire 0 (TMD0) de SUR2A, domaine essentiel pour l'interaction entre Kir6.2 et SUR dans le complexe K_{ATP} . Les résultats suggèrent que les deux mutations cause une hyperactivité du canal via 2 mécanismes distincts : (1) Une diminution de la sensibilité de l'ATP et (2) une sensibilité accrue au PIP_2 . Ces découvertes soulignent le rôle essentiel du TMD0 dans la modulation de l'ouverture de Kir6.2. En particulier, elles démontrent que ce domaine peut moduler la réponse du canal aux effecteurs intracellulaires qui se fixent sur Kir6.2, impliquant des interactions très liées entre Kir6.2 et le domaine TMD0.

Mots clés : physiologie, canaux K-ATP, Récepteur des sulfonylurées, optogénétique

Discipline : Biologie Structurale et Nanobiologie.

Laboratoire d'accueil : Institut de Biologie Structurale, Channels group, 71 Avenue des Martyrs, 38044 Grenoble Cedex 9.